

The University of Manitoba

CRYSTAL STRUCTURES OF THE TANTALUM
OXIDE MINERALS TANTALITE AND
WODGINITE, AND OF MILLERITE NiS

by

JOEL DENISON GRICE

A Thesis

Submitted to

The Faculty of Graduate Studies

In Partial Fulfillment

of the Requirements

for the Degree

Doctor of Philosophy

Department of Earth Sciences

Winnipeg, Manitoba

May, 1973



CRYSTAL STRUCTURES OF THE TANTALUM
OXIDE MINERALS TANTALITE AND
WODGINITE, AND OF MILLERITE NiS

BY: Joel D. Grice

A dissertation submitted to the Faculty of Graduate Studies of
the University of Manitoba in partial fulfillment of the requirements
of the degree of

DOCTOR OF PHILOSOPHY

© 1973

Permission has been granted to the LIBRARY OF THE UNIVER-
SITY OF MANITOBA to lend or sell copies of this dissertation, to
the NATIONAL LIBRARY OF CANADA to microfilm this
dissertation and to lend or sell copies of the film, and UNIVERSITY
MICROFILMS to publish an abstract of this dissertation.

The author reserves other publication rights, and neither the
dissertation nor extensive extracts from it may be printed or other-
wise reproduced without the author's written permission.

To my parents

ABSTRACT

Crystal structure analyses have been carried out for the three closely related Ta-oxide minerals, tantalite, pseudo-ixiolite and wodginite from the Tanco Pegmatite, Bernic Lake, Manitoba using data collected on fully automated single-crystal diffractometers. The structures were refined using full-matrix least squares and Fourier computer programs. The original structure of tantalite (columbite) of Sturdivant (1930) was confirmed and refined. The other two Ta oxide minerals are essentially isostructural with it. All three minerals have oxygens in pseudo-hexagonal close-packed layers parallel to (100). Tantalite in orthorhombic space group Pbcn with $a \sim 14.4$, $b \sim 5.8$, $c \sim 5.1 \text{ \AA}$ (but strong $a' = a/3$) has the cell content $A_4B_8O_{24}$. The structure analysis shows that A and B are mainly Mn and Ta, respectively, but an interpretation of the structure in terms of electrostatic charge distributions suggests some interchange of 2+ and 5+ cations between the two sites. For this tantalite, the structural cell content is proposed as $(Mn_{2.4}^{2+} Nb_{1.6}^{5+}) (Ta_{5.2}^{5+} Nb_{1.2}^{5+} Mn_{1.6}^{2+}) O_{24}^{2-}$, and for tantalite-columbites generally the structural formula is proposed as not $A^{2+}B^{5+}O_6^{2-}$ but rather $(A_{3-2x}^{2+} B_{2x}^{5+}) (B_{1-x}^{5+} A_x^{2+})_2 O_6^{2-}$ with A^{2+} mainly Mn^{2+} and Fe^{2+} , B^{5+} mainly Ta^{5+} and Nb^{5+} , and $x \geq 0$. Pseudo-

ixiolite in space group Pbcn with $a \sim 4.8$, $b \sim 5.8$, $c \sim 5.2 \text{ \AA}$ is shown to have a cation-disordered tantalite structure with all the cations in the one site. The cell content of this pseudo-ixiolite is $(\text{Ta}_{1.6}^{5+} \text{Mn}_{1.1}^{2+} \text{Nb}_{0.9}^{5+} \text{Ti}_{0.06}^{4+} \text{Sn}_{0.02}^{4+} \text{Fe}_{0.01}^{2+}) \text{O}_8^{2-}$, and the ideal formula is simply AO_2 where A represents all the cations. Wodginite is monoclinic with a true cell in space group C2/c and with $a \sim 9.5$, $b \sim 11.4$, $c \sim 5.1 \text{ \AA}$, $\beta \sim 91^\circ$. The relationship in the wodginite-tantalite cell dimensions is $a_w \sim 2/3 a_t$, $b_w \sim 2 b_t$, $c_w \sim c_t$. The structure analysis of wodginite confirmed it to have the structure found for the pseudo-cell ($a' = a/2$, $b' = b/2$, $c' = c$) by Elphick (1972), with origin at $0x, \frac{1}{2}y, 0z$ in the tantalite structure. For a true cell content of $(\text{A}_4\text{B}_4\text{C}_8)\text{O}_{32}$, the structure analysis showed that the A, B and C sites contain mainly 2+, 4+ and 5+ cations, respectively, but electrostatic charge considerations taken with the structure analysis suggest the best structural cell content for this wodginite to be $(\text{Sn}_{1.6}^{4+} \text{Mn}_{1.0}^{2+} \text{Fe}_{0.7}^{3+} \text{Ti}_{0.6}^{4+} \text{Nb}_{0.1}^{5+}) (\text{Ta}_{2.1}^{5+} \text{Mn}_{1.9}^{2+}) (\text{Ta}_{6.4}^{5+} \text{Sn}_{0.9}^{4+} \text{Mn}_{0.7}^{2+}) \text{O}_{32}^{2-}$. For wodginites generally, the structural formula is proposed as $\text{A}^{3.6+} \text{B}^{3.5+} \text{C}_2^{4.5+} \text{O}_8^{2-}$ where A, B and C represent some or all of the elements as distributed in the above specific formula.

The original structure of millerite NiS of Kolkmeijer and Moesveld (1931) was confirmed and refined using the same methods as for the Ta oxide minerals. The millerite crystal

was from the Marbridge Mine, Malartic, Quebec, and an electron probe microanalysis yielded an average formula of $(\text{Ni}_{0.981} \text{Fe}_{0.016} \text{Co}_{0.004}) \text{S}$. Within the structure each Ni is co-ordinated with five S atoms as previously known, but two other Ni atoms are close enough (2.53 \AA) that they must also be considered as neighbours; each S is surrounded by five Ni atoms. The bond lengths observed within the millerite structure are comparable to the expected value of an Ni-S covalent bond. Using molecular orbital energy level diagrams it is shown that the millerite structure (βNiS) with five-fold co-ordination around Ni requires less bonding energy to form than the niccolite structure (αNiS) with six fold co-ordination about each Ni, and the former thus becomes the stable phase within nature. The Ni-Ni bonding within millerite could be stabilized by the two electrons in the d_{z^2} orbital which would otherwise be non-bonding if only the S atoms were considered.

ACKNOWLEDGEMENTS

The author is very grateful to Dr. R.B. Ferguson, Professor of Mineralogy at the University of Manitoba, for his continued guidance and valuable suggestions throughout this research project.

Thanks are due to Drs. J.A. Mandarino and R.I. Gait, Department of Mineralogy, Royal Ontario Museum, Toronto, for furnishing many of the millerite specimens used in this study; to Dr. D.C. Harris, Mines Branch, Department of Mines, Energy and Resources, Ottawa, who provided standards used in the electron microprobe analysis of millerite; and to Dr. Maartence, Department of Physics, University of Manitoba for performing the magnetic measurements on millerite.

The electron microprobe at the Whiteshell Nuclear Research Establishment in Pinawa, Manitoba was made available through the generosity of Dr. A. Sawatsky and Mr. S. Jones, the probe operator, kindly aided in the analyses. Intensity data for the structural analyses were collected on single crystal diffractometers afforded through the courtesy of the following: Dr. C. Calvo, Department of Chemistry, McMaster University, Hamilton; Dr. E. Gabe, National Research Council, Chemistry Division,

Ottawa; Dr. M. James, Department of Biochemistry, University of Alberta, Edmonton; and Dr. V. Kocman, Department of Geology, University of Toronto, Toronto.

Throughout this study a number of computer programs were used. These were kindly made available by: Dr. W. Hutcheon, Department of Biochemistry, University of Alberta, Edmonton; Dr. C.K. Johnson, Oak Ridge National Laboratory, Oak Ridge, Tennessee; Dr. K.A. Kerr, Department of Chemistry and Physics, University of Calgary, Calgary; Dr. W. Kaufman, Department of Oral Biology, University of Manitoba, Winnipeg; and Dr. J.C. Rucklidge, Department of Geology, University of Toronto, Toronto.

Financial assistance was provided by fellowships granted by the University of Manitoba and the National Research Council.

TABLE OF CONTENTS

	<u>Page</u>
ABSTRACT	iii
ACKNOWLEDGEMENTS	vi
LIST OF FIGURES	xii
LIST OF TABLES	xiii
CHAPTER I - GENERAL INTRODUCTION	1
I.1 Tantalum Oxide Minerals, Tantalite, Pseudo-ixiolite and Wodginite	2
I.2 The Sulphide Mineral Millerite	3
CHAPTER II - EXPERIMENTAL AND COMPUTING METHODS	5
II.1 Choice and Preparation of Crystals	6
II.1.a Introduction	
II.1.b Tantalite and Pseudo-ixiolite	7
II.1.c Wodginite	7
II.1.d Millerite	8
II.2 X-ray Data Collection	9
II.2.a Introduction	9
II.2.b Procedure for the Picker FACSI Diffractometer	9
II.2.c Procedure for Syntex PI Diffractometer	11

CHAPTER II (Continued)

II.3	Computer Programs Used in Data Processing	12
II.3.a	Introduction	12
II.3.b	Program DATAP5 (Data Processing)	13
II.3.c	Program GONO9 (Goniostat)	14
II.3.d	Program GENLES (General Least Squares)	16
II.3.e	Program FOURIER	19
II.3.f	Program DISAGL (Distance and Angle)	20
II.3.g	Program BIJCAL (B_{ij} Calculation)	21
II.3.h	Program ORTEP-II (Oak Ridge Thermal-Ellipsoid Plot)	23

CHAPTER III - THE CRYSTAL STRUCTURES OF THE TANTALUM OXIDES TANTALITE, PSEUDO-IXIOLITE AND WODGINITE

25

III.1	Introduction	26
III.2	Tantalite	27
III.2.a	Previous Work and Sample Description	27
III.2.b	X-ray Data Collection and Data Reduction	29
III.2.c	Structure Refinement	33
III.3	Pseudo-ixiolite	44
III.3.a	Previous Work and Sample Description	44
III.3.b	Data Collection and Data Reduction	45

CHAPTER III (Continued)

III.3.c	Structure Refinement	48
III.4	Wodginite	53
III.4.a	Previous Work and Sample Description	53
III.4.b	Data Collection and Data Reduction	57
III.4.c	Structure Refinement	62
III.5	Electrostatic Charge Distributions in Tantalite, Pseudo-ixiolite and Wodginite	69
III.5.a	Introduction	69
III.5.b	Theory of the Method	79
III.5.c	Tantalite	82
III.5.d	Pseudo-ixiolite	86
III.5.e	Wodginite	87
III.6	Interpretation and Comparisons of the Structure of Tantalite, Pseudo-ixiolite, and Wodginite	89
III.6.a	Proposed Cation Distribution and Chemical Formula for Tantalite	89
III.6.b	Chemical Formula for Pseudo-ixiolite	95
III.6.c	Proposed Cation Distribution and Chemical Formula for Wodginite	96
III.6.d	Comparison of the Structures of Tantalite, Pseudo-ixiolite and Wodginite	98
(i)	The Structures Themselves	98
(ii)	Possible Origin of the Different Structures	104

CHAPTER IV - THE CRYSTAL STRUCTURE OF MILLERITE, NiS	108
IV.1 Millerite Structure Analysis: Method and Results	109
IV.1.a Introduction	109
IV.1.b Experimental Details	113
IV.1.c Structure Refinement	115
IV.2 Description and Discussion of the Millerite Structure	117
IV.2.a Description of the Millerite Structure	117
IV.2.b Discussion of the Millerite Structure	125
(i) Layering and Anisotropism of the Atoms	125
(ii) Interatomic Bonding	127
REFERENCES CITED	142
APPENDICES	
APPENDIX A - Some Job Control Language (JCL) and 'De-bugging' Procedures Used with the Computer Programs	147
APPENDIX B - Computer Program (Data Processing)	156
APPENDIX C - Computer Program GONO9 (Goniostat)	164
APPENDIX D - Computer Program GENLES (General Least Squares)	169
APPENDIX E - Computer Program FOURIER	176
APPENDIX F - Computer Program DISAGL (Distance Angle)	179
APPENDIX G - Computer Program BIJCAL (B_{ij} Calc.)	183
APPENDIX H - Computer Program ORTEP-II	187

LIST OF FIGURES

	<u>Page</u>
Figure III.2.1. Tantalite: Projection of the final structure along z .	39
Figure III.3.1. Pseudo-ixiolite: Projection of the final structure along z .	52
Figure III.4.1. Choice of origin for wodginite structure.	64
Figure III.4.2. Wodginite: Projection of the final structure along z^* .	73
Figure III.6.1. Comparison of the orientation and size of the tantalite, pseudo-ixiolite and wodginite cells.	102
Figure IV.1.1. Millerite: Projection of the final structure along z .	120
Figure IV.2.1. Millerite: Projection of the final structure along y .	126
Figure IV.2.2. Splitting of energy levels for d orbitals in various symmetries.	134
Figure IV.2.3a. Molecular orbital energy level diagram for an NiS_6 configuration with O_h symmetry.	137
Figure IV.2.3b. Molecular orbital energy level diagram for millerite assuming C_{4v} symmetry.	139
Figure C.1. Tantalite crystal as an example of input into GON09 for absorption correction.	164

LIST OF TABLES

	<u>Page</u>
Table III.2.1. Tantalite: Chemical analysis and chemical formula of specimen No. G69-58 from Grice (1970).	30
Table III.2.2. Tantalite: Space group, cell content, cell dimensions, and positional parameters.	37
Table III.2.3a. Tantalite: Anisotropic temperature factors and isotropic equivalents.	38
Table III.2.3b. Tantalite: Magnitudes and orientations of thermal ellipsoids.	40
Table III.2.4. Tantalite: Final F_o and F_c values.	41
Table III.2.5. Tantalite: Interatomic distances and interbond angles.	43
Table III.3.1. Pseudo-ixiolite: Chemical analysis and chemical formula of specimen No. G69-55, data from Grice (1970).	46
Table III.3.2. Pseudo-ixiolite: Space group, cell content, cell dimensions, and positional parameters.	50
Table III.3.3a. Pseudo-ixiolite: Anisotropic temperature factors and isotropic equivalents.	51
Table III.3.3b. Pseudo-ixiolite: Magnitudes and orientations of thermal ellipsoids.	54
Table III.3.4. Pseudo-ixiolite: Final F_o and F_c values.	55
Table III.3.5. Pseudo-ixiolite: Interatomic distances and interbond angles.	56

	<u>Page</u>
Table III.4.1. Wodginite: Chemical analysis and chemical formula of specimen No. G69-17 from Grice (1970).	58
Table III.4.2. Wodginite: Space group, cell content, cell dimensions, and positional parameters.	70
Table III.4.3. Wodginite: The electrons in each metal site by chemical analysis and by structure analysis.	71
Table III.4.4a. Wodginite: Anisotropic temperature factors and isotropic equivalents.	72
Table III.4.4b. Wodginite: Magnitudes and orientations of thermal ellipsoids.	74
Table III.4.5. Wodginite: Final F_o and F_c values.	75
Table III.4.6. Wodginite: Interatomic distances and interbond angles.	77
Table III.5.1. Tantalite: Calculation of the electrostatic charge distribution in $Mn_4^{2+} (Ta,Nb)_8^{5+} O_8^{2-}$	84
Table III.5.2a. Wodginite: Calculation of the electrostatic charge distribution in the sub-cell.	88
Table III.5.2b. Wodginite: Calculation of the electrostatic charge distribution in the true cell, $(Mn_{3.58}^{2+} Fe_{0.42}^{3+}) (Sn_{2.51}^{4+} Ti_{0.63}^{4+} Ta_{0.46}^{5+} Fe_{0.29}^{3+} Nb_{0.11}^{5+})$ $Ta_{8.00}^{5+} O_{32}^{2-}$	90
Table III.6.1. Tantalite: Calculation of the electrostatic charge distribution in $(Mn_{2.32}^{2+} Nb_{1.68}^{5+}) (Ta_{5.12}^{5+} Nb_{1.20}^{5+} Mn_{1.68}^{2+}) O_{24}^{2-}$	94

	<u>Page</u>
Table III.6.2. Wodginite: The derivation of a proposed chemical formula (cation distribution) for the true cell consistent with the chemical analysis, the derived scattering factors, the electrostatic charge distribution and the bond lengths.	99
Table III.6.3. Comparison of the tantalite pseudo-ixiolite and wodginite cells.	101
Table IV.1.1. Millerite: Microprobe analysis and chemical formula.	112
Table IV.1.2. Millerite: Space group, cell content cell dimensions, and positional parameters.	118
Table IV.1.3a. Millerite: Anisotropic temperature factors and isotropic equivalents.	119
Table IV.1.3b. Millerite: Magnitudes and orientations of thermal ellipsoids.	121
Table IV.1.4. Millerite: Final F_o and F_c values.	122
Table IV.1.5. Millerite: Interatomic distances and interbond angles.	123
Table IV.2.1. Co-ordinations and bond lengths in the Ni-Sulphide structures.	130
Table B.1. Example of output for program DATAP5: Tantalite.	159
Table C.1. Example of output for program GON09: Tantalite.	167
Table D.1. Example of output for program GENLES: Tantalite.	174
Table E.1. Example of output of program FOURIER: Tantalite ΔF .	178
Table F.1. Example of output of program DISAGL: Tantalite.	182

	<u>Page</u>
Table G.1. Example of output for program BIJCAL: Tantalite.	186
Table H.1. Example of output for program ORTEP-II: Tantalite.	190

CHAPTER I

GENERAL INTRODUCTION

CHAPTER I

I.1 Tantalum Oxide Minerals, Tantalite, Pseudo-Ixiolite and Wodginite.

The major part of this thesis describes crystal-structure analyses of the three closely-related tantalum oxide minerals tantalite, pseudo-ixiolite and wodginite from the Tanco pegmatite, Bernic Lake, Manitoba; this work is part of a continuing series of projects on many of the minerals from this pegmatite being carried out in the Department of Earth Sciences, University of Manitoba. The bulk of the work completed to date has been published recently as a series of papers which constitute most of one number of the *Canadian Mineralogist* (Vol. 11, Part 3, 1972). This thesis follows directly the research already presented on these tantalum oxides in Grice (1970) and Grice, Černý and Ferguson (1972).

The zoning in the Tanco pegmatite is described in detail by Crouse and Černý (1972), and Grice (1970) and Grice *et al.* (1972) who observed that the tantalum minerals had preferences for specific zones within the pegmatite. Tantalite is abundant in zone (6b), the albitic aplite assemblage. Pseudo-ixiolite is rare within the pegmatite

and is found primarily in zone (4), the microcline-perthite + albite + quartz + spodumene (+ amblygonite) zone, and in zone (5), the spodumene + quartz + amblygonite (+ petalite) zone. Wodginite appears to be the most common tantalum oxide in the Tanco pegmatite and it is very abundant in zone (6a), the coarse-grained K-feldspar + quartz (+ albite, beryl, spodumene) zone, and in zone (6b).

Grice, Černý and Ferguson (1972) did some initial crystallography on the Tanco tantalites, pseudo-ixiolites and wodginites which confirmed the work done by Nickel *et al.* (1963 a and 1963 b). Crystal-structural analyses of all three of these minerals are described in Chapter III of this thesis, and an attempt is made to explain why all three of these closely related structures occur in the Tanco pegmatite, and more generally to explain the extent of their stability in any tantalum deposit.

I.2 The Sulphide Mineral Millerite

Millerite NiS is, like the tantalum oxides, an important economic mineral, but because it is a sulphide its crystal-chemistry is very different from that of the oxides. Although the essential features of the millerite structure have been known for many years (Alsén, 1925; Kolkmeijer and Moesveld, 1931) the structure analysis until this time has been based on powder methods and with modern techniques a much better structure refinement could be

achieved. A very accurate refinement of the structure is described in Chapter IV.

The rather unique five-fold co-ordination of each atom type by the other provides an interesting problem for explanation. In terms of molecular orbital theory a possible explanation is derived for this structure.

CHAPTER II

EXPERIMENTAL AND COMPUTING METHODS

CHAPTER II

II.1 Choice and Preparation of Crystals

II.1.a Introduction

The choice and preparation of a crystal are important preliminary aspects in the data collection for a crystal structure analysis. In general, the crystal should (i) be a single individual and (ii) have the proper size and shape. Ideally, it is desirable to have a spherical crystal to simplify absorption corrections especially for highly absorbing crystals like those dealt with here. Where, for some reason it is impossible to prepare a spherical crystal, then one should use a polyhedral crystal whose bounding planes are known or can be estimated for calculating absorption corrections. Furthermore, the size of the crystal is important since the intensity of a diffracted beam is proportional to the volume of crystal being irradiated. If crystals are too small and reflections too weak, poor counting statistics inhibit a good structure refinement. Absorption is particularly high in the tantalum oxide minerals so one must be careful to keep crystals small enough to avoid too large a decrease in intensity due to absorption. Stout and Jensen (1968) suggest that the

optimum thickness (t , cm) should be no greater than is given by the equation $t = \frac{2}{\mu}$ where μ (per cm) is the linear absorption coefficient.

II.1.b Tantalite and Pseudo-ixiolite

It proved very difficult to get single individual crystals of tantalite and of pseudo-ixiolite because of the good cleavage associated with these two minerals. It proved impossible to grind a satisfactory sphere of either one of these minerals because they tended to yield crystal fragments displaced along the cleavage which would give multiple reflections. Due to this cleavage problem small polyhedral fragments of tantalite and pseudo-ixiolite were used for the data collections. The sizes of the crystals used were up to 5 times larger in the direction of maximum thickness than that considered optimum (0.005 cm) according to the formula given at the end of the previous section. Such crystals proved necessary in order to get good counting statistics, particularly in tantalite which has a large number of weak reflections associated with its true cell.

II.1.c Wodginite

Single crystals of wodginite also proved difficult to obtain due to the nature of the crystals. The crystals are not compact but are granular, and they tend to

crystallize in multiple growths. This made it difficult to obtain single crystals that gave neither multiple reflections nor a large mosaic spread. Two ground spheres were chosen for collecting the wodginite data, and in both cases they were approximately four times larger than the calculated optimum thickness of 0.05 mm for Mo radiation. This was necessary in order to record acceptable intensities of the weak reflections associated with the true cell.

II.1.d Millerite

The intensity data for millerite were collected on a sphere. Unfortunately, the ground spheres of the Marbridge material tended to be somewhat distorted in shape due to the good cleavage on $(10\bar{1}1)$. The sphere diameter for the crystal used was twice the calculated optimum value of 0.12 mm for Mo radiation. The main problem in finding an acceptable millerite crystal was to get one that was a single individual with no second individual twinned according to the very common twin law of reflection in $(01\bar{1}2)$. The crystal chosen for the data collection was twinned but the reflections from the second individual were very weak.

II.2 X-ray Data Collection

II.2.a Introduction

All of the X-ray data for these structures were collected using four-circle fully automated single-crystal diffractometers. Because the University of Manitoba did not have such an instrument at the time of this work, collections were made at other universities through the courtesy of the following: Dr. C. Calvo, Department of Chemistry, McMaster University, Hamilton; Dr. M. James, Department of Biochemistry, University of Alberta, Edmonton; and Dr. V. Kocman, Department of Geology, University of Toronto. All but one data collection were made on Picker FACSI instruments; the instrument at McMaster University was a Syntex P $\bar{1}$.

For all data collections Mo radiation with a Zr filter and no attenuation was used. Except for the University of Toronto instrument, graphite single-crystal monochromators were used and for all data collections scintillation counters were used. The $2\theta - \theta$ type of scan was used to get integrated intensity data.

II.2.b Procedure for the Picker FACSI Diffractometer

The details of the procedures followed in a data collection are available in the Picker Manual and only a brief summary is given here. For this instrument the

simplest procedure is to mount the crystal so it is rotating about a reciprocal axis. The goniometer head is mounted on the instrument and the crystal is carefully centred in the X-ray beam using the cross-hairs on the telescope provided. On most goniometer heads the z -axis adjustment is small (~ 2 mm) so one must use a glass fibre of nearly the correct length. The centring in the x , y , and z directions is done at $\chi = 90^\circ$ and checked at $\chi = 270^\circ$. Once the crystal is physically centred in the X-ray beam the orientation of the crystal with respect to its reciprocal lattice can begin. At $\chi = 90^\circ$ a strong low- 2θ reflection is chosen for manual centring. With adjustments to the goniometer rockers, which should be put parallel and perpendicular to the X-ray beam, the peak is maximized on the counter. Other reflections should be found at $\chi \sim 0^\circ$ to get an approximate orientation matrix. Once an approximate matrix is established the automatic mode of the instrument may be used to centre several (10 to 12 is usual) high- 2θ reflections with intensities greater than 200 cps; then the instrument's computer calculates an accurate set of cell dimensions and an accurate matrix for the intensity collection. The care with which one centres the crystal will be reflected in the quality of the cell dimensions and intensities that are obtained. Details relating to the instrumental conditions during the intensity collections are given under the descriptions of the data collection for each mineral.

II.2.c Procedure for Syntex P $\bar{1}$ Diffractometer

In the Syntex Manual a detailed explanation of the procedures for a data collection are given, and only a brief summary is presented here. On this instrument the orienting of the reciprocal lattice has been simplified and speeded up considerably in relation to the procedure used for the Picker FACSI. The crystal need not be rotating about a reciprocal axis, and in fact it may be mounted for rotation about any random direction. Once the crystal is centred in the X-ray beam, a rotation-type photograph of a few minutes' exposure using Polaroid film is taken at $\chi = 0^\circ$ with ϕ rotating through 360° several times. From the Polaroid photograph one merely chooses up to 15 strong reflections and measures in centimeters the distance between equivalent reflections. Due to the geometry of the picture there should be four symmetrically equivalent reflections if the reflections do not lie along the axis of rotation or perpendicular to this axis in the horizontal plane. The four symmetrically equivalent reflections arise due to the rotation of 360° (which gives 2) and to Friedel symmetry (which also gives 2). The metric co-ordinates are fed into the automatic scanning program which transforms them into reciprocal co-ordinates. The instrument is programmed to search out and maximize these reflections. Once this is done the computer calculates the vector magnitude and orientation between the first reflection

and each additional one. These vectors are resolved and within the print out one should be able to find vectors with the magnitude or multiples of the approximately known cell dimensions and the associated angles. Reflections may then be indexed, and from these an orientation matrix and accurate cell dimensions are calculated by the instrument computer.

II.3 Computer Programs Used in Data Processing

II.3.a Introduction

In this thesis the computer programs used for this project in the Department of Earth Sciences, University of Manitoba are described in this chapter and in Appendices B to H. This chapter gives in the following sections descriptions of all the programs used, and brief points about the use and facilities available for each program. The Appendices give examples of the input and output for each program.

Accompanying each source deck of cards there are a number of comment cards preceding the main program which explain the necessary input formats. The Los Alamos Scientific Laboratory (LASL) set of programs has an accompanying manual (Larson, 1971). Dr. K.A. Kerr of the Department of Chemistry and Physics, University of Calgary, Calgary, Alberta generously provided decks of the LASL

programs and accompanied them with her own brief manual (Kerr, 1971). One unfortunate aspect of the LASL programs is that they are not well documented within the programs themselves, and the user may experience difficulty in determining what exactly the program is doing at any particular place. The Oak Ridge National Laboratory (ORNL) program ORTEP-II is accompanied by an excellent manual (Johnson, 1971, revised for ORTEP-II). The user will find this a very well documented program and should not have any problem interpreting the thought processes within it.

II.3.b Program DATAP5 (Data Processing) - Data Reduction of Relative Intensities to Give a Set of Relative F_o Values

This program originated at the Weizmann Institute in Rehovot, Israel and was adapted for use on the IBM 360/65 by Dr. W. Kaufman of the Department of Oral Biology, University of Manitoba, from whom the program was obtained. A few changes were made to the program by the writer, and these are outlined in Appendix B.

This program corrects intensities derived from precession films, Weissenberg films, or four-circle diffractometers for spherical absorption, Lorentz and polarization factors and polarization by a graphite monochromator, if necessary. For precession and Weissenberg geometry there is a subroutine to correct for the absorption in a polyhedron

of up to 48 enclosing planes or "faces". The orientation of the crystal is defined by its rotation or precession axis and by the other two axes contained within a given photograph. The actual absorption correction is carried out in the same manner as described for the four-circle diffractometer data in program GON09 described in section (c) immediately below. Upper-level Weissenberg film intensities may be corrected for spot extension.

The input into DATAP5 may be from cards or tape. The constants necessary for the absorption correction are described in Appendix B. Each reflection is dealt with separately and there is no limit to the number that may be read in. The h,k,l indices and relative I values are the only essential data, but additional information such as a weight, scale factor, 2θ , ϕ and χ may be used. The output, an example of which is given in Appendix B, of relative F_o values (and their h,k,l indices) from the program is stored on disk in preparation for subsequent programs GON09 (section (c)) or GENLES (section (d)).

II.3.c Program GON09 (Goniostat) - Extinction and Absorption Corrections for Diffractometer (Goniostat) Intensities from Polyhedral Crystals

This program was written by W. Hamilton,
Chemistry Department, Brookhaven National Laboratory,

Long Island, N.Y., and obtained from the Department of Chemistry, University of Alberta, Edmonton through the courtesy of Dr. W. Hutcheon. The extinction part of the program was not used by the writer as it proved to be a negligible factor compared with the absorption corrections, for these structures.

This program requires that the crystal shape be described by giving the Miller Indices of the bounding planes and the distance in cm from an internal origin to each face. Up to 33 "faces" may be used to describe the polyhedron. Care must be taken to assure that the faces form a closed body, and furthermore there can be no re-entrant angles.

The input, an example of which is given in Appendix C, consists of the crystal orientation which is given in terms of the χ and ϕ values of the bounding planes. Each reflection is input with the 2θ , χ and ϕ readings, and these in turn can be used in conjunction with the crystal shape and orientation to calculate the path direction of the X-ray beam.

The absorption for a given reflection is a function of the size and shape of the crystal and the relation of the incident and diffracted beams to this shape. With the orientation matrix and dimensions of the crystal, the program calculates the absorption correction by a numerical integration over a defined grid which is part of the input data. The grid chosen must cover the whole crystal, and it should

be kept in mind that the smaller the grid interval the longer and more costly will be the computer run.

The intensities are usually corrected for Lorentz and polarization factors before being processed by program GONO9 so the output of absorption-corrected relative F_o values from GONO9 can be stored on disk ready for input into program GENLES. An example of the output is given in Appendix C.

II.3.d Program GENLES (General Least Squares) -
Structure Factor Calculations and Refinement
of Parameters by Full Matrix Least Squares

GENLES was written by A.C. Larson of the Los Alamos Scientific Laboratory in New Mexico. The present program was written in 1967 and has been improved continuously by the original author since that time.

GENLES appropriately scales the input relative F_o 's and compares them to a set of F_c 's calculated on the basis of an input trial structure. The parameters which are being refined are varied through a full-matrix least squares analysis. The program will handle without modification or user intervention any space group including those in non-standard settings provided the symbols form a group. A subroutine, SPGP, interprets the space group symbol, and determines the number and parameters of all equivalent atoms for all structurally different atoms, both general and

special. The maximum number of structurally different atoms that can be handled at present is 100 with no limit on the number of reflections.

An example of input and output for GENLES is given in Appendix D. Through the input the user has the option of refining or holding constant the following parameters:

- i) positional parameters x, y, z for each atom;
- ii) thermal parameters isotropic B or anisotropic β_{ij} for each atom;
- iii) scale factors for independent batches of reflections;
- iv) site occupancy factors for each atom;
- v) anomalous scattering factor terms $\Delta f', \Delta f''$ for individual atom types; and
- vi) an extinction parameter.

This program can also constrain interatomic distances to remain close to a predetermined value.

A choice of weighting schemes is provided in addition to unit weights or weights read from input (usually based on counting statistics). The optional weighting schemes are:

$$w_1 = \frac{1}{\sigma(F_{\text{obs}})} \quad \text{or} \quad w_2 = \frac{1}{\sigma^2(F_{\text{obs}})}$$

The function minimized may be either

$$\Sigma w_1 ||F_O| - |F_C||^2 \quad \text{or} \quad \Sigma w_2 |F_O^2 - F_C^2|^2 \quad .$$

Reflection data input may be taken entirely from cards or tape or partly from both. If the format of the reflection data differs from the 'standard' format built into GENLES it may be specified as part of the input, and it may contain some or all of the following quantities:

$$h,k,l; \quad \sin^2\theta/\lambda^2; \quad \beta(2\theta) \text{ (extinction correction);}$$

$$E^2; \quad F; \quad F^2; \quad W_{F_O}; \quad \sigma F^2; \quad N_1 \text{ (scale factor).}$$

The scattering factors used for the atoms are those tabulated by Cromer and Mann (1968). These scattering factors are computed from numerical Hartree-Fock wave functions, and the results are given in the form of coefficients a , b , and c for the analytic function:

$$f = c + \sum_{i=1,4} a_i e^{-b_i \sin^2\theta/\lambda^2}$$

The output can be varied according to what is requested by the wishes of the user. Various disks can be created for input into the programs described after this one. The printed output contains the refined positional and thermal parameters and various R factors for each cycle in the least squares refinement. Following the last cycle, the final F_O 's, F_C 's, ΔF 's and phases are printed as shown in Appendix D.

II.3.e Program FOURIER - Calculation of Electron
Density Maps, E Maps and Patterson Maps

The program FOURIER was written by P.T. Cromer in 1959 and has been modified several times since then by A.C. Larson to improve its generality.

In its present form there is no limit to the number or order of reflections used in the program. There is a size limit associated with the range of indices and the section axis chosen. The grid interval may be any value $1/n$ where n is an integer between 1 and 500. As with program GENLES, all space groups may be used.

There are three formats for input into this program:

- i) a tape produced by GENLES;
- ii) a defined format tape or a card deck containing
 $h,k,l; F_O; A_C; B_C$ (acentric); or
 $h,k,l; F_O; F_C; \Delta F$ (centric);
- iii) a data tape for Patterson synthesis containing
 $h,k,l; \sin^2 \theta/\lambda^2; PL; E^2; F_O^2; W; \sigma F_O^2, N_1$
 where PL is for extinction correction,
 W is a weighting factor based on counting statistics, and
 N_1 is used to signal scale factor index associated with the reflection.

From the appropriate input may be computed any one of

an F_o Fourier synthesis, F_c Fourier synthesis, ΔF Fourier synthesis, F^2 Patterson synthesis, sharpened F^2 Patterson synthesis or E^2 Patterson synthesis. The output is in the form of on-line printing of an area of grid points for the number of sections requested. Only sections normal to the x , y , or z -axis may be computed as there is no facility for special sections such as (110), etc. At each grid point is printed an integer representing the electron density at that point. The maps may be scaled by the volume input which is used to divide the sum of all F 's at each point. Thus, the smaller the volume the larger the printed electron density value. If an improper scaling factor is used, output may be too large or too small to be useful. The following factors were found useful to get appropriate scaling: 10X or 100X the volume for an F^2 Patterson synthesis, 1X the volume for an F_o or F_c Patterson synthesis, and 0.1X the volume for a ΔF Fourier synthesis.

An example of the input and output for this program is shown in Appendix E.

II.3.f Program DISAGL (Distance and Angle) -

Calculation of Bond Lengths and Interbond
Angles

Program DISAGL was written by A.C. Larson in 1959. This program computes and lists all inter-atomic distances in a structure which are shorter than a maximum

value which is read in. All angles are also computed according to a separately specified maximum distance. The program contains an option for a special angle calculation used to compute angles about large atoms without computing an excessive number of angles about smaller atoms. The standard deviations of the cell dimensions and atomic parameters are read into the program and these are used to calculate the sigma for the bond distances and angles.

Data may be read entirely from cards or from a disk generated by GENLES. In the output each atom is dealt with in turn and all the bond distances and angles associated with the atom, within the limits given, are listed. For the bond distances table the co-ordinates of the type atom are given and for each surrounding atom the cell and the co-ordinates within this cell are given. The angle table gives the co-ordinates of the two apical atoms and of the vertex atom.

An example of the input and output for this program is given in Appendix F.

II.3.g Program BIJCAL (B_{ij} Calculation) - Calculation of Principal Axes of Thermal Vibration Ellipsoids

Program BIJCAL was written by A.C. Larson in 1959. The purpose of the program is to determine the magnitude and orientation of the thermal vibration ellip-

soids from the β_{ij} values derived from program GENLES.

The input into this program can be from a disk created by GENLES or it can be entirely from cards, with or without standard deviations and the correlation matrix of β_{ij} . In order to get output from this program the β_{ij} 's of a particular atom must form a possible combination and they should be tested to make sure they are positive definite (see Appendix G). The beginning of this program had to be changed slightly as the subroutine SSWTCH is "built-in" for CDC computers but not for IBM which the writer was using. SSWTCH is used as a sensor to detect the mode of input (i.e., disk or cards).

In the output, atoms are dealt with individually in the order of presentation. The root mean square amplitude and the β_{ij} associated with each ellipsoid axis are given. The orientation of the ellipsoid is indicated in two ways: (i) the angles that the ellipsoid axes make with the real lattice axes are given in degrees, measured in a clockwise direction from the positive axis; (ii) directional cosines of the ellipsoid axes relative to the orthogonal lattice axes.

An example of the input and output for BIJCAL is given in Appendix G.

II.3.h Program ORTEP-II (Oak Ridge Thermal-Ellipsoid Plot) - Thermal-Ellipsoid Plot Program for Crystal Structure Illustration

Program ORTEP-II is C.K. Johnson's latest version (1971) of his earlier program ORTEP. A copy of the program was obtained directly from C.K. Johnson in the Oak Ridge National Laboratory, Oak Ridge, Tennessee. The program is used for drawing crystal structure illustrations with an off-line mechanical plotter such as the CalComp which is available at the University of Manitoba. A very thorough manual written by Johnson accompanies the program, and it describes the computational procedures and necessary input for the program. Examples of input and output are given in the manual and one is given in Appendix H of this thesis. ORTEP-II differs from ORTEP in that the new version has a routine that eliminates overlapping of lines in the drawing and thus requires very little manual touch-up.

The input into ORTEP-II is entirely from cards. The crystal structure data required includes cell dimensions, space group symmetry, atomic parameters, and temperature factors. The instruction input is quite varied and depends on what the user desires in the output. Input must include instructions such as projection orientation, scale, how much of the structure is to be drawn, type of atom and bond representation, labelling, and whether or not a stereo-

scopic pair is to be drawn.

The output consists of two parts; the printed output and the plotted figure. The printed output can contain a listing of interatomic bond lengths and principal axes of thermal motion. Also, it usually contains all of the input data and a listing of all the atoms with their co-ordinates to be plotted. The program has a convenient listing of fault indicators which, if present in the output, will aid the user in determining his error in his input instructions.

CHAPTER III

THE CRYSTAL STRUCTURES OF THE TANTALUM OXIDES
TANTALITE, PSEUDO-IXIOLITE AND WODGINITE

CHAPTER III

III.1 Introduction

To date there have been only two significant studies made on any of the three tantalum oxide minerals, tantalite, pseudo-ixiolite and wodginite: Sturdivant (1930) solved the structure of "niobite" (= Columbite), $(\text{Fe}, \text{Mn}) \text{Nb}_2\text{O}_6$, and Elphick (1972) derived the structure of wodginite, based on the sub-cell; no structural work had been done on pseudo-ixiolite until this work. In view of the probable close structural relationships of these three minerals first suggested by Nickel *et al.* (1963 a and 1963 b) and emphasized by Grice *et al.* (1972), it was considered desirable to choose crystals for all three minerals from the Tanco mine because of the detailed knowledge of their chemistry and occurrence (Grice, 1970; Grice *et al.*, 1972). For each of the minerals, data was collected by a fully-automated single-crystal diffractometer to get the best possible set of intensity measurements. For each structure refinement the data was processed in a similar manner in order to give the best comparable results. This part of the thesis describes structure analyses of tantalite, pseudo-ixiolite and wodginite in Chapter III.2, III.3, and

III.4 respectively. Chapter III.5 presents the theory and calculations of the electrostatic charge distribution in each of these oxides, and the results of this coupled with the crystal-chemistry are given in a comparative analysis in the final Chapter III.6.

III.2 Tantalite

III.2.a Previous Work and Sample Description

Although tantalite and pseudo-ixiolite are very similar in the hand specimen, the samples from the Tanco Mine, Bernic Lake may be tentatively identified as one or the other according to grain shape and location within the mine. As discussed in Chapter I, General Introduction, tantalite is confined to the aplitic albite (Zone (6), Assemblage (b)), and it occurs as subhedral to euhedral grains up to 2 mm in size. As described later, pseudo-ixiolite has on the other hand, a larger platy shape and is in a different zone. A positive distinction between tantalite and pseudo-ixiolite can, however, only be made by X-ray identification.

The specimen chosen for a structural analysis, No. G69-58, was not actually in the albitic albite but lay immediately adjacent to it in a quartz-muscovite-albite matrix (see Grice, 1970, p. 8). This specimen was chosen because the crystals were fairly large and because, on the basis of the author's earlier X-ray work (Grice, 1970), it

was classified as a partially disordered tantalite on the strength of the hkl reflections: those with $h = 3n$ are generally present, but those with $h = ln$ or $h = 2n$ which are absent in the disordered mineral were present as weak reflections on photographs of this specimen. Also as described below, the chemistry is essentially that of a manganotantalite containing Mn, Ta and Nb with very little Fe, Sn or Ti substitution. The specific gravity for this specimen was measured to be 6.76(3) gm/cc, (Grice *et al.*, 1972) but this value is probably low due to silicate inclusions.

Preliminary crystallographic data for this specimen (heated and unheated) are given in Grice (1970, p. 54) and in Table 3 of Grice *et al.* (1972). The space group derived from single-crystal photographs is Pbcn, and the cell dimensions (with standard deviations in brackets), for the heated material, refined from powder diffractometer data are:

$$a = 14.430(3) \text{ \AA}$$

$$b = 5.763(2) \text{ \AA}$$

$$c = 5.091(1) \text{ \AA}$$

Slightly different cell dimensions from those above were derived using the single-crystal diffractometer on the actual material. The latter cell dimensions are given in the next section and they were used in the structure

analysis.

The chemical analysis for G69-58 and the number of cations calculated on the basis of 24 oxygens (Grice, 1970) are given in Table III.2.1. The general formula for tantalite is $A_4B_8O_{24}$ where $A = Mn^{2+}, Fe^{2+}, Sn^{4+}, Ti^{4+}$ and $B = Ta^{5+}, Nb^{5+}$. To ensure that this material was as ordered as possible with respect to its cation arrangement, it was heated to $1000^\circ C$ for sixteen hours (Grice, 1970). To prevent oxidation of Mn^{2+} and Fe^{2+} , the specimen was heated in a controlled atmosphere with $fO_2 = 10^{-14}$ atm. which is just below the wustite-magnetite oxidation curve. Mn^{2+} oxidizes at much higher oxygen pressures than Fe^{2+} .

It is likely the Mn content in this analysis is low because it is a much lighter element than Ta and due to the nature of probe analyses the Ta would have an effect of "overshadowing" the Mn. In the discussion below of the structure analysis, the total of Mn + Fe + Sn + Ti is thus assumed to be 4.0 rather than 3.8.

III.2.b X-ray Data Collection and Data Reduction

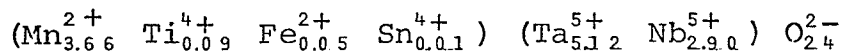
For the X-ray data collection, several tantalite fragments were chosen and ground into spheres. The spheres were found to give unsatisfactory single-crystal reflections because the fragmental qualities of this material caused the grinding to give split crystals. For this reason a blocky polyhedral fragment was chosen to

Table III.2.1. Tantalite: Chemical analysis and chemical formula of specimen No. G69-58 from Grice (1970, p. 44).

<u>Oxide</u>	<u>Weight %</u>	<u>Element</u>	<u>No. of Cations*</u>
MnO	14.6	Mn ²⁺	3.66
FeO	0.2	Fe ²⁺	0.05
SnO ₂	0.1	Sn ⁴⁺	0.01
TiO ₂	0.4	Ti ⁴⁺	0.09
Ta ₂ O ₅	64.2	Ta ⁵⁺	5.12
Nb ₂ O ₅	21.0	Nb ⁵⁺	2.90
Total	<u>100.5</u>	Total	<u>11.83</u>

3.81
 8.02

Chemical formula:



* Number of atoms calculated on the basis of 24 oxygens in the unit cell.

collect data on. The dimensions of the crystal were carefully measured across the bounding planes, and possible Miller indices for these planes deduced. The dimensions of the fragment were approximately 0.33 mm x 0.22 mm x 0.17 mm. The crystal was mounted perpendicular to a cleavage plane which proved subsequently to be the (310) plane.

Data was collected on a Picker FACSI fully automated four-circle single crystal diffractometer in the crystal structures laboratory of Dr. M. James, Department of Biochemistry, University of Alberta, Edmonton. Mo radiation with a Zr filter was used with a graphite monochromator ($2d = 6.708 \text{ \AA}$) to irradiate the specimen.

Intensities for tantalite were collected on an orthorhombic cell assuming no space group extinctions. Accurate cell dimensions were derived from a least squares refinement of 20 reflections whose intensities had been maximized by a computer-controlled scanning program. The refined cell dimensions and their standard deviations (in brackets) are :

$$a = 14.4134(34) \text{ \AA}$$

$$b = 5.7600(14) \text{ \AA}$$

$$c = 5.0838(13) \text{ \AA}$$

The intensities were collected using $2\theta - \theta$ scans with a scanning speed of $2^\circ 2\theta$ per minute. Background counts

were made for 10 seconds on either side of the peak. One octant of the sphere of reflections was collected out to $2\theta = 60^\circ$. Except for a few striking reflections which could be attributed to the Renninger effect, the extinct reflections corresponded to the space group determined by Sturdivant (1930), namely Pbcn. In the description of this tantalite given here as in Grice (1970) and in Grice, Černý and Ferguson (1970), the orientation of the cell is that of Strunz and Tennyson (1970). For this space group, 615 reflections were measured of which 602 were observed.

As a consequence of the high content of Ta and Nb in tantalite, the linear absorption coefficient is very large ($\mu = 390$ units per cm for Mo radiation), and this large absorption correction proved to be one of the most limiting factors in the structure refinement. The Lorentz and polarization corrections were carried out using the computer program DATAP5 (Appendix B). The polarization correction included the factor contributed by a single-crystal monochromator (Appendix B, c). The absorption correction for the tantalite polyhedron was processed by the computer program GON09 (Appendix C). For both the programs DATAP5 and GON09 the tantalite data is used as given in the example in the Appendices.

III.2.c Structure Refinement

For the refinement of the tantalite structure the starting parameters for all the atomic positions were those determined by Sturdivant in 1930 (see Table III.2-2, p. 37, for Sturdivant's results). Sturdivant showed that in this structure there are five structurally different atoms, and their sites are outlined in the same table. The site symbols are those given for this space group Pbcn (No. 60) in the International Tables for X-ray Crystallography, Volume I. From Table III.2-2 it can be seen that the 'Mn'-type or A site is in a four-fold special position $0, y, \frac{1}{4}$ because it lies on a two-fold axis; the 'Ta'-type or B site and the three oxygen sites are all in eight-fold general positions, x, y, z .

Initially a least squares refinement of the structure was carried out using the least squares program, GENLES and assuming only the two metal sites. The one metal site was given the scattering values of pure Mn^{2+} while the other was given a combination of the Ta^0 and Nb^{5+} scattering values in proportions consistent with the chemical analyses (5 Ta to 3 Nb) given in Table III.2-1. The scattering factor Ta^0 was used because that of Ta^{5+} is not available in Cromer and Mann's (1968) tabulation. After each group of least squares cycles, a ΔF Fourier synthesis was computed to aid in decisions regarding the refinement

procedure. Using 363 reflections and isotropic temperature factors, several cycles of the first refinement gave a value of $R = 0.26$. After this, the three oxygens were added and, with the same number of reflections and isotropic temperature factors, the R factor was reduced to 0.13. At this point in the refinement several difficult features about the results were becoming evident: (i) the $\rho_o - \rho_c$ map had apparent anomalies around the metal sites which suggested a possible "splitting of the Ta-site (see Table E1); (ii) there were groups of reflections for which the F_c values agreed very poorly with the F_o values, in particular reflections of the types 001, 0k1, and 311; (iii) the weighted R factor was considerably higher than the unweighted R (approximately four times higher); (iv) the isotropic temperature factor B of oxygen II was considerably higher than that of the other two, 3.98 \AA^2 as opposed to 0.53 and 0.44 \AA^2 . There was nothing on any of the electron density or difference maps to indicate any essential misplacing of the atoms so other factors had to be considered.

The first improvement in the R factor was brought about by adding the rest of the data and converting all isotropic temperature factors to anisotropic ones. At this point R was reduced to 0.11 and, although all four problems were reduced somewhat in magnitude, they were still there. In an attempt to correct problem ii it was thought that changes in the absorption correction would help. A clay

model was made of the crystal in an attempt to better define the bounding planes and estimate the distances from the planes to the origin as required by the absorption program. Figure C.1 in Appendix C shows a sketch of this model and its use in the program GON09. With an improved absorption correction the R index reduced slightly to 0.105. The groups of reflections referred to previously improved somewhat but not entirely. With the seven worst reflections removed (002, 004, 022, 023, 111, 311, 313) the R index dropped to 0.093. The reason that the weighted R factor was so much higher than the unweighted one could also have been due to the absorption correction. Since some of the corrections are up to 200 times the initially observed intensities, this might have been the effect of increasing relatively weak reflections to large F_o values which would thus give an unreasonably high weight to a possibly poor reflection. This would have the effect of drastically upsetting the weighting scheme. In an attempt to deal with the problem of the apparently 'split' Ta-atom, this atomic site was divided into two close Ta-sites each with one-half the scattering power of Ta. Somewhat surprisingly in the program GENLES the refinement routine attempted to take all the electrons from one site and put them in the other. This was manifested by a drastic increase and decrease respectively of the temperature factors of the two sites. As might be expected under the

circumstances, the run ended in "chaos" with $R = 0.43$, but it did indicate that this "splitting" was not the proper way to handle this curious feature on the difference map. In fact this problem remained unsolved, but it may also be due to absorption, and possibly also to the close O_{II} atom with a large anisotropic temperature factor.

The F_o 's and F_c 's for the final structure adopted are listed in Table III.2.4, and these correspond to a final $R = 0.106$. These are not for $Mn_4(Ta_5Nb_3)O_{24}$ as one might expect, but rather they are for $(Mn_{2.32}Nb_{1.68})(Ta_{5.12}Nb_{1.20}Mn_{1.68})O_{24}$. The reason for adopting this particular site occupancy is discussed in section 5(b)iii. The co-ordinates for the final atomic positions are given in Table III.2.2, a projection of the structure is shown in Figure III.2.1, the temperature factors are given in Table III.2.3a, and the conversion of the β_{ij} 's to B_{ij} 's and the magnitudes and orientations of the thermal ellipsoids are given in Table III.2.3b. The much greater atomic numbers of the metals relative to oxygen causes the metals to interfere with the positional parameters and the temperature factors of the oxygens. In the least squares refinement of the anisotropic temperature factors for the oxygens, O_I and O_{III} ended with impossible combinations and were thus assigned the isotropic equivalents. From the final atomic parameters, bond lengths

Table III.2.2. Tantalite: Space group, cell content, cell dimensions, and positional parameters.

<u>Space Group</u>	Pbcn = P	$2_1/b$	$2/c$	$2_1/n$	(No. 60)
<u>Cell Content</u>	Z	(Mn _{2,3,2} ²⁺ Nb _{1,6,8} ⁵⁺)	(Ta _{5,1,2} ⁵⁺ Nb _{1,2,0} ⁵⁺ Mn _{1,6,8} ²⁺)	O _{2,4} ²⁻	
<u>Cell Dimensions and Standard Deviations (in brackets), Å</u>	a	= 14.4134	(34)		
	b	= 5.7600	(14)		
	c	= 5.0838	(13)		
<u>Atomic Equivalent Positions</u>	4 Mn in (a)	: $\pm(0, y, \frac{1}{4}; \frac{1}{2}, \frac{1}{2}+y, \frac{1}{4})$			
	8 Ta in (d)	: $\pm(x, y, z; \frac{1}{2}+x, \frac{1}{2}-y, z;$ $x, y, \frac{1}{2}-z; \frac{1}{2}-x, \frac{1}{2}-y, \frac{1}{2}+z)$			
	8 O _I in (d)				
	8 O _{II} in (d)				
	8 O _{III} in (d)				

Positional Parameters

Standard Deviations are Given in Brackets.

<u>Site</u>	<u>Co-ordinate</u>	<u>Sturdivant (1930)</u>	<u>This Work</u>
A (= 'Mn')	x	0	0
	y	0.350	0.3231 (6)
	z	$\frac{1}{4}$	$\frac{1}{4}$
B (= 'Ta')	x	0.163	0.1625 (1)
	y	0.175	0.1766 (2)
	z	0.750	0.7367 (3)
O _I	x	0.090	0.0956 (5)
	y	0.095	0.0942 (15)
	z	0.083	0.0605 (18)
O _{II}	x	0.410	0.4183 (5)
	y	0.100	0.1146 (19)
	z	0.083	0.0998 (22)
O _{III}	x	0.750	0.7597 (6)
	y	0.080	0.1193 (16)
	z	0.070	0.0940 (19)

Table III.2.3a. Tantalite: Anisotropic temperature factors and isotropic equivalents.
Standard deviations are given in brackets

<u>Atomic Site.</u>	<u>β_{11}</u>	<u>β_{22}</u>	<u>β_{33}</u>	<u>β_{12}</u>	<u>β_{13}</u>	<u>β_{23}</u>	Equivalent Isotropic B, <u>(\AA^2)</u>
A	0.0028 (3)	0.0114 (16)	0.0171 (22)	0.0	0.00038 (59)	0.0	1.86
B	0.0013 (1)	0.0032 (8)	0.0033 (9)	-0.00016 (5)	-0.00012 (11)	-0.00052 (19)	0.61
O _I	0.0013 (2)	0.0080 (21)	0.0102 (34)	0.0	0.0	0.0	1.06
O _{II}	0.0017 (3)	0.0194 (29)	0.0154 (43)	-0.00115 (126)	-0.00696 (147)	-0.02904 (632)	2.02
O _{III}	0.0010 (4)	0.0064 (18)	0.0082 (35)	0.0	0.0	0.0	0.84

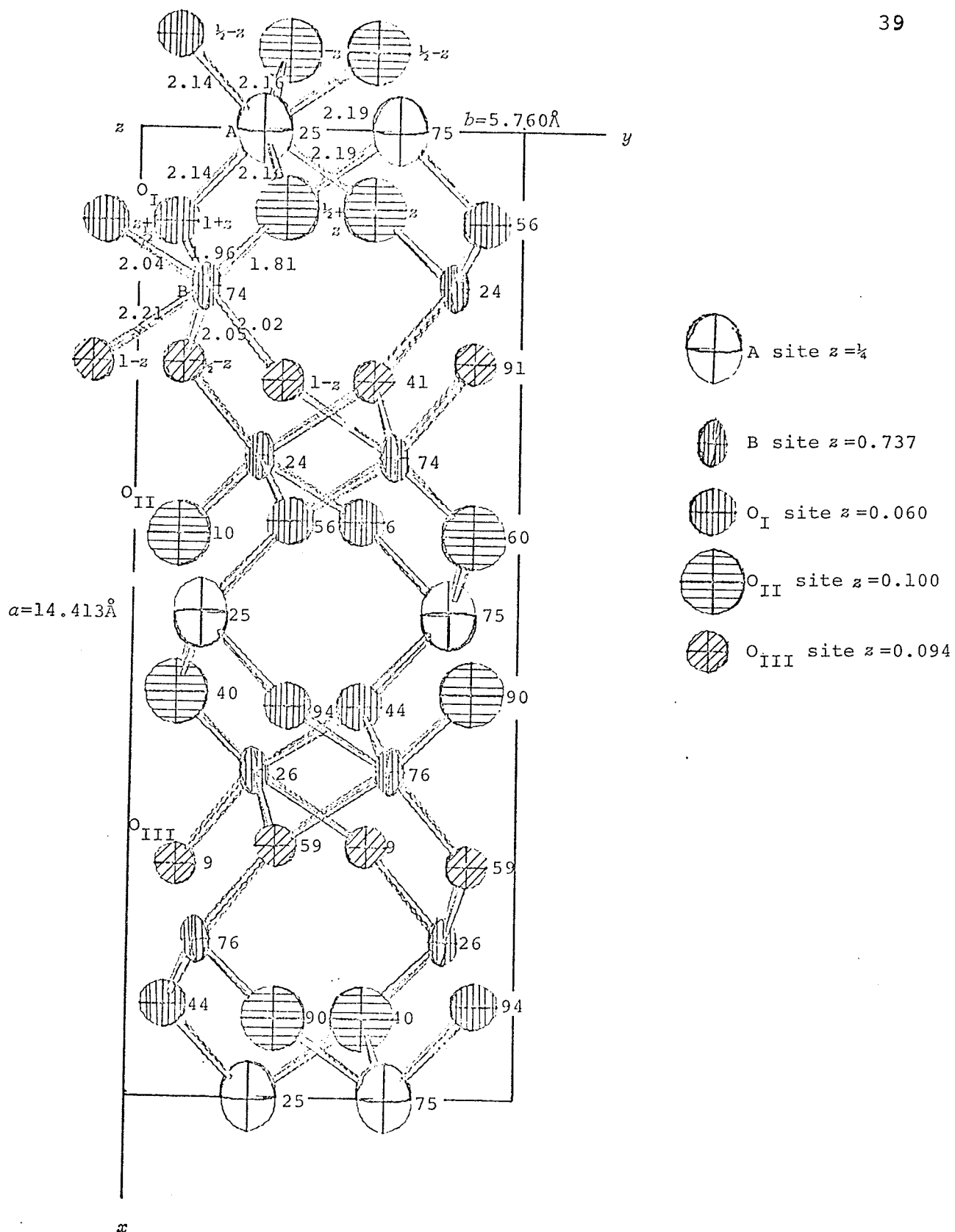


Figure III.2.1. Tantalite: projection of the final structure along z . Heights are shown above the plane of projection in hundredths of the c period,

Table III.2.3b. Tantalite: Magnitudes and orientations of thermal ellipsoids.

Site	Ellipsoid Axes	Root Mean Square Amplitude, (Å)	Equivalent B (Å ²)	Angles Between Ellipsoid Axes and Real Axes*		
				A	B	C
A	1	0.172	2.32	5.7°	90.0°	95.7°
	2	0.138	1.51	90.0	0.0	90.0
	3	0.149	1.76	84.3	90.0	5.7
B	1	0.115	1.05	2.8	92.4	91.3
	2	0.075	0.40	88.1	17.6	107.5
	3	0.065	0.33	88.0	72.5	17.6
O _{II}	1	0.154	1.88	32.5	117.2	106.4
	2	0.224	3.95	78.6	41.2	128.9
	3	0.053	0.22	60.0	61.7	43.5

Standard deviations were not calculated for these measurements.

* A,B,C are the angles between the ellipsoid axes 1,2,3 and the crystallographic lattice axes x,y,z , respectively measured in a clockwise direction from the positive axis.

Table III.2.4. Tantalite: Final F_o and F_c values

H	K	L	FOB	FCALC	DEL-F	A-PT
0 0 2	636	491	236	-401		
0 0 4	457	295	172	-285		
0 0 6	237	236	-4	-236		
0 2 0	197	267	-64	-267		
0 2 2	304	301	-1	301		
0 2 4	201	257	49	257		
0 2 6	399	351	48	-351		
0 2 8	201	194	15	-186		
0 2 10	166	182	-17	182		
0 2 12	129	117	12	117		
0 4 0	128	161	-33	-161		
0 4 1	323	351	-28	-351		
0 4 2	55	62	-7	62		
0 4 3	253	260	-7	260		
0 4 4	45	50	-5	50		
0 4 5	213	204	6	-206		
0 4 6	69	57	3	67		
0 6 0	184	233	-39	-233		
0 6 1	112	102	3	109		
0 6 2	237	237	5	-232		
0 6 3	56	59	-2	-58		
0 6 4	181	192	-11	192		
0 8 0	127	144	-20	-146		
0 8 1	98	176	-7	176		
1 0 0	14	9	6	8		
1 1 0	14	9	3	1		
1 1 1	71	67	63	-1	69	
1 1 2	12	17	2	-10		
1 1 3	66	62	4	-62		
1 1 4	52	49	3	49		
1 1 5	13	11	2	-11		
1 1 6	22	21	1	-23		
1 1 7	2	3	3	-2		
1 1 8	55	55	-1	56		
1 1 9	61	59	3	-58		
1 2 0	67	66	1	-66		
1 2 1	45	43	2	43		
1 2 2	43	44	0	44		
1 2 3	41	45	-5	-45		
1 2 4	22	24	-2	24		
1 2 5	64	53	1	-63		
1 2 6	16	17	-2	-17		
1 2 7	50	51	-1	51		
1 2 8	9	1	-1	1		
1 2 9	30	27	3	-27		
1 3 0	81	84	-6	-88		
1 3 1	16	15	2	-15		
1 3 2	102	93	13	89		
1 3 3	17	13	7	10		
1 3 4	92	11	11	-81		
1 3 5	24	25	0	-24		
1 3 6	54	55	-1	55		
1 3 7	49	49	0	49		
1 3 8	61	55	6	55		
1 3 9	55	45	9	-46		
1 4 0	69	56	12	-56		
1 4 1	27	22	5	-22		
1 4 2	19	21	-1	21		
1 4 3	55	53	2	53		
1 4 4	180	131	78	133		

H	K	L	FOB	FCALC	DEL-F	A-PT
1 1 2	54	30	24	-30		
1 1 3	102	79	23	-79		
1 1 4	46	46	1	46		
1 1 5	56	58	-2	58		
1 1 6	21	21	-8	-31		
1 1 7	47	55	-8	-55		
1 1 8	110	92	21	-90		
1 1 9	70	75	-5	75		
1 2 0	41	49	-8	-49		
1 2 1	107	88	17	-88		
1 2 2	93	78	16	78		
1 2 3	54	55	-1	-55		
1 2 4	59	56	4	56		
1 2 5	72	73	-1	-73		
1 2 6	48	48	3	-48		
1 2 7	66	68	-2	68		
1 2 8	31	25	7	25		
1 2 9	87	73	14	-73		
1 2 10	24	18	6	-18		
1 2 11	35	29	7	28		
1 2 12	52	53	1	53		
1 2 13	76	53	22	-53		
1 2 14	57	42	15	-42		
1 2 15	78	60	18	60		
1 2 16	46	35	11	35		
1 2 17	51	49	3	-48		
1 2 18	32	31	1	-31		
1 2 19	86	81	5	81		
1 2 20	23	18	6	-18		
1 2 21	74	72	2	-72		
1 2 22	7	2	5	-2		
1 2 23	35	33	2	33		
1 2 24	11	13	-2	-13		
1 2 25	25	30	-5	30		
1 2 26	57	42	10	-42		
1 2 27	19	18	1	-18		
1 2 28	72	63	9	-63		
1 2 29	14	8	6	8		
1 2 30	48	51	-3	51		
1 2 31	19	19	0	-19		
1 2 32	38	34	4	-34		
1 2 33	33	32	1	32		
1 2 34	28	27	1	-27		
1 2 35	18	20	-1	-20		
1 2 36	60	60	0	-60		
1 2 37	26	28	-2	-28		
1 2 38	56	54	1	54		
1 2 39	18	11	7	11		
1 2 40	47	48	0	-48		
1 2 41	34	31	3	-31		
1 2 42	6	5	1	5		
1 2 43	16	16	0	16		
1 2 44	37	33	4	33		
1 2 45	24	27	-4	-27		
1 2 46	18	18	0	-18		
1 2 47	215	215	0	-215		
1 2 48	21	17	4	17		
1 2 49	192	184	8	184		
1 2 50	15	13	2	13		

H	K	L	FOB	FCALC	DEL-F	A-PT
3 0 3	8	20	6	-12		
3 0 4	20	12	7	12		
3 0 5	28	25	3	25		
3 1 0	182	213	-31	-213		
3 1 1	104	193	-9	193		
3 1 2	199	206	-7	206		
3 1 3	157	166	-9	-166		
3 1 4	160	163	-3	-163		
3 1 5	119	126	-6	126		
3 1 6	1	0	-1	0		
3 1 7	7	3	4	3		
3 1 8	27	24	2	24		
3 1 9	11	8	3	8		
3 1 10	45	43	1	43		
3 1 11	28	21	7	-21		
3 1 12	313	400	-87	400		
3 1 13	75	78	-3	78		
3 1 14	343	346	-3	-346		
3 1 15	56	50	6	-50		
3 1 16	260	261	-1	261		
3 1 17	50	45	5	45		
3 1 18	168	184	3	-184		
3 1 19	8	6	2	6		
3 1 20	38	34	4	34		
3 1 21	13	10	4	-10		
3 1 22	9	0	9	0		
3 1 23	11	14	-3	-14		
3 1 24	115	95	20	-95		
3 1 25	221	241	-20	-241		
3 1 26	437	422	15	422		
3 1 27	196	182	15	182		
3 1 28	358	332	25	332		
3 1 29	143	132	11	-132		
3 1 30	219	219	0	-219		
3 1 31	6	52	46	52		
3 1 32	149	147	2	147		
3 1 33	7	4	3	-4		
3 1 34	36	35	1	-35		
3 1 35	112	108	4	-108		
3 1 36	128	145	-18	-145		
3 1 37	120	110	10	110		
3 1 38	109	101	8	-101		
3 1 39	63	73	-10	73		
3 1 40	27	25	2	25		
3 1 41	80	70	11	-70		
3 1 42	36	38	-2	-38		
3 1 43	49	46	3	46		
3 1 44	28	23	5	23		
3 1 45	20	24	-4	-24		
3 1 46	58	62	-4	62		
3 1 47	115	96	19	-96		
3 1 48	86	71	15	-71		
3 1 49	96	83	13	83		
3 1 50	62	58	4	58		
3 1 51	62	61	1	-61		
3 1 52	39	42	-2	-42		
3 1 53	66	67	-1	67		
3 1 54	9	12	-3	-12		
3 1 55	62	59	3	59		
3 1 56	21	21	0	-21		

H	K	L	FOB	FCALC	DEL-F	A-PT
4 1 2	46	4	-42			
4 1 3	5	3	2	-3		
4 1 4	30	24	6	24		
4 1 5	111	175	6	109		
4 1 6	23	25	-2	-25		
4 1 7	84	91	2	-81		
4 1 8	27	39	-6	39		
4 1 9	76	75	1	75		
4 1 10	13	14	-1	-14		
4 1 11	40	42	-1	42		
4 1 12	26	32	4	-32		
4 1 13	76	78	-2	-78		
4 1 14	20	24	-4	-24		
4 1 15	13	7	2	7		
4 1 16	68	74	-6	-74		
4 1 17	32	26	6	-26		
4 1 18	87	82	5	82		
4 1 19	31	37	-6	37		
4 1 20	66	70	-4	-70		
4 1 21	39	39	1	39		
4 1 22	3	3	3	3		
4 1 23	12	8	4	-3		
4 1 24	12	14	-2	-14		
4 1 25	46	44	2	44		
4 1 26	3	3	0	3		
4 1 27	38	34	4	-38		
4 1 28	45	47	-2	-47		
4 1 29	15	21	-5	21		
4 1 30	23	23	2	23		
4 1 31	17	14	-3	-14		
4 1 32	39	35	4	35		
4 1 33	37	36	1	-36		
4 1 34	32	25	7	-25		
4 1 35	34	47	-2	40		
4 1 36	38	33	5	38		
4 1 37	24	21	2	-23		
4 1 38	67	63	-1	68		
4 1 39	10	12	-2	-12		
4 1 40	50	49	1	-49		
4 1 41	18	19	-1	-19		
4 1 42	16	13	-3	-18		
4 1 43	63	57	3	-59		
4 1 44	14	12	2	-12		
4 1 45	57	45	12	45		
4 1 46	11	11	0	11		
4 1 47	41	31	7	-31		
4 1 48	6	6	1	6		
4 1 49	13	42	-5	42		
4 1 50	52	49	3	-49		
4 1 51	70	69	1	-69		
4 1 52	45	44	0	44		
4 1 53	51	45	6	44		
4 1 54	33	33	3	-30		
4						

Table III.2.5. Tantalite: Interatomic distances and interbond angles.

<u>Equivalent Position Code</u>			<u>Interatomic Distances</u>			
<u>x</u>	<u>y</u>	<u>z</u>	<u>Distance, Å</u>	<u>Multiplicity</u>		
a	$\frac{1}{2}-x$	$\frac{1}{2}+y$	z	A-O _I (p,h)	2.138 (08)	2
b	$\frac{1}{2}-x$	$\frac{1}{2}-y$	$\frac{1}{2}+z$	A-O _{II} (a,j)	2.188 (11)	2
c	x	$-y$	$\frac{1}{2}+z$	A-O _{II} (b,i)	2.162 (10)	2
d	x	y	$1+z$	Mean A-O	2.163 (10)	
e	$1-x$	$-y$	$1-z$			
f	$1-x$	y	$\frac{1}{2}-z$	B-O _I (c)	2.040 (09)	1
g	$\frac{1}{2}+x$	$\frac{1}{2}-y$	$1-z$	B-O _I (d)	1.964 (09)	1
h	$-x$	y	$\frac{1}{2}-z$	B-O _{II} (b)	1.813 (10)	1
i	$x-\frac{1}{2}$	$\frac{1}{2}-y$	$-z$	B-O _{III} (e)	2.214 (09)	1
j	$x-\frac{1}{2}$	$\frac{1}{2}+y$	$\frac{1}{2}-z$	B-O _{III} (f)	2.048 (09)	1
k	$x-\frac{1}{2}$	$\frac{1}{2}-y$	$1-z$	B-O _{III} (g)	2.021 (09)	1
p	x	y	z	Mean B-O	2.017 (09)	

<u>Interbond Angles</u>			
	<u>Angle</u>		<u>Angle</u>
O _I (h)-A-O _I (p)	103.9 (5)°	O _I (c)-B-O _I (d)	87.3 (3)°
O _I (h)-A-O _{II} (i)	97.0 (3)°	O _I (c)-B-O _{II} (b)	92.0 (4)°
O _I (h)-A-O _{II} (j)	88.2 (3)°	O _I (c)-B-O _{III} (e)	79.7 (3)°
O _I (h)-A-O _{II} (a)	167.9 (4)°	O _I (c)-B-O _{III} (f)	77.0 (4)°
O _I (h)-A-O _{II} (b)	94.8 (4)°	O _I (c)-B-O _{III} (k)	163.4 (3)°
O _{II} (i)-A-O _{II} (j)	82.3 (3)°	O _I (d)-B-O _{II} (b)	99.6 (4)°
O _{II} (i)-A-O _{II} (a)	83.0 (4)°	O _I (d)-B-O _{III} (e)	74.7 (3)°
O _{II} (i)-A-O _{II} (b)	160.9 (6)°	O _I (d)-B-O _{III} (f)	156.5 (4)°
O _{II} (j)-A-O _{II} (a)	79.8 (5)°	O _I (d)-B-O _{III} (k)	97.1 (4)°
		O _{II} (b)-B-O _{III} (e)	170.1 (4)°
		O _{II} (b)-B-O _{III} (f)	98.2 (4)°
		O _{II} (b)-B-O _{III} (k)	102.9 (4)°
		O _{III} (e)-B-O _{III} (f)	85.3 (3)°
		O _{III} (e)-B-O _{III} (k)	86.1 (2)°
		O _{III} (f)-B-O _{III} (k)	93.6 (2)°

and interbond angles were calculated, and these are listed in Table III.2.5.

This structure is discussed later in Chapter III.5.

III.3 Pseudo-ixiolite

III.3.a Previous Work and Sample Description

As pointed out in Chapter III.2 pseudo-ixiolite and tantalite occur in different zones within the pegmatite at Bernic Lake, Manitoba. Pseudo-ixiolite occurs in zone (4) which consists of microcline-perthite, albite, quartz, spodumene and occasionally amblygonite or petalite. Pseudo-ixiolites are usually larger than tantalites, being 1 mm to 10 mm in size, and they are often euhedral and platy.

Specimen G69-55 which was chosen for the structural analysis came from zone (4), and it has the following crystallographic characteristics (Grice, 1970; Grice *et al.*, 1972). From single-crystal work this material appeared to be a true pseudo-ixiolite with no indication of the supercell that characterizes tantalite. The space group was determined as Pbcn, and the cell dimensions (with standard deviations in brackets) refined from powder diffraction data are:

$$a = 4.763(1) \text{ \AA}$$

$$b = 5.750(2) \text{ \AA}$$

$$c = 5.162(2) \text{ \AA}$$

Slightly different cell dimensions derived from the single-crystal diffractometer for the actual material, and given in the next section, were actually used for the structure analysis.

The electron probe analysis is given in Table III.3.1 and, as with the tantalite chosen, the pseudo-ixiolite contains very little Fe, Sn or Ti. In the table, the number of cations is calculated on the basis of eight oxygens in the unit cell. The general formula for pseudo-ixiolite is A_4O_8 where A represents all the cations. The specific gravity measured for this specimen was 6.94(3) gm/cc.

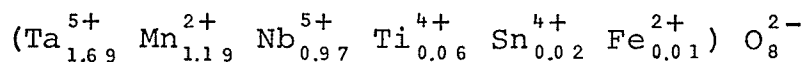
III.3.b Data Collection and Data Reduction

As indicated earlier the pseudo-ixiolite crystal chosen for data collection was Grice's (1970) specimen No. G69-55 from the Tanco Mine, Bernic Lake, Manitoba. This particular specimen was chosen because the chemical composition of this sample was close to that of the tantalites in the same deposit, and because the crystals from this specimen showed none of the tantalite super-cell reflections (Grice, 1970). As with the tantalite, ground spheres yielded unsatisfactory X-ray reflections because of the good cleavage of the mineral which tended to split the crystals. Consequently a polyhedral fragment was again chosen in this case; it had x, y, z dimensions of 0.15 mm, 0.20 mm, and 0.20 mm, respectively. The crystal was

Table III.3.1. Pseudo-ixiolite: Chemical analysis and chemical formula of specimen No. G69-55, data from Grice (1970, p. 45).

<u>Oxide</u>	<u>Weight %</u>	<u>Element</u>	<u>No. of Cations*</u>
MnO	14.4	Mn ²⁺	1.19
FeO	0.1	Fe ²⁺	0.01
SnO ₂	0.6	Sn ⁴⁺	0.02
TiO ₂	0.8	Ti ⁴⁺	0.06
Ta ₂ O ₅	64.0	Ta ⁵⁺	1.69
Nb ₂ O ₅	22.0	Nb ⁵⁺	0.97
	<hr/>		<hr/>
Total	101.9	Total	3.94
	<hr/>		<hr/>

Chemical formula:



* Number of atoms calculated on the basis of 8 oxygens in the unit cell.

mounted perpendicular to the largest cleavage plane which proved to be the (100) plane.

Single-crystal X-ray data were collected on a Picker FACS I fully-automated four-circle diffractometer using Mo radiation with a Zr filter. The data was collected in the Department of Geology, University of Toronto, through the generosity of Dr. V. Kocman. Two or three reflections were manually maximized on each axis and used to calculate an orientation matrix and cell refinement. The cell dimensions derived and used in the final data collection were:

$$a = 4.785 \text{ \AA}$$

$$b = 5.758 \text{ \AA}$$

$$c = 5.160 \text{ \AA}$$

Standard deviations were not calculated for these cell dimensions but they are presumed to be of a comparable accuracy as those for tantalite ($\pm 0.002 \text{ \AA}$). The difference between these cell dimensions, particularly the a values, and those quoted in the previous section from Grice's (1970) powder work are presumably due to the different actual material used.

Initially intensities were collected on the tantalite cell to check for weak reflection corresponding to the tripled a cell dimension. It became evident that all of the reflections characteristic of the larger cell were probably of negligible intensity, and thus the final

collection was made on the small cell with the dimensions given above. All possible reflections in the primitive cell for two octants (hkl and $\bar{h}kl$) out to $2\theta = 50^\circ$ were collected. The space group $Pbcn$ determined by Nickel *et al.* (1963b) was confirmed, and the cards for the space group extinct reflections were withdrawn from the data deck of the computer program.

Program DATAP5 was used to correct the initial intensities for Lorentz and polarization factors. The absorption correction was made by the computer program GON09 assuming the crystal to be a plate bounded by the planes (100) , $(\bar{1}00)$, (010) , $(0\bar{1}0)$, (001) and $(00\bar{1})$. As with tantalite the absorption corrections were severe with $\mu = 390 \text{ cm}^{-1}$. The equivalent relative F 's for the two octants were averaged and weighted on the basis of the size of the F 's and the agreement of the F 's between the two octants. There were 126 reflections, all of which are observed, used in the structure analysis.

III.3.c Structure Refinement

Although the actual structure of pseudo-ixiolite had not been analysed until now, it was believed to be closely related to the tantalite structure as has already been discussed in the Introduction to this chapter. Given the cell dimensions and space group that pseudo-ixiolite have, and assuming that the structure is essentially the same as

that of tantalite, then all the metal atoms must be in one four-fold special site (a) $0, y, \frac{1}{2}$, and all the O's in one eight-fold general site (d) x, y, z . Thus it follows that the metal atoms must be disordered in pseudo-ixiolite. The two atomic sites (a) and (d) are spelled out in Table III.3.2 below.

In the least squares program, GENLES, the scattering curve used for the one metal site was that for Ta° modified by an appropriate occupancy factor which took into consideration the other metals occupying this site. The occupancy factor was based on the chemical analysis given in Table III.3.1, and it was not allowed to vary throughout the refinement. Using only the metal site with half the reflection data and an isotropic temperature factor, the structure refined in three iterations to $R = 0.27$ with $B = 1.81 \text{ \AA}^2$. Using the phases determined from this run, a ΔF synthesis was computed and the position of the oxygen site was determined. In the final least squares refinement using both the metal and oxygen sites, all of the data, and anisotropic temperature factors, the structure refined to $R = 0.135$ and $R_w = 0.085$. The co-ordinates for the final atomic positions are given in Table III.3.2, a projection of the structure along z is given in Figure III.3.1, the anisotropic temperature factors are given in Table III.3.3a, and the conversion of the β_{ij} 's to B_{ij} 's and the magnitudes and orientations of the thermal ellipsoids

Table III.3.2. Pseudo-ixiolite: Space group, cell content, cell dimensions, and positional parameters.

<u>Space Group</u>	Pbcn = P	$2_1/b$	$2/c$	$2_1/n$	(No. 60)			
<u>Cell Content</u>	Z	(Ta _{1.69} ⁵⁺	Mn _{1.19} ²⁺	Nb _{0.97} ⁵⁺	Ti _{0.06} ⁴⁺	Sn _{0.02} ⁴⁺	Fe _{0.01} ²⁺)	O ₈ ²⁻
<u>Cell Dimensions,</u> (All $\pm \sim 0.002$), Å		$a = 4.785$		$b = 5.758$		$c = 5.160$		
<u>Atomic Equivalent Positions</u>		4 Metl in (a): $\pm(0, y, \frac{1}{4}; \frac{1}{2}, \frac{1}{2}+y, \frac{1}{4})$						
		8 O in (d): $\pm(x, y, z; \frac{1}{2}+x, \frac{1}{2}-y, z;$ $x, y, \frac{1}{2}-z; \frac{1}{2}-x, \frac{1}{2}-y, \frac{1}{2}+z)$						

Positional Parameters

Standard deviations are given in brackets

<u>Site</u>	<u>Co-ordinate</u>	<u>Parameter</u>
A	x	0
	y	0.3318 (8)
	z	$\frac{1}{4}$
O	x	0.72244 (88)
	y	0.1216 (58)
	z	0.4161 (83)

Table III.3.3a. Pseudo-ixiolite: Anisotropic temperature factors and isotropic equivalents. (Standard deviations are in brackets)

<u>Atomic Site</u>	<u>β_{11}</u>	<u>β_{22}</u>	<u>β_{33}</u>	<u>β_{12}</u>	<u>β_{13}</u>	<u>β_{23}</u>	Equivalent Isotropic B, (\AA^2)
A	0.0527 (31)	0.0055 (13)	0.0123 (17)	0.0	0.0001 (57)	0.0	2.25
O	0.0438 (18)	0.0049 (95)	0.0377 (174)	0.0018 (253)	0.0388 (375)	-0.0272 (270)	3.02

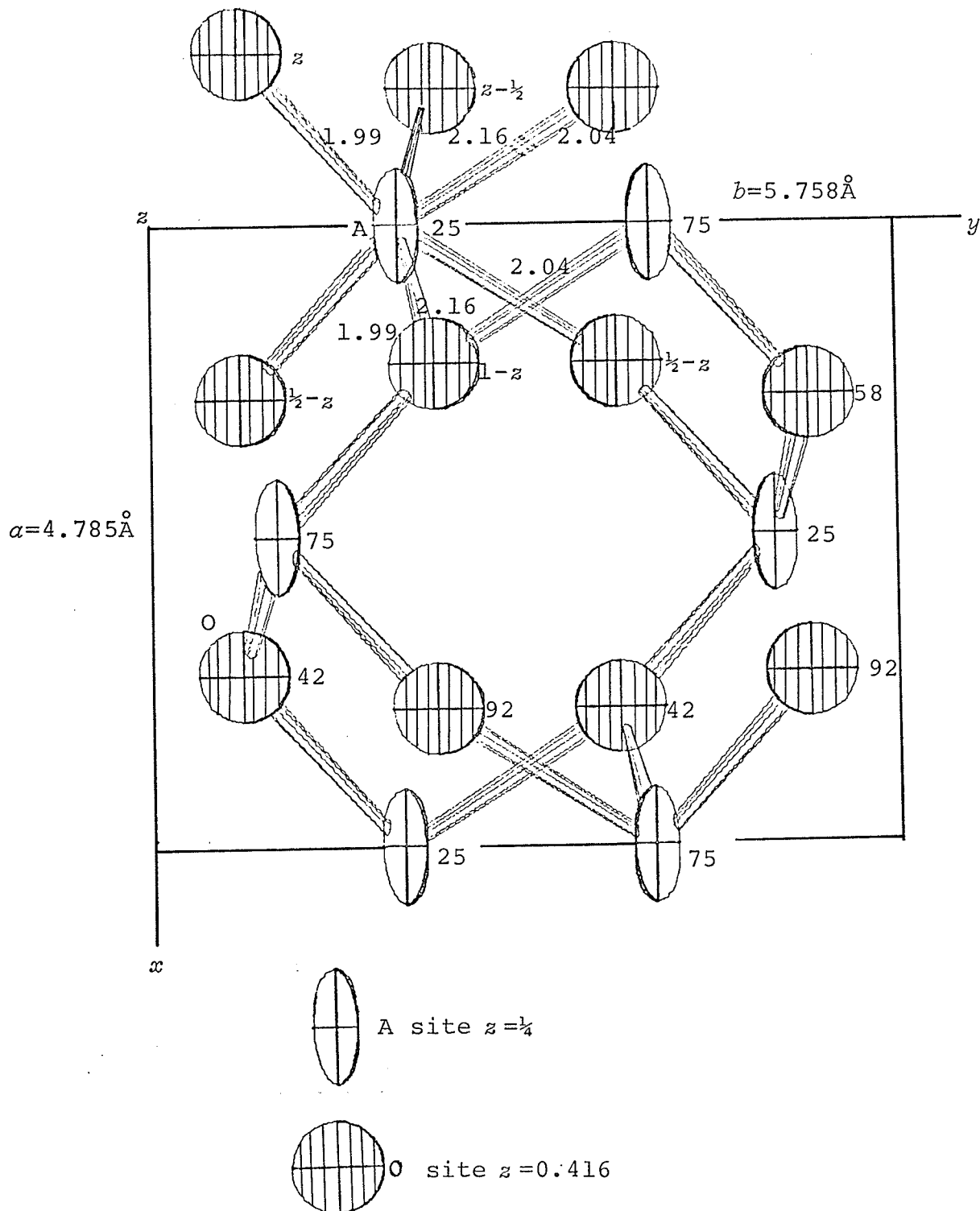


Figure III.3.1. Pseudo-ixiolite: projection of the final structure along z .

are given in Table III.3.3b. The F_o and F_c values for the refined structure are listed in Table III.3.4. From the final atomic parameters, bond lengths and interbond angles were calculated and these are listed in Table III.3.5.

This structure, which is essentially isostructural with that of tantalite, is discussed below in Chapter III.5.

III.4 Wodginite

III.4.a Previous Work and Sample Description

Wodginite from the Tanco Mine can often be distinguished from tantalite or pseudo-ixiolite within the hand specimen. Most commonly the grains are anhedral to subhedral in crystal outline, the subhedral ones showing a prismatic habit, and these grains are reddish-brown in colour. Rarely well-formed black crystals are found. In the Tanco pegmatite the wodginite occurs mainly in coarse-grained K-feldspar + quartz (Zone (6), Assemblage (a)) or in albitic aplite (Zone (6), Assemblage (b)) (see Grice, Černý and Ferguson, 1972).

The specimen chosen for structure analysis, No. G69-17, in Grice (1970) and in Grice *et al.* (1972), came from Zone (6), Assemblage (a). The following crystallographic and chemical description of this specimen is taken from these two references. The wodginite grains were anhedral, compact, and occur in a matrix of K-feldspar which had not

Table III.3.3b. Pseudo-Ixiolite: Magnitudes and orientations of thermal ellipsoids.

<u>Site</u>	<u>Ellipsoid Axes</u>	<u>Root Mean Square Amplitude, (Å)</u>	<u>Equivalent B (Å²)</u>	<u>Angles Between Ellipsoid Axes and Real Axes*</u>		
				A	B	C
A	1	0.247	4.83	0.0°	90.0°	90.0°
	2	0.096	0.73	90.0	0.0	90.0
	3	0.129	1.31	90.0	90.0	0.0
O	1	0.279	6.16	49.6	101.8	42.8
	2	0.048	0.19	102.8	29.3	64.1
	3	0.185	2.71	136.8	116.5	58.7

Standard deviations were not calculated for these measurements.

* A,B,C are the angles between the ellipsoid axes 1,2,3 and the crystallographic lattice axes x,y,z , respectively measured in a clockwise direction from the positive axis.

Table III.3.4. Pseudo-ixiolite: Final F_O and F_C values

H	K	L	F _{OB}	F _{CALC}	DFL-F	A-PT	H	K	L	F _{OB}	F _{CALC}	DFL-F	A-PT
0	0	2	166	125	41	-125	2	3	3	5	1	4	-1
0	0	4	87	92	-4	92	2	3	2	3	4	-1	-4
0	0	6	60	65	-6	-65	2	3	1	4	5	-1	5
0	2	0	91	77	14	-77	2	4	0	23	24	0	-24
0	2	1	133	103	30	103	2	4	1	74	75	-2	-76
0	2	2	74	71	3	71	2	4	2	42	44	-2	44
0	2	3	146	115	30	-116	2	4	3	57	62	-5	62
0	2	4	64	46	17	-46	2	4	4	29	31	-2	-31
0	2	5	74	60	14	60	2	5	3	3	2	1	2
0	4	0	85	80	5	-80	2	5	2	6	3	2	-3
0	4	1	137	98	39	-98	2	5	1	6	2	4	-2
0	4	2	55	39	16	39	2	6	0	58	56	-8	66
0	4	3	85	77	6	79	2	6	1	4	2	2	-2
0	4	4	36	31	5	-31	2	6	2	54	56	-2	-56
0	6	0	71	32	-11	82	3	5	0	32	34	-2	-34
0	6	1	5	12	-7	12	3	5	1	47	47	-1	47
0	6	2	97	81	16	-81	3	5	2	23	26	-2	26
1	6	2	4	1	3	-1	3	4	3	6	2	3	2
1	5	1	10	11	-1	11	3	4	2	7	7	0	-7
1	5	0	43	48	-5	-48	3	4	1	7	1	5	1
1	5	1	74	74	0	74	3	3	0	64	65	0	65
1	5	2	53	45	7	46	3	3	1	4	1	3	-1
1	5	3	65	64	2	-64	3	3	2	59	62	-3	-62
1	5	4	38	36	2	-36	3	3	3	7	5	1	-6
1	4	4	12	3	5	8	3	3	4	49	50	-2	50
1	4	3	9	4	5	-4	3	2	4	3	1	2	1
1	4	2	15	15	-1	15	3	2	3	3	2	1	2
1	4	1	9	3	6	-3	3	2	2	3	1	2	-1
1	3	0	124	127	-3	127	3	2	1	10	13	-3	13
1	3	1	5	5	0	6	3	1	0	30	32	-2	-32
1	3	2	103	110	-6	-110	3	1	1	52	72	-21	-72
1	3	3	4	0	3	0	3	1	2	34	36	-3	36
1	3	4	77	73	-1	78	3	1	3	55	51	4	51
1	3	5	6	2	4	2	3	1	4	29	27	0	-29
1	2	5	4	5	-1	6	3	1	5	39	37	2	-37
1	2	4	4	2	2	-2	3	0	4	8	5	2	6
1	2	3	4	0	4	0	3	0	2	12	11	1	11
1	2	2	5	1	4	1	4	0	0	67	59	9	59
1	2	1	31	33	-2	-33	4	0	2	49	40	9	-40
1	1	0	75	32	-7	-82	4	0	4	35	34	3	34
1	1	1	93	123	-31	-123	4	1	4	4	2	3	-2
1	1	2	53	53	-5	63	4	1	3	3	2	1	2
1	1	3	100	93	2	78	4	1	2	4	4	0	-4
1	1	4	42	43	0	-43	4	1	1	4	3	0	-3
1	1	5	55	64	-8	-64	4	2	0	26	24	2	-24
1	0	6	1	0	1	0	4	2	1	36	36	0	36
1	0	4	12	11	1	-11	4	2	2	23	23	0	23
2	0	2	32	30	2	-30	4	2	3	39	38	2	-38
2	0	0	90	85	4	86	4	3	3	1	1	0	1
2	0	2	120	113	2	-113	4	3	2	3	3	-1	3
2	0	4	74	77	-5	79	4	3	1	4	3	1	-3
2	1	5	6	2	4	-2	4	4	0	26	24	2	-24
2	1	4	6	1	4	1	4	4	1	42	33	8	-33
2	1	3	3	3	0	-3	4	4	2	15	13	2	13
2	1	2	6	5	0	6	5	3	0	34	27	11	27
2	1	1	4	5	-2	5	5	3	1	4	2	2	2
2	2	0	55	51	-3	-53	5	2	2	3	0	3	0
2	2	1	82	103	-21	103	5	2	1	6	3	2	-3
2	2	2	39	44	-5	43	5	1	0	20	17	4	-17
2	2	3	51	53	-7	-53	5	1	1	23	21	7	-21
2	2	4	35	33	-3	-33	5	1	2	15	11	4	11
2	2	5	53	52	1	52	5	0	2	4	2	2	-2
2	3	5	1	2	-2	-2	0	0	0	260	251	0	251
2	3	4	1	0	1	0							

Table III.3.5. Pseudo-ixiolite: Interatomic distances and interbond angles.

<u>Equivalent Position Code</u>			<u>Interatomic Distances</u>			
<u>x</u>	<u>y</u>	<u>z</u>	<u>Distance, Å</u>	<u>Multiplicity</u>		
a	$x-\frac{1}{2}$	$\frac{1}{2}+y$	$\frac{1}{2}-z$	A-O (a,d)	2.04 (4)	2
b	$1+x$	y	$\frac{1}{2}-z$	A-O (b,e)	1.99 (4)	2
c	$x-\frac{1}{2}$	$\frac{1}{2}-y$	$1-z$	A-O (c,f)	2.16 (4)	2
d	$\frac{1}{2}-x$	$\frac{1}{2}-y$	$z-\frac{1}{2}$	Mean A-O	2.06 (4)	
e	$x-1$	y	z			
f	$\frac{1}{2}-x$	$\frac{1}{2}+y$	z			

Interbond Angles

	<u>Angle</u>
O (d)-A-O (e)	95.5 (0.9)°
O (d)-A-O (f)	88.7 (1.4)°
O (d)-A-O (a)	79.6 (1.7)°
O (d)-A-O (b)	93.7 (0.8)°
O (d)-A-O (c)	164.9 (1.9)°
O (e)-A-O (f)	88.3 (1.0)°
O (e)-A-O (a)	166.1 (2.1)°
O (e)-A-O (b)	105.1 (2.1)°
O (e)-A-O (c)	93.7 (0.8)°
O (f)-A-O (a)	78.6 (2.1)°

been sericitized to any extent. The space group of the true cell is C2/c or Cc with a strong sub-cell in space group P2/c or Pc. The cell dimensions (with standard deviations in brackets) from powder diffraction data are:

$$a = 9.436(21) \text{ \AA}$$

$$b = 11.409(20) \text{ \AA}$$

$$c = 5.097(11) \text{ \AA}$$

$$\beta = 91^{\circ}8(5)'$$

The cell dimensions above differ slightly from those derived using the single-crystal diffractometer. The latter cell dimensions are given in the next section and used in the structure analysis. This specimen was used in Elphick's (1972) structure analysis of the wodginite based on the sub-cell. Her structure has the space-group symmetry P2/c.

The chemical analysis given in Table III.4.1 is an average for two analyses given in Grice (1970) for this specimen. The number of cations is calculated on the basis of 32 oxygens per (true) unit cell as suggested by Nickel *et al.* (1963a). The general formula for wodginite is discussed later.

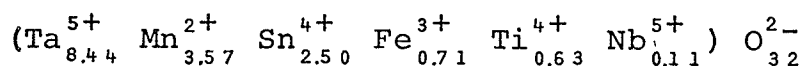
III.4.b Data Collection and Data Reduction

Wodginite crystals suitable for single-crystal X-ray work were found to be difficult to obtain due to the granular nature of the mineral. TANCO specimen G69-17 was

Table III.4.1. Wodginite: Chemical analysis and chemical formula of specimen No. G69-17 from Grice (1970, p. 22).

<u>Oxide</u>	<u>Weight %*</u>	<u>Element</u>	<u>Number of Cations**</u>
MnO	10.0	Mn ²⁺	3.57
Fe ₂ O ₃ [†]	2.2	Fe ³⁺	0.71
SnO ₂	14.9	Sn ⁴⁺	2.50
TiO ₂	2.0	Ti ⁴⁺	0.63
Ta ₂ O ₅	73.9	Ta ⁵⁺	8.44
Nb ₂ O ₅	0.7	Nb ⁵⁺	0.11
<hr/>			
Total	<u>103.6</u>	Total	<u>15.96</u>

Chemical formula:



* Mean of two analyses given in Grice (1970) and in Grice *et al.* (1972).

** Number of atoms calculated on the basis of 32 oxygens in the unit cell.

† Turnock (1966) has shown that the Fe in wodginite is probably Fe³⁺.

chosen as the best sample from which to obtain single crystals because it was compact and because a considerable amount of work had already been done on this specimen (see Grice (1970), Grice *et al.* (1972), and Elphick (1972)). Spheres were ground from this material, and a suitable crystal chosen. Most crystals proved to be multiple, or else they gave a large mosaic spread along one axis, presumably due to this granularity. It proved difficult to get a sphere of suitable diameter. The absorption correction for wodginite is very large necessitating a small sphere, while at the same time the super-cell for this mineral results in a large number of weak reflections (hkl reflections with h and k odd are weak), and in order to get suitable intensities for recording these reflections a large crystal is needed. However, two spherical crystals were eventually chosen for study, and data collections were made on both. The first collection was made by Dr. V. Kocman in the Mineralogical Laboratory, in the Department of Geology, University of Toronto. The crystal was a sphere of 0.45 mm diameter, and with these data the essential features of the structures were determined, but it was not possible to refine the structure below $R = 0.20$. The refinement using data from the first crystal was terminated due to the limitations imposed by the poor intensities. The reasons for the poor data were (i) a mosaic spread of the reflections making them poorly defined, and (ii) a large

absorption correction. The second collection was made on a smaller sphere with a diameter of 0.35 mm. The collection was made in the Department of Chemistry, McMaster University through the courtesy of Dr. C. Calvo and with the aid of Mr. R. Faggiani. The instrument used was a Syntex fully-automated four-circle diffractometer equipped with a graphite single-crystal monochromator. MoK_α radiation with a Zr filter was used for the data collection.

Using the centering routine of the Syntex instrument, 10 reflections were chosen and maximized by a computer-controlled scanning routine. These were then used to refine the monoclinic cell and to establish the orientation matrix. The refined cell dimensions are:

$$\begin{aligned}a &= 9.489(5) \text{ \AA} \\b &= 11.429(7) \text{ \AA} \\c &= 5.105(3) \text{ \AA} \\ \beta &= 91^\circ 6(3)'\end{aligned}$$

One half of the MoK_α sphere of reflections was collected out to $2\theta = 60^\circ$ using $2\theta - \theta$ scans; the octants collected were hkl , $hk\bar{l}$, $\bar{h}kl$ and $\bar{h}\bar{k}\bar{l}$. The computer programs for this instrument are set up to provide for variable scanning rates: each reflection is initially scanned at a fast rate, and on the basis of its intensity, a proportional scan rate is automatically chosen and the reflection is recorded at this speed. The operator has the

option of choosing the minimum and maximum scanning rates. For all octants the maximum rate was chosen as $24^\circ 2\theta$ per minute; the minimum chosen for the first two octants was $2^\circ 2\theta$ per minute, and for the latter two octants it was $4^\circ 2\theta$ per minute.

The intensities of symmetry-related reflections were averaged to give a final intensity value for each of 483 unique reflections. When the agreement between symmetry-related reflections was poor, the measurement with the higher intensity was kept and the weaker one rejected from the averaging. The unique reflections were corrected for Lorentz, polarization (including polarization by the single-crystal monochromator), and absorption (assuming a perfect sphere) factors using the computer program DATAP5.

The agreement of intensities between symmetry-related reflections was very poor for this data collection. It is difficult to account for this, for although the crystal had a very large absorption correction ($\mu = 491 \text{ cm}^{-1}$ for Mo radiation), it was very close to being spherical in shape. This could hardly account for the large intensity variations of up to 2x as were recorded here. Friedel pairs have identical absorption corrections for any crystal shape. Across each axis, Friedel pairs were recorded and compared. There was good agreement along the y -axis but poor agreement along both the x - and z -axes. From the peak profiles, the reflections appeared well centred and

were not "hollow" in the centre from marked absorption. It was not possible to account for this apparently anomolous characteristic of the measured intensities, and the structure analysis was carried out, as noted above, using the higher of the intensities for a given reflection when a marked discrepancy did exist.

III.4.c Structure Refinement

Nickel *et al.* (1963a) proposed that the structure of wodginite should be, from a variety of evidence, closely related to that of tantalite. Grice *et al.* (1972) confirmed the conclusion of Nickel *et al.* about the probable structure and Elphick (1972) derived a structure for wodginite based on the sub-cell. Her structure is discussed below in relation to the tantalite structure and to the author's results for wodginite. For the two possible space groups, for the true cell of wodginite, C2/c and Cc, Nickel *et al.* (1963) pointed out that the 16 cations could be either in two sets of four-fold positions and one eight-fold position if the space group were C2/c, or in four sets of four-fold positions if the space group were Cc. From their chemical analyses, they were unable to group the atoms appropriately to give whole numbers of atoms in one site, and they thus concluded that the cations may be randomly distributed in the 16 available sites in either space group.

Elphick's (1972) analysis of the wodginite structure

was done on the sub-cell with $a \sim 4.7 \text{ \AA}$, $b \sim 5.7 \text{ \AA}$, $c \sim 5.1 \text{ \AA}$ and $\beta \sim 91^\circ$. In the present analysis data were collected on the true cell which has twice the a and b periods of the sub-cell, that is $a \sim 9.5 \text{ \AA}$, $b \sim 11.4 \text{ \AA}$, $c \sim 5.14 \text{ \AA}$ and $\beta \sim 91^\circ$. In Elphick's thesis, the relationship of possible origins in the sub-cell of wodginite to the origin in the cell of the prototype tantalite structure is described. In the present work similar arguments hold for the choice of origin and hence of atomic parameters for the true cell.

In order to arrive at starting parameters for the wodginite structure, two initial decisions had to be made: (i) whether the space group is C2/c or Cc, and (ii) the choice of origin relative to the tantalite structure. The existence of two-fold axes in the true cell of wodginite seems probable from a consideration of the structure of tantalite such as in the projection along z shown in Figure III.4.1 where it can be seen that there are parallel to the y axis, two-fold axes through the A(=Mn) sites and pseudo two-fold axes through the B(=Ta) sites if the general metal site occupancy is taken to be disordered and if one is dealing with the sub-cell of wodginite which has one-third the a dimension of tantalite. Furthermore, Elphick's structure of the sub-cell refined satisfactorily on centrosymmetric space group P2/c, so that all the evidence pointed to centrosymmetric C2/c as being the space group for the true cell of wodginite.

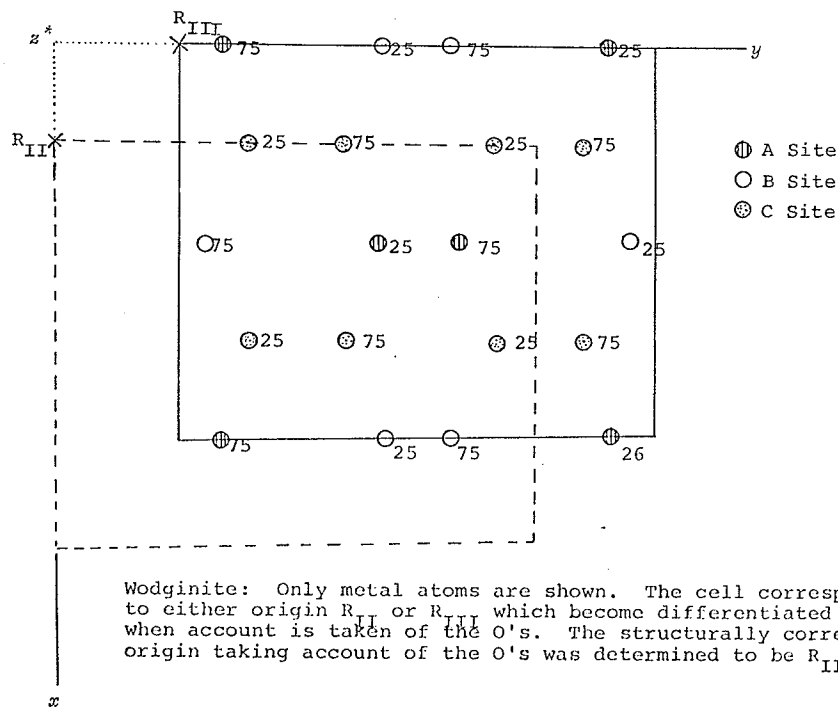
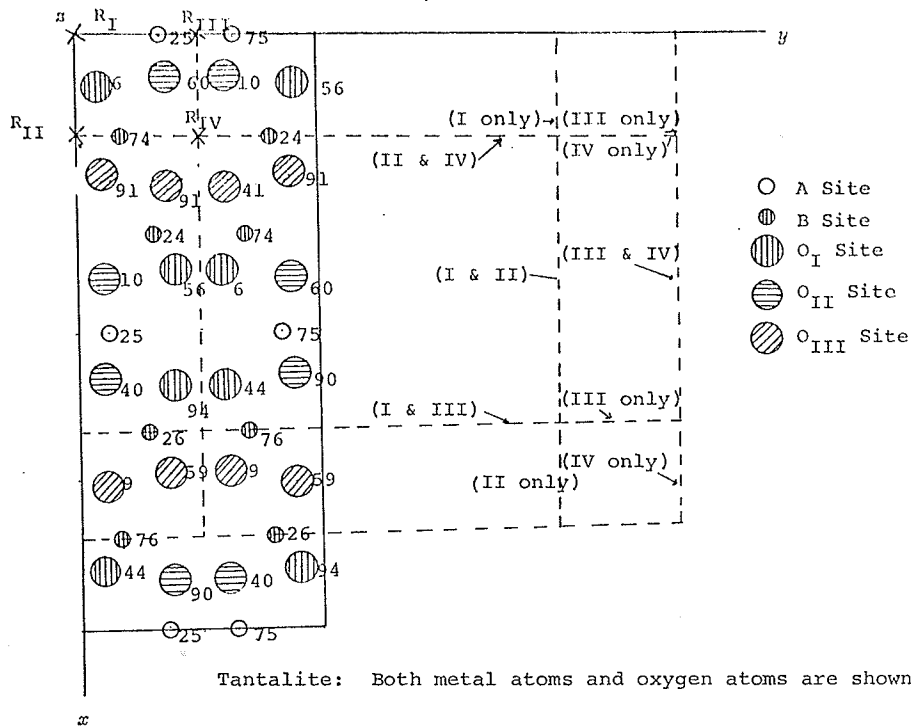


Figure III.4.1. Choice of origin for wodginite structure.

Regarding possible origins within the tantalite structure for wodginite, Figure III.4.1 shows in comparable orientation the tantalite cell with space group $Pbcn$, and the true wodginite cell with space group $C2/c$. All of the atoms are shown for the former, but only the metal atoms for the latter. On the tantalite cell are marked the four possible choices of origin for the wodginite cell, R_I , R_{II} , R_{III} , and R_{IV} . The origins R_I and R_{III} lie on centres of symmetry and origins R_{II} and R_{IV} lie on pseudo-centres of symmetry in the space group $Pbcn$. Origins R_I and R_{II} correspond to Elphick's A and B origins, respectively. The fact that Elphick does not have origins corresponding to R_{III} and R_{IV} only becomes significant in relation to the oxygen positions. Considering only disordered metal sites again, it can be seen that R_I is equivalent to R_{IV} , and R_{II} is equivalent to R_{III} . Elphick found origin R_{II} the correct choice for the metal co-ordinates, but when account is taken of her oxygen positions, her structure becomes equivalent to origin R_{III} described here even though she did not express it in these terms.

Tantalite has the general cell content $A_4B_8O_{24}$, and in Chapter III.2 it was shown that A and B represent essentially Mn, Fe, Nb and Ta, Nb, Mn, respectively. In wodginite the sub-cell has, as indicated above, two two-fold metal sites, and the true cell has two four-fold and one eight-fold metal sites; thus the general formula

for the true cell of wodginite is $A_4B_4C_8O_{32}$. Later it will be seen that A, B and C each have a different metal occupancy. For the wodginite sub-cell, sites A and B are equivalent and the general formula is thus $(A,B)_2C_2O_8$. Elphick (1972) found for the sub-cell that site C contains essentially Ta, and site (A,B) all other cations.

With a set of parameters for the metal atoms only, in order not to bias the O positions, based on origins R_{II} and R_{III} as Elphick's work indicated (Figure III.4.1) the structure analysis of wodginite was started using the least squares refinement program GENLES and the first (poorer) set of 483 intensities before the second set of better intensities was available. In Table III.4.2 the equivalent positions for the possible atomic sites in wodginite are given as taken from the International Tables for X-ray Crystallography, Volume I for space group C2/c (No. 15). In correlation with Elphick's results, the scattering factor for metal site C in a general eight-fold position with co-ordinates 0.25, 0.16, 0.25 and equivalent to Elphick's site M1 was taken as that for pure Ta. The two metal sites A and B in special four-fold positions are equivalent to Elphick's one metal site M2. Site A was given the parameters 0, 0.40, $\frac{1}{4}$ with the scattering curve of Ta but with a fixed occupancy of 0.5 which gave an effective scattering power between Mn and Sn, the two other most abundant constituents of wodginite from this deposit.

For site B parameters $\frac{1}{2}$, 0.1, $\frac{3}{4}$ were used initially with the same scattering curve and occupancy as site A. Using the three metal sites (but no oxygen sites), 475 reflections and isotropic temperature factors, the structure refined to $R = 0.23$ after four cycles of least squares. Site A ended with a temperature factor that was very large compared with that of site B (2.4 \AA^2 as compared with 0.8 \AA^2). This difference in temperature factor for two atomic positions with the same scattering power seemed to indicate that the positions were not equivalent with respect to effective scattering power. A ΔF synthesis based on this least squares output was computed, and it also indicated that A needed fewer electrons and B needed more electrons than those assumed. The ΔF map also gave a rough indication of the oxygen positions in four sets of eight fold positions. As pointed out previously, the differentiation in origins R_{II} and R_{III} comes when the oxygens are considered. From the ΔF map, origin R_{III} appeared to be the correct choice and furthermore it gave oxygen parameters comparable to Elphick's which is further proof of its correctness. Because origin R_{III} was not realized by Elphick, she falsely concluded that wodginite and tantalite are not completely isostructural due to differences in the oxygen positions.

For the second least squares "run" on the first data set, all 483 intensities were used with positions assumed for all of the atoms. The scattering curves used

were Mn^{2+} and Fe^{3+} for site A, Sn^{4+} and Ti^{4+} for site B, and Ta° and Nb^{5+} for site C with occupancies proportional to the chemical analysis given in Table III.4.1. The isotropic temperature factors were replaced by anisotropic temperature factors for all atoms, and the R factor dropped to 0.20. As mentioned in the previous section under Data Collection and Data Reduction, the refinement of the structure ended at this point for this set of data because it seemed impossible to refine any further on this data set.

At this point arrangements were made for the second more accurate data collection through the kindness of Dr. C. Calvo, Department of Chemistry, McMaster University, from which the intensities for 814 reflections were derived. Using 589 of these intensities, positions for all atoms, isotropic temperature factors, and variable occupancies for the cation sites, the structure refined to $R = 0.14$. As with the tantalite and pseudo-ixiolite structure refinements, the oxygen atoms were found difficult to refine because they are so much 'lighter' than the cations. Here two of the four oxygens had temperature factors of 0.0 \AA^2 and the other two oxygens had temperature factors of 0.9 \AA^2 with standard deviations of the same magnitude. In a subsequent least squares run with anisotropic temperature factors, oxygens O_{III} and O_{IV} still had temperature factors of 0.0 \AA^2 . When O_{II} was permitted to

refine anisotropically, it refined to impossible anisotropic parameters, according to the test "for non-positive definite" described in Appendix G. In the final refinement all 814 reflections were used, occupancies for the cations were refined, anisotropic temperature factors were refined for the cations and for O_I and O_{II} , and a fixed isotropic temperature factor of 1.5 \AA^2 was used for O_{III} and O_{IV} . The isotropic equivalent for O_{II} is given in Table III.4.4a because it refined to non-positive definite values. The final agreement factor was $R = 0.124$ and $R_w = 0.106$ where the weighting scheme is based on counting statistics.

A projection along z^* of the final structure is shown in Figure III.4.2, and the final results are given in Tables III.4.2 to III.4.6: the positional parameters in Table III.4.2; the effective scattering powers for each of the three cation sites A, B, and C in relation to the chemical analysis, which is discussed later, in Table III.4.3; the temperature factors in Tables III.4.4a and 4b; the final F_o and F_c values in Table III.4.5; and the bond lengths and interbond angles in Table III.4.6.

III.5 Electrostatic Charge Distributions in Tantalite, Pseudo-ixiolite and Wodginite

III.5.a Introduction

In all three of these structures the cation

Table III.4.2. Wodginite, true cell: Space group, cell content, cell dimensions, and positional parameters.

<u>Space Group</u>	C2/c (No. 15)
<u>Cell Content</u>	(Ta _{8.44} ⁵⁺ Mn _{3.57} ²⁺ Sn _{2.50} ⁴⁺ Fe _{0.71} ³⁺ Ti _{0.63} ⁴⁺ Nb _{0.11} ⁵⁺) O ₃₂ ²⁻
<u>Cell Dimensions and Standard Deviations (in brackets), Å</u>	$a = 9.489(5)$ $b = 11.429(7)$ $c = 5.105(3)$ $\beta = 91^\circ 6'(3)$
<u>Atomic Equivalent Positions</u>	4 A, B in (e): (0,0,0; $\frac{1}{2}, \frac{1}{2}, 0$) + (0, $y, \frac{1}{4}$; 0, $\bar{y}, 3/4$) 8 C, O _I , O _{II} , O _{III} , O _{IV} in (f): (0,0,0; $\frac{1}{2}, \frac{1}{2}, 0$) + (x, y, z ; $\bar{x}, \bar{y}, \bar{z}$; $\bar{x}, y, \frac{1}{2}-z$; $x, \bar{y}, \frac{1}{2}+z$)

Positional Parameters

<u>Site</u>	<u>Co-ordinates</u>	<u>Positional Parameters</u>	
		<u>Elphick (1972)*</u>	<u>This Work</u>
A	x	M_2	0
	y		0.4151(6)
	z		$\frac{1}{4}$
B	x		$\frac{1}{2}$
	y		0.0917(3)
	z		3/4
C	x	M_1	$\frac{1}{4}$
	y		0.1625(3)
	z		$\frac{1}{4}$
O _I	x	O ₁	0.141(6)
	y		0.312(05)
	z		0.104(11)
O _{II}	x	O ₂	0.123(4)
	y		0.057(6)
	z		0.078(5)
O _{III}	x		0.1424(36)
	y		0.1960(29)
	z		0.5689(65)
O _{IV}	x		0.1200(39)
	y		0.4388(30)
	z		0.5895(70)

*In order to compare Elphick's sub-cell with the author's, her x and y parameters have been divided by 2.

Table III.4.3. Wodginite: The electrons in each metal site by chemical analysis and by structure analysis

<u>Metal Site</u>	<u>Cation</u>	From Chemical Analysis (Table III.4.1)		From Scattering Factors of the Refined Structure Analysis		
		<u>No. of Cations*</u>	<u>e⁻/atom</u>	<u>e⁻/site</u>	<u>e⁻/site</u>	
A	Mn ²⁺	3.58	4.00	20.6	27 (1)	
	Fe ³⁺	0.42				
	Fe ³⁺	0.29	1.7			
B	Sn ⁴⁺	2.51	28.9	42	45 (2)	
	Ti ⁴⁺	0.63	2.8			
	Nb ⁵⁺	0.11	1.0			
	Ta ⁵⁺	0.46	7.8			
C	Ta ⁵⁺	8.00	8.00	68.0	68	73 (1)

General Formula: $A_4 B_4 C_8 O_{32}$

Proposed Formula: $(Mn_{3.58}^{2+} Fe_{0.42}^{3+}) (Sn_{2.51}^{4+} Ti_{0.63}^{4+} Ta_{0.46}^{5+} Fe_{0.29}^{3+} Nb_{0.11}^{5+}) Ta_{8.00}^{5+} O_{32}^{2-}$

* Number of cations have been recalculated to total to 16.00

Table III.4.4a. Wodginite: Anisotropic temperature factors and isotropic equivalents.
(Standard deviations are given in brackets.)

Atomic Site	β_{11}	β_{22}	β_{33}	β_{12}	β_{13}	β_{23}	Equivalent Isotropic $B, \text{\AA}^2$
A	0.0000 (7)	0.0000 (5)	0.0068 (26)	0.0	0.0000 (17)	0.0	0.24
B	0.0010 (4)	0.0010 (2)	0.0035 (13)	0.0	0.0032 (9)	0.0	0.41
C	0.0012 (1)	0.0010 (1)	0.0064 (5)	0.0001 (2)	0.0028 (3)	0.0016 (4)	0.40
O _I	0.0027 (31)	0.0053 (29)	0.0191 (121)	-0.0065 (50)	0.0031 (100)	0.0175 (98)	2.32
O _{II} *	0.0105 (31)	0.0072 (92)	0.0363 (138)	0.0	0.0007	0.0	3.78
O _{III} **	0.0042	0.0029	0.0144	0.0	0.0003	0.0	1.50
O _{IV} **	0.0042	0.0029	0.0144	0.0	0.0003	0.0	1.50

* Equivalent isotropic temperature factor from refinement.

** Fixed isotropic temperature factor.

β_{ij} for O_{II}, O_{III} and O_{IV} are calculated from the isotropic temperature factor.

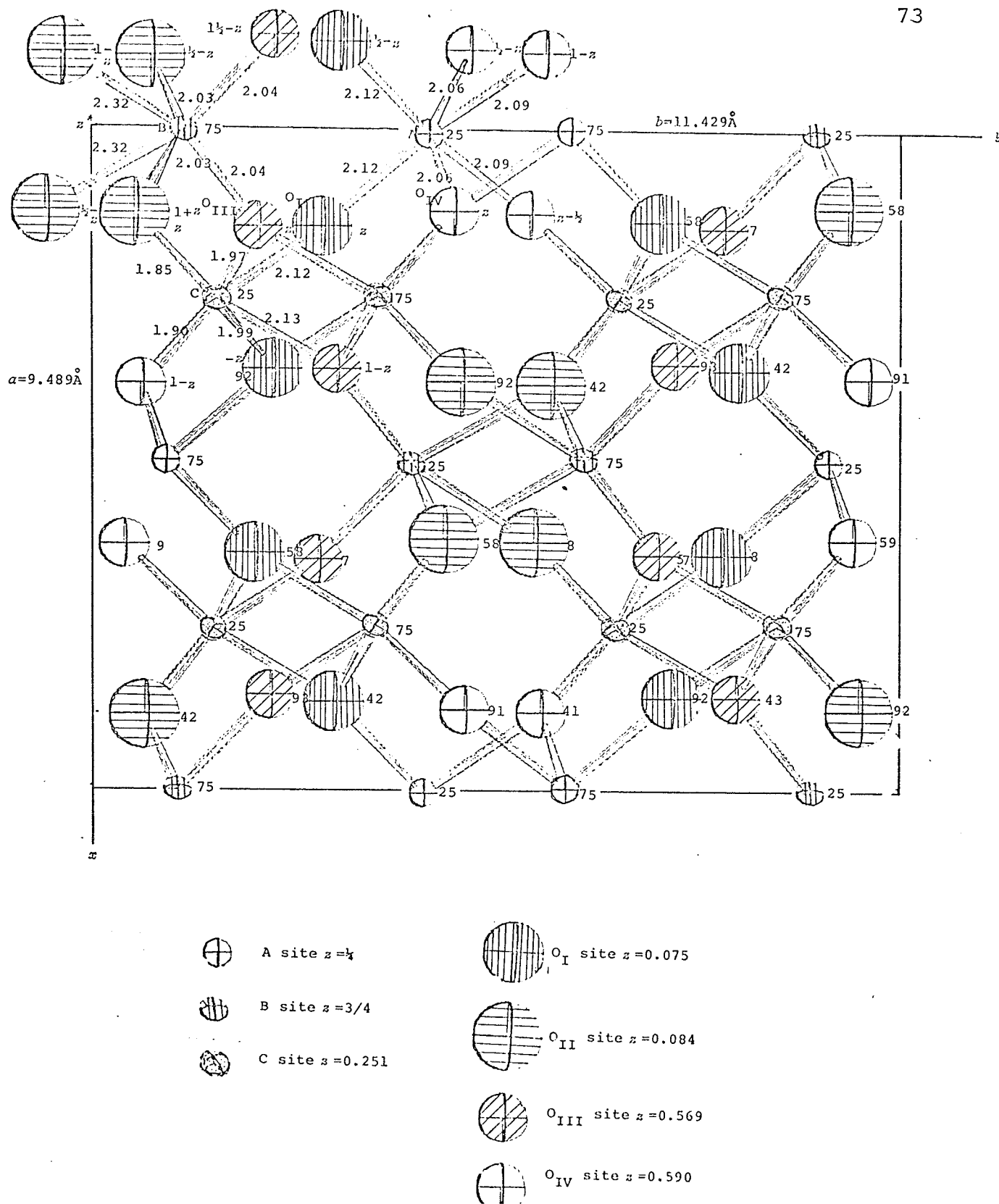


Figure III.4.2. Wodginite: projection of the final structure along z^* . Heights are shown above the plane of projection in hundredths of the c period.

Table III.4.4b. Wodginite: Magnitudes and orientations of thermal ellipsoids.

<u>Atomic Site</u>	<u>Ellipsoid Axes</u>	<u>Root Mean Square Amplitude, (Å)</u>	<u>Equivalent B (Å²)</u>	<u>Angles Between Ellipsoid Axes and Real Axes*</u>		
				A	B	C
A	1	0.000	0.00	1.1°	90.0°	90.0°
	2	0.000	0.00	90.0	0.0	90.0
	3	0.095	0.71	91.1	90.0	0.0
B	1	0.028	0.06	44.4	90.0	135.5
	2	0.079	0.50	90.0	0.0	90.0
	3	0.092	0.66	45.6	90.0	45.5
C	1	0.052	0.22	42.1	70.3	126.3
	2	0.076	0.45	120.1	31.5	97.9
	3	0.107	0.91	63.7	66.5	37.5
O _I	1	0.143	1.61	42.8	102.3	50.9
	2	0.245	4.73	105.4	38.3	55.6
	3	0.088	0.61	128.7	125.6	57.9

Standard deviations were not calculated for these measurements.

* A,B,C are the angles between the ellipsoid axes 1,2,3 and the crystallographic axes x,y,z , respectively.

Table III.4.5. (Continued)

H	K	L	FOB	FCALC	DEL-F	A-PT
6 2 1	533	526	7	575		
6 2 -1	519	517	-1	-532		
6 2 2	267	255	12	-255		
6 2 -2	319	236	34	-289		
6 2 3	411	238	9	438		
6 2 4	211	190	29	190		
6 2 -4	224	222	5	223		
6 2 5	348	302	47	302		
6 2 -5	372	367	6	-367		
6 2 6	165	134	32	-134		
6 2 -6	141	146	-5	-146		
6 4 0	113	125	-11	129		
6 4 1	98	94	4	-94		
6 4 -1	242	226	16	226		
6 4 2	98	98	0	-98		
6 4 -2	124	112	12	-112		
6 4 3	112	119	-7	119		
6 4 -3	129	133	-4	-133		
6 4 4	92	84	8	84		
6 4 -4	94	91	4	94		
6 4 5	153	121	29	-121		
6 4 -5	78	94	-16	94		
6 4 6	73	61	12	-61		
6 4 -6	77	72	5	-72		
6 4 7	518	550	17	-507		
6 4 -7	42	51	-9	-51		
6 4 8	39	36	3	36		
6 4 -8	430	454	-26	456		
6 6 -7	511	493	17	493		
6 6 7	51	49	1	49		
6 6 8	79	78	1	-79		
6 6 -8	374	363	11	-363		
6 6 9	4	4	0	-408		
6 6 -9	33	32	1	-32		
6 6 5	26	31	-7	31		
6 8 0	26	42	-17	42		
6 8 1	187	171	-4	-171		
6 8 -1	183	165	-12	-165		
6 8 2	42	36	6	-73		
6 8 -2	47	25	21	-25		
6 8 3	133	145	-12	-145		
6 8 -3	158	158	-10	169		
6 8 4	14	15	-1	15		
6 8 -4	55	71	-6	71		
6 8 5	49	50	-4	98		
6 8 -5	122	120	2	-120		
6 10 0	243	272	21	272		
6 10 -1	311	297	14	-297		
6 10 2	323	327	21	307		
6 10 -2	222	274	5	-224		
6 10 3	242	249	-7	-249		
6 10 -3	23	247	-13	247		
6 10 4	235	274	23	-274		
6 10 -4	176	193	-17	193		
6 10 5	210	208	-7	208		
6 12 0	145	156	-11	-156		
6 12 -1	93	96	3	-66		
6 12 2	32	32	1	32		
6 12 -2	130	126	-23	126		

H	K	L	FOB	FCALC	DEL-F	A-PT
6 12 3	145	145	-5	145		
6 12 -3	48	47	1	47		
6 14 0	88	77	11	77		
6 14 -1	236	274	12	-274		
6 14 1	303	275	28	-275		
7 1 0	25	35	-10	35		
7 1 1	62	31	50	-31		
7 1 -1	82	31	50	-31		
7 1 2	30	29	1	-29		
7 1 -2	34	38	0	-38		
7 1 3	36	19	16	-19		
7 1 -3	79	45	35	45		
7 1 4	45	28	17	28		
7 1 -4	42	36	-24	36		
7 1 5	31	14	14	14		
7 1 -5	60	40	20	-40		
7 1 6	40	21	13	-21		
7 1 -6	14	32	-18	32		
7 3 0	69	30	39	-30		
7 3 1	31	49	-17	49		
7 3 -1	10	47	-37	47		
7 3 2	95	29	35	29		
7 3 -2	71	15	57	-15		
7 3 3	37	39	-7	-39		
7 3 -3	9	45	-35	45		
7 3 4	42	29	33	-29		
7 3 -4	75	52	-18	52		
7 3 5	16	32	-22	32		
7 3 -5	41	-25	-41	-25		
7 3 6	39	11	28	11		
7 3 -6	40	69	-20	-60		
7 5 0	63	25	38	-25		
7 5 1	30	11	19	11		
7 5 -1	45	4	9	4		
7 5 2	2	65	-11	69		
7 5 -2	48	17	31	17		
7 5 3	39	21	18	-21		
7 5 4	32	38	-6	-38		
7 5 5	76	63	12	-63		
7 5 6	39	11	28	11		
7 5 -6	39	15	24	-15		
7 7 0	10	2	8	-2		
7 7 1	67	71	-4	-71		
7 7 -1	77	67	10	67		
7 7 2	4	12	-8	12		
7 7 -2	11	6	5	6		
7 7 3	69	66	3	66		
7 7 -3	55	59	-3	-58		
7 7 4	14	8	6	-8		
7 7 -4	23	7	16	-7		
7 7 5	56	52	3	-53		
7 7 -5	30	36	-6	36		
7 9 0	61	73	-12	73		
7 9 -1	22	27	-5	-27		
7 9 2	39	35	6	35		
7 9 -2	46	50	-4	-50		
7 9 3	81	80	0	-80		
7 9 -3	19	11	8	11		
7 9 4	23	48	-19	48		

H	K	L	FOB	FCALC	DEL-F	A-PT
7 9 4	50	45	6	45		
7 9 -4	40	54	-14	54		
7 11 0	71	65	6	65		
7 11 -1	28	49	-21	49		
7 11 2	54	61	-8	-61		
7 11 -2	39	49	-10	-49		
7 11 3	29	42	-13	-42		
7 11 -3	26	45	-19	45		
7 13 0	13	22	-9	22		
7 13 -1	59	71	-13	71		
7 13 -2	15	11	5	11		
8 0 0	556	581	-25	581		
8 0 2	422	435	-13	-435		
8 0 -2	483	464	19	-464		
8 0 4	360	333	27	333		
8 0 -4	416	416	0	416		
8 2 0	62	74	-12	-74		
8 2 -1	129	138	-9	-138		
8 2 2	85	85	0	85		
8 2 -2	56	57	0	57		
8 2 3	121	120	2	120		
8 2 -3	136	141	-3	-141		
8 2 4	46	48	-2	-48		
8 2 -4	95	91	4	-91		
8 2 5	118	99	19	-99		
8 2 -5	98	114	-15	114		
8 4 0	273	269	3	-269		
8 4 -1	348	351	-3	351		
8 4 2	409	428	21	-428		
8 4 -2	231	235	-4	235		
8 4 3	291	267	24	267		
8 4 -3	366	357	9	-357		
8 4 4	423	397	25	397		
8 4 -4	206	195	11	-195		
8 4 5	225	223	2	-223		
8 4 -5	276	280	-4	280		
8 6 0	159	163	-4	163		
8 6 1	54	47	7	47		
8 6 -1	28	11	17	-11		
8 6 2	149	157	-8	-157		
8 6 -2	154	159	-4	-159		
8 6 3	29	23	6	-23		
8 6 -3	33	27	6	27		
8 6 4	121	107	14	107		
8 6 -4	147	148	-1	-148		
8 6 5	14	18	-5	18		
8 6 -5	33	38	-5	-38		
8 8 0	207	178	29	-178		
8 8 1	370	369	1	-369		
8 8 -1	397	369	28	369		
8 8 2	115	128	-13	128		
8 8 -2	132	125	7	125		
8 8 3	276	298	-22	298		
8 8 -3	337	351	-14	-351		
8 8 4	87	84	3	-84		
8 8 -4	123	120	3	-120		

H	K	L	FOB	FCALC	DEL-F	A-PT
8 13 0	113	117	4	-107		
8 13 -1	75	68	-7	93		
8 13 2	102	107	-4	-107		
8 13 -2	54	94	-11	94		
8 13 3	126	125	1	125		
8 13 -3	69	79	-15	79		
8 12 0	192	269	2	269		
8 12 -1	97	76	12	76		
8 12 2	74	74	0	-74		
8 12 -2	237	274	-37	-274		
9 1 0	40	35	5	35		
9 1 -1	86	72	14	72		
9 1 2	97	96	32	-95		
9 1 -2	6	24	-14	-24		
9 1 3	62	29	35	-29		
9 1 -3	46	27	19	27		
9 1 4	4	18	-7	18		
9 1 -4	44	37	7	37		
9 1 5	41	16	24	16		
9 1 -5	30	14	25	-14		
9 3 0	52	24	27	-24		
9 3 1	12	37	-22	37		
9 3 -1	14	36	-21	-39		
9 3 2	68	29	36	29		
9 3 -2	76	33	42	33		
9 3 3	7	27	-27	27		
9 3 -3	26	57	-24	57		
9 3 4	65	16	31	-16		
9 3 -4	72	34	33	-34		
9 3 5	19	16	3	16		
9 3 -5	65	37	28	-37		
9 3 6	45	56	-11	-56		
9 3 -6	31	11	21	11		
9 5 -1	47	12	20	12		
9 5 2	44	46	-1	46		
9 5 -2	34	42	-8	42		
9 5 3	37	21	16	21		
9 5 -3	69	14	53	-14		
9 5 4	63	66	-14	-66		
9 5 -4	24	47	-24	-47		
9 7 0	29	3	22	3		
9 7 1	57	54	3	-54		
9 7 -1	80	68	11	68		
9 7 2	21	9	11	9		
9 7 -2	3	44	5	44		
9 7 3	69	65	3	-65		
9 7 4	16	5	12	5		
9 7 -4	3	5	-9	5		
9 9 0	60	98	-9	98		
9 9 -1	33	33	0	-33		
9 9 2	21	30	-9	30		
9 9 -2	45	57	-11	-57		
9 9 3	36	44	-8	-44		
9 9 -3	37	34	4	34		
9 9 4	21	27	-6	-27		
9 9 -4	49	51	-1	51		

Table III.4.6. Wodginite: Interatomic distances and interbond angles.

<u>Equivalent Position Code</u>				<u>Interatomic Distances</u>		
				<u>Distance, Å</u>	<u>Multiplicity</u>	
a	x	1-y	z-½	A-O _I (p,f)	2.12 (4)	2
b	x	-y	½+z	A-O _{IV} (p,f)	2.06 (4)	2
c	x	y	1+z	A-O _{IV} (a,g)	2.09 (4)	2
d	½-x	½-y	-z	Mean A-O	2.09 (4)	
e	½-x	½-y	1-z			
f	-x	y	½-z	B-O _{II} (b,h)	2.32 (6)	2
g	-x	1-y	1-z	B-O _{II} (c,f)	2.03 (4)	2
h	-x	-y	1-z	B-O _{III} (p,i)	2.04 (3)	2
i	-x	y	1½-z	Mean B-O	2.13 (4)	
p	x	y	z			
				C-O _I (p)	2.12 (4)	1
				C-O _I (d)	1.99 (3)	1
				C-O _{II} (p)	1.85 (5)	1
				C-O _{III} (p)	1.97 (3)	1
				C-O _{III} (e)	2.13 (3)	1
				C-O _{IV} (e)	1.90 (4)	1
				Mean C-O	1.99 (4)	

Interbond Angles

	<u>Angle</u>
O _I (f)-A-O _I (p)	97.6 (1.9) °
O _I (f)-A-O _{IV} (f)	93.6 (1.4) °
O _I (f)-A-O _{IV} (g)	88.5 (1.4) °
O _I (f)-A-O _{IV} (p)	91.4 (1.4) °
O _I (f)-A-O _{IV} (a)	173.9 (1.4) °
O _{IV} (f)-A-O _{IV} (g)	89.1 (1.3) °
O _{IV} (f)-A-O _{IV} (p)	172.5 (1.9) °
O _{IV} (f)-A-O _{IV} (a)	85.3 (1.5) °
O _{IV} (g)-A-O _{IV} (a)	85.4 (1.9) °

Table III.4.6. (Continued)

	<u>Angle</u>		<u>Angle</u>
O _{II} (h)-B-O _{II} (f)	87.1(1.7)°	O _I (p)-C-O _I (d)	117.9(0.9)°
O _{II} (h)-B-O _{II} (b)	74.8(2.5)°	O _I (p)-C-O _{II} (p)	85.1(2.0)°
O _{II} (h)-B-O _{II} (c)	81.6(1.9)°	O _I (p)-C-O _{III} (p)	86.5(1.4)°
O _{II} (h)-B-O _{III} (i)	88.4(1.6)°	O _I (p)-C-O _{III} (e)	58.8(1.3)°
O _{II} (h)-B-O _{III} (p)	163.1(1.6)°	O _I (p)-C-O _{IV} (e)	127.6(1.4)°
O _{II} (f)-B-O _{II} (c)	165.8(3.7)°	O _I (d)-C-O _{II} (p)	147.3(1.9)°
O _{II} (f)-B-O _{III} (i)	95.5(1.7)°	O _I (d)-C-O _{III} (p)	63.7(1.4)°
O _{II} (f)-B-O _{III} (p)	92.8(1.7)°	O _I (d)-C-O _{III} (e)	88.3(1.4)°
O _{III} (i)-B-O _{III} (p)	108.4(1.9)°	O _I (d)-C-O _{IV} (e)	97.6(1.5)°
		O _{II} (p)-C-O _{III} (p)	97.6(1.6)°
		O _{II} (p)-C-O _{III} (e)	124.4(1.8)°
		O _{II} (p)-C-O _{IV} (e)	83.5(1.9)°
		O _{III} (p)-C-O _{III} (e)	118.5(0.9)°
		O _{III} (p)-C-O _{IV} (e)	145.7(1.4)°
		O _{III} (e)-C-O _{IV} (e)	87.3(1.4)°

sites are surrounded by 6 oxygens in varying degrees of distortion from an octahedral configuration. Although there are differences between the structures which are described in Chapter III.6, it is possible to treat the three structures similarly as far as the calculation of charge distribution is concerned. The electrostatic charge distributions calculated in this chapter are used in the following chapter in conjunction with the available chemical data to interpret the structure data obtained in this study.

III.5.b Theory of the Method

The theory governing accurate electrostatic charge distribution calculations in oxide and silicate structures is discussed by Gait (1967) and by Gait, Ferguson and Coish (1970) who have applied it to some feldspar structures. The following description of the method is a brief résumé taken from these two references.

The basic hypothesis for electrostatic charge distributions is given in Pauling's second rule governing ionic structures which is stated in Evans (1966) as follows:

"In a stable co-ordinated structure the total strength of the valency bonds which reach an anion from all the neighbouring cations is equal to the charge of the anion."

A simple example would be NaCl in which case Na^+ is

co-ordinated octahedrally by Cl^- and each anion would then receive $+1/6$ e.s.u. from each of six surrounding cations for a total $+1$ e.s.u. Gait (1967) and Gait *et al.* (1970) found that in order to derive accurate charge distributions, it is necessary to distribute the positive charges to the anions in amounts that are inversely proportional to the square of the cation-anion distance. They show that for such a charge calculation the following two equations are necessary:

$$W = \sum_{i=1}^n \left[\frac{1}{\text{CO}^2} \right]$$

where: W is the 'weighting factor' for a particular cation,
 CO is the cation-oxygen bond distance (\AA), and
 n is the number of anions surrounding the cation;
 and

$$C_c = \frac{P_c}{(\text{CO})^2 \times W}$$

where: C_c is the positive charge (e.s.u.) contributed to a particular oxygen atom from a given cation,
 P_c is the positive charge (e.s.u.) on the cation,
 CO as above, and
 W as above.

These authors have also pointed out that the significant positive charge summation is not that to a single oxygen which might be expected to ideally be exactly $+2$, but

rather than to a polyhedral group of oxygens, say a (pseudo-) octahedral group of six oxygens which would ideally be exactly +12. The reason for this is that the substitution of differently charged cations in one cation site would affect the charge given to the oxygens in groups of six (for octahedral co-ordination) rather than individually.

In cases where there is only one cation site the charge distribution must calculate to an ideal answer, provided the composition is chemically balanced, whether all cation-anion distances are the same (e.g. NaCl) or not (e.g. pseudo-ixiolite). This argument is explained further under the discussion below of the electrostatic charge distribution in pseudo-ixiolite. For all such single-cation structures, the calculation of a charge distribution is thus pointless.

The calculation of charge distribution is carried out as follows: (i) the proportioned charge C_c to each oxygen in a polyhedron is calculated for each cationic site; (ii) C_c is totalled for each unique oxygen from all its associated cations; and (iii) the total positive charge contributed to each cationic group of oxygens is obtained by summing the charges contributed to each oxygen in the polyhedron concerned as determined in (ii).

With each number given in the tables following is the associated standard deviation calculated on the basis

of the errors in the cation-oxygen bond distances. To calculate the standard deviation of one number that is a function of two or more other numbers the following relationships are used (see Gait, Ferguson and Coish, after Baird, 1962):

$$\begin{aligned} \text{For : } \bar{z} &= \bar{x} + \bar{y} & \sigma_{\bar{z}}^2 &= \sigma_{\bar{x}}^2 + \sigma_{\bar{y}}^2 \\ \bar{z} &= \bar{x}^a \bar{y}^b & \sigma_{\bar{z}}^2 / \bar{z}^2 &= a^2 \sigma_{\bar{x}}^2 / \bar{x}^2 + b^2 \sigma_{\bar{y}}^2 / \bar{y}^2 \end{aligned}$$

It appears that accurate electrostatic charge distribution calculations of the kind described here have not been carried out on oxide minerals to date. In the discussion that follows, these calculations are applied to the three tantalum oxides, tantalite, pseudo-ixiolite and wodginite in an effort to aid, in conjunction with the effective scattering power and the mean bond length, in the interpretation of the elements occurring in each cationic site.

III.5.c Tantalite

The structure of tantalite is described in detail in Chapter III.2, and it is pointed out that there are two cationic sites and three oxygen sites. The structure was first refined in this analysis using scattering curves based on the formula $\text{Mn}_4(\text{Ta}_{5.1}\text{Nb}_{2.9})\text{O}_{24}$ which represents closely the chemical analysis (Table III.2.1). If one assumes that the cations are completely ordered, which was believed to be the case for a tantalite

which had been heated in the manner described, then site A would consist of all Mn^{2+} , and site B of Ta^{5+} and Nb^{5+} in the proportion shown by the formula. The cations could be expected to order themselves readily in this structure because there is a great difference in size and charge between Mn^{2+} and $(\text{Ta},\text{Nb})^{5+}$ with radii of 0.82 \AA and 0.64 \AA , respectively. Assuming this ordered distribution, the structure refined to $R = 0.105$ with anisotropic temperature factors. On the basis of this refinement, bond distances were calculated and these were used to calculate an electrostatic charge distribution. These bond distances are different from those given in Table III.2.5 which are, as explained on page 36, for a partially ordered structure (see also page 93). Table III.5.1 gives the results of this calculation. The table shows C_c , the positive charge contributed to each oxygen from a particular cationic site, the total positive charge contributed to each of the three unique oxygens, and the total positive charge contributed to the two (pseudo-) octahedral groups of six oxygens. Ideally the total charge to an octahedral group of six oxygens would be 12 e.s.u., but Table III.5.1 shows that around the divalent 'Mn' site it is for this ordered arrangement considerably less than this, 10.86(03) e.s.u., whereas around the pentavalent 'Ta' site it is too large, 12.57(02) e.s.u. To explain the charge unbalance one might invoke such arguments as (i) shifts in the bond distances such that the proportioned charge is shifted from one site to the other;

Table III.5.1. Tantalite: Calculation of the electrostatic charge distribution in $Mn_4^{2+} (Ta,Nb)_8^{5+} O_{24}^{2-}$

Positive charge from each cation site to each oxygen:

<u>Mn²⁺ Site</u>			<u>Ta⁵⁺ Site</u>		
<u>Bond</u>	<u>CO, Å</u>	<u>Cc, e.s.u.</u>	<u>Bond</u>	<u>CO, Å</u>	<u>Cc, e.s.u.</u>
Mn-I	2.17 (1)	0.339 (1)	Ta-I	1.93 (1)	0.885 (3)
Mn-I	2.17 (1)	0.339 (1)	Ta-I	2.03 (1)	0.805 (3)
Mn-II	2.26 (2)	0.313 (2)	Ta-II	1.78 (2)	1.040 (8)
Mn-II	2.26 (2)	0.313 (2)	Ta-III	2.21 (1)	0.677 (3)
Mn-II	2.15 (2)	0.348 (2)	Ta-III	2.04 (1)	0.790 (4)
Mn-II	2.15 (2)	0.348 (2)	Ta-III	2.03 (1)	0.803 (4)

Total positive charge to each oxygen site, e.s.u.:

	<u>Total to I</u>		<u>Total to II</u>		<u>Total to III</u>
Mn	0.339 (1)	Mn	0.313 (2)	Ta	0.677 (3)
Ta	0.885 (3)	Mn	0.348 (2)	Ta	0.790 (4)
Ta	<u>0.805 (3)</u>	Ta	<u>1.040 (8)</u>	Ta	<u>0.803 (4)</u>
	2.029 (5)		1.701 (8)		2.270 (6)

Total positive charge to octahedral groups of 6 O's, e.s.u.:

	<u>Around Mn</u>		<u>Around Ta</u>
2I	4.058 (10)	2I	4.058 (10)
4II	6.804 (32)	1II	1.701 (08)
		3III	<u>6.810 (18)</u>
	<u>10.862 (34)</u>		12.569 (22)

(ii) changes in the valence of manganese and tantalum and/or niobium; or (iii) interchange of some of the different valent cations between the two sites. The first argument does not seem valid because the shifts required to bring about a charge balance are far greater than the standard deviations would allow. To bring about a charge balance in the manganese site one would need only 0.60 weight per cent Mn_2O_3 , and although Mn^{3+} does occur in nature, it is present only in geological environments with very highly oxidizing conditions. Tantalite is unlikely to be formed in nearly high enough fO_2 to produce Mn^{3+} (Grice, 1970; Turnock, 1966). The possibility of a lower valence for Ta or Nb in nature seems negligible as no valence other than 5+ has been found in nature for either of these elements; thus, the second argument appears invalid. The third suggestion above seems the most plausible, and the effective charge on each of the two cationic sites necessary to give an ideal electrostatic charge balance was calculated using the bond lengths calculated for the ordered structure refinement. The necessary effective charge on the A and B sites calculated to be +3.256 and +4.372 e.s.u., respectively in place of +2 and +5 e.s.u. These new effective charges on the two cationic site result in each of the two groups of octahedral oxygens receiving almost exactly +12 e.s.u. An interpretation regarding the atomic content of the A and B

sites is given in Chapter III.6.

III.5.d Pseudo-ixiolite

The structure of pseudo-ixiolite is described in Chapter III.3 where it is pointed out that the structure has one cation site and one oxygen site. In the single cation site all the metals are, of necessity, randomly distributed and the atoms are thus 'disordered' within this site. The oxygens are in a distorted octahedral co-ordination around the metal site (Table III.3.5).

The calculation of an electrostatic charge distribution is meaningless for a structure that has only one cationic site. When one considers the weighting factor based on bond lengths, the charge on the cation is, in the case of (pseudo-) octahedral co-ordination, proportioned among the six oxygens around it, and the sum of these proportions, C_c , must total to the charge on the cation. Thus, if there is only one cation, the charge balance between cations and oxygens can only occur if there is an electrostatic charge or valence balance within the chemistry itself, and the 'structural charge balance' has no significance. Pseudo-ixiolite is of this structure type; it has a 'chemical charge balance' and thus the total charges to the octahedral group of six oxygens around the cation site must be exactly 12 e.s.u.

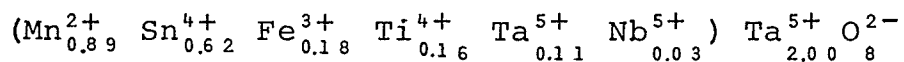
III.5.e Wodginite

The structure of wodginite is described in Chapter III.4 where it is pointed out that there are three cationic sites and four oxygen sites in the true cell, and two cationic and two oxygen sites in the sub-cell. Since the sub-cell has fewer structural sites, the electrostatic charge distribution calculations are simpler and these will be discussed first. The bond distances for the sub-cell were calculated from Elphick's (1972) structure analysis.

Table III.5.2a gives the electrostatic charge distribution values in the wodginite sub-cell using Elphick's (1972) structure analysis. The one metal site B contains, from the structure analysis, only Ta^{5+} , and the total charge to the six oxygens around it is 12.30(11) e.s.u. (Table III.5.2a) which is slightly higher than the ideal. The other metal site A contains all the other cations, namely Mn^{2+} , Sn^{4+} , Fe^{3+} , Ti^{4+} , Ta^{5+} and Nb^{5+} in the proportions given in the analysis in Table III.4.1; this site has an effective charge of +3.07 e.s.u. The total charge to the six oxygens around this site is 11.91(11) e.s.u.; this actual value is a little lower than the ideal of 12, but it is equal to the ideal within the limits of error. The results are discussed briefly in the following Chapter III.6.

Table III.5.2a. Wodginite: Calculation of the electrostatic charge distribution in the sub-cell.

Composition (Table III.4.1) and cation distribution is



A ^{3.07+} Site			Ta ⁵⁺ Site		
<u>Bond</u>	<u>CO, Å</u>	<u>Cc, e.s.u.</u>	<u>Bond</u>	<u>Co, Å</u>	<u>Cc, e.s.u.</u>
A-I	1.95 (6)	0.572 (9)	Ta-I	2.12 (6)	0.774 (15)
A-I	1.95 (6)	0.572 (9)	Ta-I	2.12 (6)	0.774 (15)
A-II	2.05 (5)	0.516 (9)	Ta-I	2.13 (6)	0.769 (15)
A-II	2.05 (5)	0.516 (9)	Ta-I	2.13 (6)	0.769 (15)
A-II	2.20 (6)	0.447 (9)	Ta-II	1.91 (5)	0.957 (22)
A-II	2.20 (6)	0.447 (9)	Ta-II	1.91 (5)	0.957 (22)

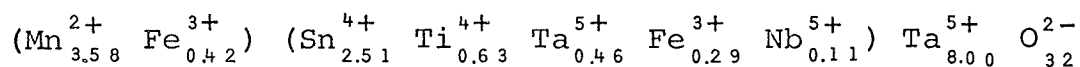
Total charge to each oxygen site:

	<u>Total to I</u>		<u>Total to II</u>
A	0.572 (09)	A	0.516 (09)
Ta	0.774 (15)	A	0.447 (09)
Ta	<u>0.769 (15)</u>	Ta	<u>0.957 (22)</u>
	2.115 (23)		1.920 (26)

Total charge to octahedral groups of 6 O's:

	<u>Around A</u>		<u>Around Ta</u>
2I	4.230 (046)	4I	8.460 (092)
4II	<u>7.680 (104)</u>	2II	<u>3.840 (052)</u>
	11.910 (112)		12.300 (106)

The electrostatic charge distribution for the true cell of wodginite with more structural sites is necessarily more involved. In Table III.5.2b the charge distribution calculations are shown for effective charges on each cationic site implied by the formula



which has been shown previously as being crystal-chemically and structurally reasonable. The effective charges on each site for this formula are, in e.s.u. A = +2.10, B = +4.07, and C = +5.00. In Table III.5.2b it can be seen that this cation distribution yields large charge unbalances on the octahedral groups of six oxygens: the oxygens around the A site receive a low total charge of only 10.28(7) e.s.u., whereas the six oxygens around the B and C sites both receive an excess of charge with 13.66(11) and 12.29(5) e.s.u., respectively. An interpretation of the electrostatic charge distribution and its relation to the chemical analysis and the observed bond lengths is given in Chapter III.6.

III.6 Interpretation and Comparisons of the Structures of Tantalite, Pseudo-ixiolite, and Wodginite

III.6.a Proposed Cation Distribution and Chemical Formula for Tantalite

It was shown in the previous section that, in order

Table III.5.2b. Wodginite: Calculation of the electrostatic charge distribution in the true cell,

$$(Mn_{3.58}^{2+} Fe_{0.42}^{3+}) (Sn_{2.51}^{4+} Ti_{0.63}^{4+} Ta_{0.46}^{5+} Fe_{0.29}^{3+} Nb_{0.11}^{5+}) Ta_{8.00}^{5+} O_{32}^{2-}$$

<u>A^{2.10+} Site</u>			<u>B^{4.07+} Site</u>		
<u>Bond</u>	<u>CO,A</u>	<u>Cc,e.s.u.</u>	<u>Bond</u>	<u>CO,A</u>	<u>Cc,e.s.u.</u>
A-I	2.12 (4)	0.340 (4)	B-II	2.32 (6)	0.564 (09)
A-I	2.12 (4)	0.340 (4)	B-II	2.32 (6)	0.564 (09)
A-IV	2.06 (4)	0.360 (5)	B-II	2.03 (4)	0.737 (11)
A-IV	2.06 (4)	0.360 (5)	B-II	2.03 (4)	0.737 (11)
A-IV	2.09 (4)	0.350 (4)	B-III	2.04 (3)	0.734 (10)
A-IV	2.09 (4)	0.350 (4)	B-III	2.04 (3)	0.734 (10)

<u>C⁵⁺ Site</u>		
<u>Bond</u>	<u>CO,A</u>	<u>Cc,e.s.u.</u>
C-I	2.12 (4)	0.726 (09)
C-I	1.99 (3)	0.831 (12)
C-II	1.85 (5)	0.962 (21)
C-III	1.97 (3)	0.846 (09)
C-III	2.13 (3)	0.724 (09)
C-IV	1.90 (4)	0.911 (14)

Total charge to each oxygen site:

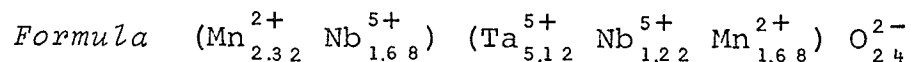
<u>Total to I</u>		<u>Total to II</u>		<u>Total to III</u>		<u>Total to IV</u>	
A	0.340 (04)	B	0.564 (09)	B	0.734 (10)	A	0.360 (05)
C	0.726 (09)	B	0.737 (11)	C	0.846 (09)	A	0.350 (04)
C	<u>0.831 (12)</u>	C	<u>0.962 (21)</u>	C	<u>0.724 (09)</u>	C	<u>0.911 (14)</u>
	1.897 (16)		2.263 (25)		2.304 (18)		1.621 (16)

Total charges to octahedral groups of 6 O's:

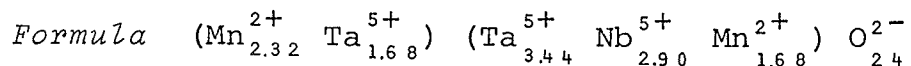
<u>Around A</u>		<u>Around B</u>		<u>Around C</u>	
2I	3.794 (31)	4II	9.052 (100)	2I	3.794 (31)
4IV	6.484 (64)	2III	4.608 (036)	1II	2.263 (25)
				2III	4.608 (36)
				1IV	<u>1.621 (16)</u>
	<u>10.278 (70)</u>		<u>13.660 (108)</u>		12.286 (51)

to have an 'ideal' charge distribution to the two octahedral groups of oxygens, one would have to assume that the cation sites A and B have effective charges of +3.256 and +4.372 e.s.u., respectively. It is now possible to consider what numbers of atoms for the three major cations from the chemical analysis can be assigned to the two sites to give the ideal effective charge on each site. The three most likely formulae based on types of order-disorder in the two cation sites are as follows:

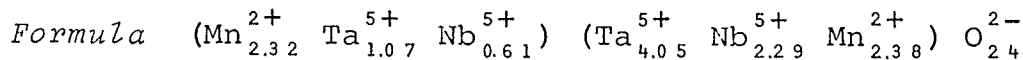
Type 1. All the 5+ cations in the A site necessary to increase its effective charge from +2 to +3.256 present as Nb⁵⁺:



Type 2. All the necessary 5+ cations in the A site present as Ta⁵⁺:



Type 3. All the necessary 5+ cations in the A site present as both Ta⁵⁺ and Nb⁵⁺ in their original chemical proportions:



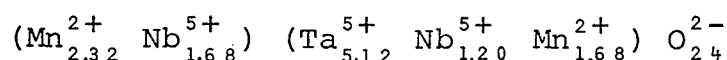
The formula which was the most logical to try was that which resulted in effective scattering powers for the

two metal sites most like those for Mn_4^{2+} ($Ta_{5.1}^{5+}$ $Nb_{2.9}^{5+}$) $O_{2.4}^{2-}$ on which the original refinement was based. It can be seen that Type 1 would be the best choice since only the lighter of the pentavalent cations, Nb^{5+} (effective atomic No. 36) is substituted for light Mn^{2+} (effective atomic No. 23). For comparison the effective number of electrons per site are given here:

	<u>Effective Simplest Formula*</u>	<u>Site A</u>	<u>Site B</u>
<i>Original</i>	Mn_4^{2+} ($Ta_{5.1}^{5+}$ $Nb_{2.9}^{5+}$)	23	56
<i>Type 1</i>	$(Mn_{2.3}^{2+}$ $Nb_{1.6}^{5+})$ ($Ta_{5.1}^{5+}$ $Nb_{1.2}^{5+}$ $Mn_{1.6}^{2+}$)	28	54
<i>Type 2</i>	$(Mn_{2.3}^{2+}$ $Ta_{1.6}^{5+})$ ($Ta_{3.4}^{5+}$ $Nb_{2.9}^{5+}$ $Mn_{1.6}^{2+}$)	42	47
<i>Type 3</i>	$(Mn_{2.3}^{2+}$ $Ta_{1.0}^{5+}$ $Nb_{0.6}^{5+})$ ($Ta_{4.0}^{5+}$ $Nb_{2.2}^{5+}$ $Mn_{2.3}^{2+}$)	37	49
* Ideal	$A_4 B_8 O_{2.4}$		

A least squares refinement was carried out, after these calculations were made, using effective scattering factors for A and B implied by formula Type 1 and the structure refined to $R = 0.106$ which was approximately the same R factor as before. This indicates that the structure could in fact be partially disordered which was not indicated until one calculated the electrostatic charge distribution. Since the effective scattering powers of the cationic sites was changed it was felt that the

atomic parameters should be allowed to refine in this run. This brought about minor changes in the co-ordinates and hence the bond lengths. Table III.6.1 shows a recalculation of the electrostatic charge balance with the new bond lengths, and although the positive charge to the octahedral groups of oxygens is not the ideal 12 e.s.u., it is much closer. The inherent error in the formula due to the method of chemical analysis does not warrant any further minor adjustments needed in the formula to achieve the ideal electrostatic charge balance. All the data listed in Chapter III.2 is for the partially ordered formula

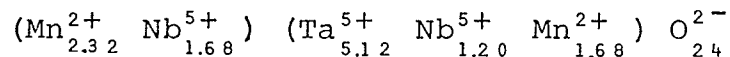


which corresponds to $\text{A}^{+3.26} \text{B}_2^{+4.37} \text{O}_6^{2-}$

Although the R factor does not indicate a preference for the partially ordered formula the improved electrostatic charge balance indicates that the simplest, structurally-sound formula for our tantalite is not $\text{Mn}^{2+} (\text{Ta}_{1.3}^{5+} \text{Nb}_{0.7}^{5+}) \text{O}_6^{2-}$ but rather $(\text{Mn}_{0.6}^{2+} \text{Nb}_{0.4}^{5+}) (\text{Ta}_{1.3}^{5+} \text{Nb}_{0.3}^{5+} \text{Mn}_{0.4}^{2+}) \text{O}_6^{2-}$, and it is further suggested that the structurally-sound formula for tantalites generally may not be $\text{A}^{2+} \text{B}_2^{5+} \text{O}_6^{2-}$ but rather $(\text{A}_{1-2x}^{2+} \text{B}_{2x}^{5+}) (\text{B}_{1-x}^{5+} \text{A}_x^{2+})_2 \text{O}_6^{2-}$ where A^{2+} is mainly Mn^{2+} and Fe^{2+} , B^{5+} is mainly Ta^{5+} and Nb^{5+} , and for this tantalite $x \sim 0.20$.

In tantalite the mean metal-oxygen distance for site A is 2.16(1) Å and that for site B is 2.02(1) Å (Table III.2.5). This is what one might expect for the

Table III.6.1. Tantalite: Calculation of electrostatic charge distribution in



Positive charge from each cation site to each oxygen:



Effective charge +3.256 e.s.u. Effective charge +4.372 e.s.u.

<u>Bond</u>	<u>CO, Å</u>	<u>Cc, e.s.u.</u>	<u>Bond</u>	<u>CO, Å</u>	<u>Cc, e.s.u.</u>
A-I	2.14 (1)	0.555 (2)	B-I	2.04 (1)	0.705 (2)
A-I	2.14 (1)	0.555 (2)	B-I	1.96 (1)	0.760 (3)
A-II	2.16 (1)	0.543 (2)	B-II	1.81 (1)	0.892 (4)
A-II	2.16 (1)	0.543 (2)	B-III	2.21 (1)	0.598 (2)
A-II	2.19 (1)	0.530 (2)	B-III	2.05 (1)	0.699 (2)
A-II	2.19 (1)	0.530 (2)	B-III	2.02 (1)	0.718 (1)

Total positive charge to each oxygen site, e.s.u.:

<u>Total to I</u>		<u>Total to II</u>		<u>Total to III</u>	
A	0.555 (2)	A	0.543 (2)	B	0.598 (2)
B	0.705 (2)	A	0.530 (2)	B	0.699 (2)
B	<u>0.760 (3)</u>	B	<u>0.892 (4)</u>	B	<u>0.718 (1)</u>
	2.020 (4)		1.965 (5)		2.015 (3)

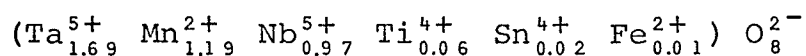
Total positive charge to octahedral groups of 6 O's, e.s.u.:

<u>Around A</u>		<u>Around B</u>	
2I	4.040 (8)	2I	4.040 (8)
4II	7.860 (18)	1II	1.965 (5)
	<u>11.900 (20)</u>	3III	<u>6.046 (10)</u>
			12.051 (13)

metal occupancies postulated in Chapter III.2 for the two sites: A contains more large-sized low-charged Mn^{2+} atoms whereas B contains mainly smaller sized, highly charged Ta^{5+} and Nb^{5+} atoms. Using the proportions of ions in the chemical formula given above, the corresponding bond lengths are only slightly different than those calculated from ionic radii of Shannon and Prewitt (1969): for six-fold co-ordination, the authors give Mn^{2+} as 0.82 Å, Ta^{5+} as 0.64 Å and O^{2-} as 1.40 Å; thus in an ionic structure as tantalite is considered to have, the A-O bond length would be 2.15 Å and the B-O bond length would be 2.08 Å. These bond lengths are calculated using the proper proportions of the cations in each site.

III.6.b Chemical Formula for Pseudo-ixiolite

The chemical formula for a true pseudo-ixiolite is that proposed by Nickel *et al.* (1963b). As explained in Chapter III.5 the cations must be disordered in the one metal site and the formula for the cell is:



The occupancy used in the structure refinement was based on this chemistry and there was no indication that the occupancy should be changed. There is an electrostatic charge balance within the chemistry and as was pointed out in the previous section, it is pointless to carry out any

electrostatic charge balance calculation for such a simple structure. The average bond length for the pseudo-octahedral co-ordination was found to be $2.06(4) \text{ \AA}$ (Table III.3.5) which is intermediate between the averages for the A and B sites for tantalite, $2.16(1) \text{ \AA}$ and $2.02(1) \text{ \AA}$, respectively. Such an intermediate value is what would be expected for this disordered structure.

III.6.c Proposed Cation Distribution and Chemical Formula for Wodginite

In the previous section, it was shown that for Elphick's (1972) structure of wodginite based on the sub-cell with Ta^{5+} filling the B site and all other cations, the A site, the two octahedral groups of oxygens receive close to the ideal 12 e.s.u. (Table III.5.2a). The structural interpretation of a cation distribution which has Ta^{5+} fully ordered is thus for this sub-cell nearly compatible with an ideal electrostatic charge distribution. As the table shows, a slight interchange of the 2+ and 5+ cations between the two sites would give an even better charge distribution.

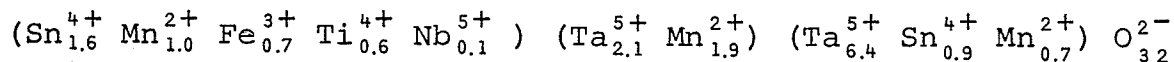
The electrostatic charge distributions given in Table III.5.2b in Chapter III.5 for the true cell of wodginite indicate that, if the octahedral groups of oxygens are to total close to +12 e.s.u., then some exchange of cations is needed between all three sites: cations with a

higher valence are needed in site A whereas those with a lower valence are required in sites B and C. Solving the appropriate simultaneous equations as was done with tantalite, the 'ideal effective charge', (in e.s.u.) on these sites leading to a balanced electrostatic charge distribution calculated to be +3.56 for the A site, +3.52 for the B site and +4.46 for the C site. This implies a considerably different cation distribution from that originally proposed on the basis of the structure analysis, namely that the A site was mainly divalent, the B tetravalent, and the C pentavalent.

It now remains to derive a possible cation distribution which is consistent with (i) the chemistry; (ii) the scattering factors derived from the structure analysis; (iii) the electrostatic charge distribution; and (iv) the effective size of each cationic site. Table III.6.2 shows the derivation of such a formula by trial and error. In the table the cations in total amounts consistent with the chemical analysis (Table III.4.1) have been assigned to the A, B, and C sites such that the effective charge, the effective scattering powers and the effective bond lengths of the three sites are reasonably compatible with respectively, effective charges calculated for the 'ideal' charge distribution, the structurally derived scattering factors, and the structurally derived mean cation-oxygen distances. In the table it can be seen that the

three compare reasonably well. However, the numbers of electrons/site (Column (8)) do not agree with the effective scattering powers (Column (9)) within the limits of error of the latter, but as was pointed out earlier wodginite is fairly variable in composition even within one grain. It would not take very large changes in the chemistry to compensate for the differences in scattering powers seen in this table.

From Table III.6.2, one can conclude that it is possible to derive a cation distribution for the true cell of wodginite which reconciles in a reasonably satisfactory way the chemistry, electrostatic charge distribution, structurally derived scattering factors and bond lengths. From the considerations embodied here, the author proposes the general formula for wodginite to be $A_4^{3.6+} B_4^{3.5+} C_8^{4.5+} O_{32}^{2-}$, and the specific formula for this wodginite to be



III.6.d Comparison of the Structures of Tantalite, Pseudo-ixiolite and Wodginite

(i) The Structures Themselves

A close relationship between the structures of tantalite, pseudo-ixiolite, and wodginite was proposed by Nickel *et al.* (1963a) and by Grice *et al.* (1972), but not until the present work have all three structures

Table III.6.2. Wodginite: The derivation of a proposed chemical formula (cation distribution) for the true cell consistent with the chemical analysis, the derived scattering factors, the electrostatic charge distribution and the bond lengths

(1) Cation Site	(2) Cation	(3) Effective Atomic No.	(4) Ionic Radius, Å (S. and P.* 1969)	(5) No. of Cations for 32 O's from Chem. Anal. (Table III.4.1)	(6) Effective Weighted Charge on Site, e.s.u. for Distrib. (5)	(7) Effective Charge Calc. for Ideal Charge Distrib., e.s.u.	(8) e ⁻ /Site Implied by Distrib. (5)	(9) e ⁻ /Site Implied by Derived Scattering Factors	(10) Cat.-Ox. Dist., Å Implied by (4) and (5)	(11) Observed Mean Cat.-Ox. Dist., Å
A	Sn ⁴⁺	46	0.69	1.6	4.0	+3.4	32	27(1)	2.10	2.09(4)
	Mn ²⁺	23	0.82	1.0						
	Fe ³⁺	23	0.645	0.7						
	Ti ⁴⁺	18	0.605	0.6						
	Nb ⁵⁺	36	0.64	0.1						
B	Ta ⁵⁺	68	0.64	2.1	4.0	+3.5	47	45(2)	2.13	2.13(4)
	Mn ²⁺	23	0.82	1.9						
C	Ta ⁵⁺	68	0.64	6.4	8.0	+4.6	62	73(1)	2.06	1.99(5)
	Sn ⁴⁺	46	0.69	0.9						
	Mn ²⁺	23	0.82	0.7						

Proposed General Formula: $A_4^{3.6+} B_4^{3.5+} C_8^{4.5+} O_{32}^{2-}$

Proposed Specific Formula: $(Sn_{1.6}^{4+} Mn_{1.0}^{2+} Fe_{0.7}^{3+} Ti_{0.6}^{4+} Nb_{0.1}^{5+}) (Ta_{2.1}^{5+} Mn_{1.9}^{2+}) (Ta_{6.4}^{5+} Sn_{0.9}^{4+} Mn_{0.7}^{2+}) O_{32}^{2-}$

*Shannon, V. and Prewitt, C.T. (1969).

been analysed to make a comparison possible. In Table III.6.3 are given the cell dimensions, space groups and cell volumes for all three minerals taken from the two references above. The orientation of these three cells is that given by Strunz and Tennyson (1971). It can be seen that pseudo-ixiolite can be regarded as having the basic cell for both tantalite and wodginite. In tantalite the a period is three times that of pseudo-ixiolite, with b and c the same, and in wodginite the a and b periods are double those of pseudo-ixiolite with c the same and with the cell having a slight monoclinic distortion with $\beta \sim 91^\circ$. Figure III.6.1 exemplifies the relationship of the three cells with respect to orientation and size (Ferguson, 1972).*

Tantalite can be considered the prototype structure because the mineral has been known the longest and because it was the only one of the three structures known previously (Sturdivant, 1930). Tantalite also formed the basis for the naming by Nickel *et al.* (1963a) of their new mineral wodginite, and it further formed the basis on which these authors defined the new mineral or variety pseudo-ixiolite (1963b). From the projected structures of tantalite shown in Figure III.2.1 it can be seen that the tantalite structure is layered parallel to the (100) planes: the O atoms in any one such layer are pseudo-close-packed and the O's in alternate layers nearly repeat themselves so that throughout the structure the O atoms can be regarded

*personal communication

Table III.6.3. Comparison of the tantalite, pseudo-ixiolite and wodginite cells.

	<u>Tantalite</u>	<u>Pseudo-Ixiolite</u>	<u>Wodginite</u>
System	Orthorhombic	Orthorhombic	Monoclinic
Space Group	Pbcn	Pbcn	C2/c
$a, \text{\AA}$	3x4.81	4.79	2x4.74
$b, \text{\AA}$	5.76	5.76	2x5.70
$c, \text{\AA}$	5.09	5.16	5.10
β Angle	(90°)	(90°)	~91°
Cell Vol., (\AA) ³	3x141	142	4x138

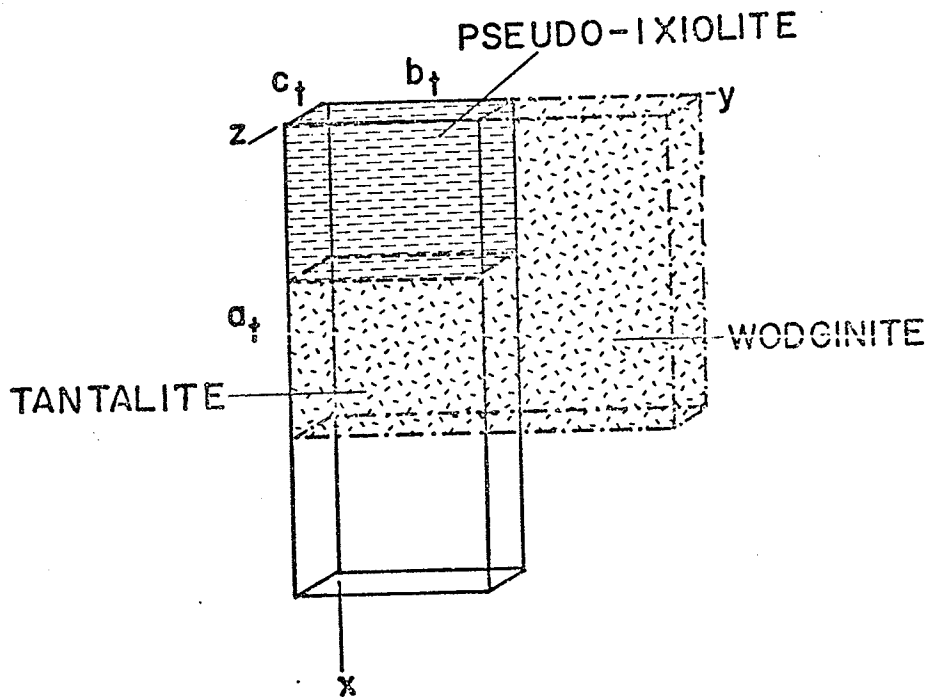


Figure III.6.1. Comparison of the orientation and size of the tantalite, pseudo-ixiolite and wodginite cells

as being pseudo-hexagonal close-packed parallel to (100). The metal atoms occupy one-half the six-fold distorted octahedral holes within the O's.

The other two minerals, pseudo-ixiolite and wodginite, are essentially isostructural with tantalite (Figures III.3.1 and III.4.2, respectively). When the atoms in the two metal sites in tantalite become disordered between the two sites, and there are slight necessary shifts in some oxygen positions, then the a period of tantalite is reduced to one-third that of the true cell and it becomes the pseudo-ixiolite cell as defined by Nickel *et al.* (1963b). The shifts in the atomic positions necessary to give the pseudo-ixiolite structure cause a greater distortion to the pseudo-octahedral configuration than is seen in the tantalite structure. In wodginite the layering of the oxygens and cations is still evident. Figure III.4.1 shows that the A and B cation sites in wodginite lie in positions comparable to the A site of tantalite, and the C site of the former corresponds to the B site of the latter. To compare atomic positions in the two minerals one must, as discussed in Chapter III.4, transfer the wodginite origin to $0, \frac{1}{2}, 0$ in the tantalite structure and take into consideration that the a and b periods of wodginite correspond to $\frac{2}{3}a$ and $2b$ of tantalite (Figure III.6.1). The oxygen positions in the two minerals are also comparable, but there are significant

shifts in those of wodginite to accommodate the different cations. In wodginite the A and B sites have pseudo-octahedral co-ordination but that of the C site, although six-fold, does not resemble any regular configuration (Table III.4.6).

(ii) Possible Origin of the Different Structures

It is likely that both physical and chemical considerations have to be taken into account in assessing which of these three phases will likely form in natural or synthetic systems. The formation of wodginite in preference to tantalite or pseudo-ixiolite is probably due largely to the oxygen pressure within the system. Turnock (1966) has shown that wodginite forms at a higher oxygen pressure than tantalite, and that wodginite has Fe^{3+} in preference to the Fe^{2+} which is found in tantalite. In keeping with the electrostatic charge balance considerations, the more electropositive ions Sn^{4+} and Ti^{4+} would prefer the wodginite structure to the tantalite structure and this is observed in the Tanco specimens. If oxygen pressures were not sufficiently high to form the wodginite phase, the Sn and Ti would probably form separate phases, cassiterite and ilmenite along with tantalite. This of course remains speculative until more is understood

in the system of 'tin tantalites' which would include other mineral phases such as sukulaite, olovotantalite, and stiringite. In the Tanco Pegmatite, Grice, Černý and Ferguson (1972) have shown that most of the wodginite does occur in an assemblage formed later than the main tantalite bearing assemblage and the former assemblage would be expected to have the higher oxygen pressure.

The reasons for the preference for the formation of the pseudo-ixiolite structure over the tantalite structure in a given environment is less clear. It appears that there are two factors which may control the formation of these minerals. Heating pseudo-ixiolite results in the ordering of the cations to some degree and the resultant adoption of the tantalite structure. Grice, Černý and Ferguson (1972) point out that this ordering takes place at elevated temperatures despite the oxygen pressure. This could explain the lack of this phase in Turnock's (1966) synthetic work which was conducted at 1200°C. The degree of ordering at a particular temperature may, however, depend on the oxygen pressure with the formation of pseudo-ixiolite favoured in the more oxidizing environment. Evidence for this is the preference of ions with higher oxidation states than Mn^{2+} and Fe^{2+} that are found in tantalite. Knorring *et al.* (1969) report Fe^{3+} , Sc^{3+} , Ti^{4+} and Sn^{4+} in their scandian ixiolite. Grice, Černý and Ferguson (1972) report a slight preference of Sn^{4+} and Ti^{4+}

in pseudo-ixiolite as opposed to tantalite for the Tanco pegmatite minerals. Černý and Turnock (1971) report up to 4.8 wt.% TiO_2 and 1.6 wt.% SnO_2 in the pseudo-ixiolites they studied. Their one partially ordered columbite contained 0.2 wt.% TiO_2 and no SnO_2 . The significance of the more highly positive ions in pseudo-ixiolite is realized when the electrostatic charge balance is considered. In ideally ordered tantalite there is a divalent and a pentavalent site whereas in pseudo-ixiolite the one metal site has an average quadrivalent charge. The trivalent and quadrivalent ions would thus prefer the disordered pseudo-ixiolite phase to that of ordered tantalite phase. In the Tanco pegmatite tantalite is found primarily in the albitic aplite (Zone 6b) which would be formed at a higher temperature with less water (Jahns and Burnham, 1969) (hence presumably lower $f\text{O}_2$) than the coarser-grained zones (4) and (5) which contain pseudo-ixiolite. The relationship of the time sequence of formation between the wodginite phase and the pseudo-ixiolite phase within the pegmatite is not clear.

In conclusion it would appear that the observation made by Grice, Černý and Ferguson (1972) on the formation of tantalite, pseudo-ixiolite and wodginite in the Tanco pegmatite support the structural evidence that: (i) tantalite formation is preferred to pseudo-ixiolite formation at higher temperatures and (ii) in order of

increasing fO_2 , the preferred phase formation would be tantalite, then pseudo-ixiolite, then wodginite.

CHAPTER IV

THE CRYSTAL STRUCTURE OF MILLERITE, NiS

CHAPTER IV

IV.1 Millerite Structure Analysis: Method and Results

IV.1.a Introduction

Millerite occurs as tufts or crusts in cavities and more rarely as cleavable masses in sulfide bodies such as those of the Marbridge Mine, Malartic, Quebec. Millerite is a low-temperature mineral which is stable up to 379°C (Kullerud and Yund, 1962). It is both a primary and a secondary mineral resulting in the second case by, for example, the oxidation of pentlandite. The crystal structure of millerite as originally derived, is of particular crystal - chemical interest because of an unusual five-fold co-ordination of the Ni atoms by S atoms. The structure has not previously been refined by modern techniques.

A structure for millerite was first derived by Alsén in 1925. Although the atomic positions he proposed for the two types of atoms were essentially correct, he had the Ni and S atoms reversed. This reversal of the two kinds of atom was demonstrated by Kolkmeijer and Moesveld in 1931. Even though the structure of millerite was known, the writer and his supervisor felt that a modern refinement would be

valuable particularly in view of the unusual co-ordination of the Ni atom. We also felt that with accurate interatomic distances it might be possible to interpret the Ni-S bonding and co-ordination in terms of present-day bonding theories.

The particular millerite chosen for study came from the Marbridge Mine, Malartic, Quebec. This material was chosen because it is coarse with a prominent perfect cleavage, and so it is easy to get single-crystalline fragments for a structural data collection. This is discussed more fully later.

There are four nickel-iron sulfide ore deposits on the Marbridge property. Deposit No. 1 is described by Clark (1965), No. 2 by Buchan and Blowes (1968), and Nos. 3 and 4 by Graterol and Naldrett (1969); interested readers are referred to these accounts for the details of each deposit. The ore deposits occur in a belt of meta-ultramafic, metavolcanic and metasedimentary rocks which strike south-east between two batholithic intrusions, the Preissac and La Motte adamellites. In general, the sulfides occur both as massive bodies and as disseminations within the country rock. It is interesting to note that millerite is very common in these ores, and in fact it carries over 60 per cent of the Ni in the whole Marbridge deposit. The millerite is commonly associated with pentlandite, pyrite, pyrrhotite, violarite and magnetite. Minor and trace minerals include chalcopyrite, bornite, heazlewoodite,

valleriite, sphalerite, gersdorffite and sperrylite.

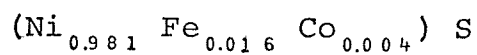
Electron microprobe analyses were carried out on the material that was used for the structure refinement. These analyses were done on a Philips AMR/3 electron microprobe at the Whiteshell Nuclear Research Establishment, Pinawa, Manitoba through the kindness of Dr. A. Sawatsky and with the valuable assistance of Mr. S. Jones. Standards were supplied by Dr. D.C. Harris of the Mines Branch, Department of Mines, Energy and Resources in Ottawa. The standards were Elba Island pyrite (FeS_2), synthetic $\text{NiS}_{1.07}$, and synthetic CoS_2 . The probe data were corrected for dead time, generation or atomic number, absorption, and fluorescence using a program written by J.C. Rucklidge and E.L. Gasparrini (1969).

Counts were recorded on five spots on each of three different grains. The material was found to be homogeneous within each grain, and consistent in composition from grain to grain. The analysis for one grain measured on five spots is given in Table IV.1.1. Note that the Ni + Fe + Co to S ratio is very close to 1:1, and that Ni is the strongly predominant metal so that the material has a composition close to the ideal formula, NiS. The atomic proportions assuming S = 1 are also given in this Table from where it can be seen the simplest formula for this millerite is $(\text{Ni}_{0.981}\text{Fe}_{0.016}\text{Co}_{0.004})\text{S}$. Although no direct measure of accuracy was made on these results, the Ni and S contents

Table IV.1.1. Millerite: Microprobe analysis and chemical formula.

<u>Element</u>	<u>Weight Percent</u>	<u>Atomic Proportions</u>	<u>Atomic Proportions For S=1</u>
Ni	63.68	1.085	0.981
Fe	1.03	0.018	0.016
Co	0.21	0.004	0.004
Cu	0.00	0.000	0.000
S	35.47	1.106	1
Total	<u>100.39</u>		

1.107 1.001

Chemical Formula

should be good to within ± 2 per cent of the weight per cent given due to the close relation between the standard and the sample. The Fe and Co results may be more suspect due to larger difference between standard and sample but they should be good to at least ± 4 per cent of the amounts shown.

IV.1.b Experimental Details

In the search for single crystals of millerite suitable for X-raying, it proved to be very difficult to find one that was entirely single. Several millerite specimens from various localities were supplied by Dr. R.I. Gait of the Department of Mineralogy, Royal Ontario Museum, Toronto, Ontario. "Single-crystal" fragments of the fibrous varieties from Oxford Twp., Sherbrooke Co., Quebec; Eugenia Mine, Tarragona, Spain; Heinrichsegen Mine Siegerland, Westphalia; Wissen-on-the Seig, Prussia, Westphalia; Grube Friedrich, Germany; and Niederhovel, Germany, all proved upon X-raying to consist of bundles of individual crystals; on the other hand "single-crystal" fragments of the platey material from Marbridge Mine, Malartic, Quebec; Strathcona Mine, Sudbury, Ontario; and Timagami Copper Mine, Timagami, Ontario all yielded X-ray photographs characteristic of regular intergrowths. A number of spheres were, however, ground from the platey Marbridge material and a suitable crystal, showing only very weak reflections from a second individual, was chosen for detailed X-ray analysis.

As described in detail later, millerite is rhombohedral R with hexagonal $a \sim 9.6\text{\AA}$ and $c \sim 3.1\text{\AA}$. In the regularly intergrown crystals, the second individual was found, from precession photographs, to be related to the first by a rotation about the y axis of an angle close to $20^\circ 40'$. From the angle table given for millerite in Palache, Berman and Frondel (1944) it can be seen that this is almost certainly the ρ angle for $(10\bar{1}1)$, $20^\circ 42.5'$; thus, the (0001) plane of one individual is parallel to $(10\bar{1}1)$ of the other. When the lattice in real space is plotted one can see that this intergrowth corresponds to a twin by reflection across $(01\bar{1}2)$ which is the common twin law for millerite.

Because no single-crystal diffractometer was available at the University of Manitoba, the data collection was carried out in the crystal structures laboratory of Dr. M. James in the Department of Biochemistry, University of Alberta, Edmonton. The instrument used was a four-circle, fully automated single-crystal diffractometer (the Picker FACSI).

The intensities for millerite were collected on a rhombohedral cell, in this case, referred to hexagonal axes and assuming the well-established acentric space group R3m. An orientation matrix and cell refinement were calculated using a least squares analysis of 20 reflections whose intensities had been maximized by the computer-controlled scanning program. The refined hexagonal cell dimensions are:

$$a = 9.6071(12) \text{ \AA}$$

$$c = 3.1434(9) \text{ \AA}$$

and these were used for the structure refinement. The intensities were collected using 2θ scans with a scanning speed of $2^\circ 2\theta$ per minute. Background counts were made for 10 seconds on either side of each peak. The peaks for this crystal were sharp. Reflections were collected using MoK_α radiation, and the instrument was equipped with a graphite single-crystal monochromater. All reflections compatible with the R lattice were collected out to $2\theta = 60^\circ$. This gave 155 unique reflections in the hkl segment, and all had measurable intensities.

IV.1.c Structure Refinement

Using the computer program DATAP5 the initial intensities were collected for the Lorentz factor, the polarization factor (including polarization by the monochromater), and absorption. In the absorption correction the crystal was assumed to be a perfect sphere with radius of 0.125 mm, and $\mu = 179.6 \text{ cm}^{-1}$ for MoK_α radiation.

Larson's computer program GENLES was used for a full-matrix least squares refinement of the positional and thermal parameters. The scattering factors used for Ni° and S° are those tabulated by Cromer and Mann (1968).

The hexagonal cell of the rhombohedral lattice of millerite with the cell dimensions given earlier contains

9 [NiS]. In the acentric space group of millerite, $R3m$, both the Ni and S atoms are, in the hexagonal cell, in nine-fold special positions (b) x, \bar{x}, z whose equivalent positions may be described as follows (International Tables for X-ray Crystallography, Vol. I):

$$(0,0,0; 1/3,2/3,2/3; 2/3,1/3,1/3) + (x,\bar{x},z; x,2x,z; 2\bar{x},\bar{x},z)$$

Kolkmeijer and Moesveld (1931) retained the rhombohedral setting initiated by Alsén (1925) for the millerite structure as well as the arbitrarily chosen origin which set rhombohedral x_1 of Ni to be 0. In the present refinement it was decided to use hexagonal axes and to shift the arbitrary origin such that the prototype sulfur would be at (hexagonal) height $z = 0$. Table IV.1.2 contains Kolkmeijer and Moesveld's positional parameters in relation to both hexagonal and rhombohedral cells, and relative to both their origin and the new origin used here. Starting with the transformed positional parameters of Kolkmeijer and Moesveld (1931) which are given in Table IV.1.2, and arbitrarily chosen isotropic temperature factors of $B = 1 \text{ \AA}^2$ for both atoms, the structure was refined to the point where, after three least squares cycles, $R = 0.090$ and $R_w = 0.084$ at which stage the isotropic temperature factors were

$$B_S = 0.585 (64) \text{ \AA}^2$$

$$B_{Ni} = 0.550 (48) \text{ \AA}^2$$

A ΔF map computed from this run indicated that anisotropic temperature factors were needed. After three cycles of full-matrix least squares refinement using anisotropic temperature factors, the refinement improved to $R = 0.066$ and $R_w = 0.056$, and at this point the refinement was terminated. The final positional parameters are given in Table IV.1.2, and the final anisotropic temperature factors for Ni and S derived from the structure refinement are given in Table IV.1.3a and the corresponding magnitudes and orientations for the thermal ellipsoids calculated using the computer program BIJCAL are given in Table IV.1.3b. Using the computer program ORTEP-II a z -axis projection of the structure was drawn, and it is shown as Figure IV.1.1. F_o and F_c values are listed in Table IV.1.4 and from the positional parameters, interatomic distances and interbond angles were calculated using program DISAGL, and these are listed in Table IV.1.5.

IV.2 Description and Discussion of the Millerite Structure

IV.2.a Description of the Millerite Structure

The millerite structure is a simple one with only one nickel and one sulfur atomic position. In this structure, which is shown in projection in Figure IV.1.1, the atoms are in one sense layered in planes parallel to (0001) but the layering is not one of the simple packing configurations with all of the Ni atoms in one layer and all of the

Table IV.1.2. Millerite: Space group, cell content, cell dimensions, and positional parameters.

Space Group	<u>R3m (No. 160)</u>	
	<u>Hexagonal</u>	<u>Rhombohedral</u>
Cell Content	(Ni _{8.83} Fe _{0.14} Co _{0.04}) S ₉	(Ni _{2.94} Fe _{0.04} Co _{0.01}) S ₃
Cell Dimensions, Å (this work)	$a = 9.6071(12)$ $c = 3.1434(9)$	$a_r = 5.6448$ $\alpha = 116^\circ 38'$
Positional Parameters	9 Ni in (b) x, \bar{x}, z 9 S in (b) x, \bar{x}, z	3 Ni in (b) x_1, x_1, x_3 3 S in (b) x_1, x_1, x_3
Kolkmeijer and Moesveld (1931)	$x_{Ni} = -0.088, z_{Ni} = 0.088$ $x_S = 0.118, z_S = 0.596$	$x_{Ni} = 0, z_{Ni} = 0.264$ $x_S = 0.714, z_S = 0.361$
Kolkmeijer and Moesveld (1931), new origin*	$x_{Ni} = 0.912, z_{Ni} = -0.508$ $x_S = 0.114, z_S = 0$	$x_{Ni} = 0.404, z_{Ni} = -0.332$ $x_S = 0.114, z_S = 0.772$
This work*	$x_{Ni} = 0.91225(9)$ $z_{Ni} = 0.47546(102)$ $x_S = 0.11224(19)$ $z_S = 0$	$x_{Ni} = 0.3877$ $z_{Ni} = 0.3499$ $x_S = 0.1122$ $z_S = 0.7756$

* In the present work, the original origin of Kolkmeijer and Moesveld (1931) has been shifted parallel to z to a new origin to set (hexagonal) $z_S = 0$.

Table IV.1.3a. Millerite: Anisotropic temperature factors and isotropic equivalents.
 (Standard deviations are given in brackets. Parameters without standard deviations were not refined since they were not independent parameters.)

<u>Atom</u>	<u>β_{11}</u>	<u>β_{22}</u>	<u>β_{33}</u>	<u>β_{12}</u>	<u>β_{13}</u>	<u>β_{23}</u>	<u>Equivalent Isotropic $B, \text{\AA}^2$</u>
Ni	0.00143 (17)	0.00143	0.02303 (145)	0.00160 (31)	0.00017 (43)	-0.00017	0.557
S	0.00223 (26)	0.00223	0.02111 (243)	0.00305 (59)	-0.00029 (78)	0.00029	0.640

Table IV.1.3b. Millerite: Magnitudes and orientations of thermal ellipsoids.

<u>Site</u>	<u>Ellipsoid Axes</u>	<u>Root Mean Square Amplitude, (Å)</u>	<u>Equivalent B (Å²)</u>	<u>Angles Between Ellipsoid Axes and Real Axes*</u>		
				A	B	C
Ni	1	0.066	0.35	30.0°	150.0°	91.8°
	2	0.072	0.41	60.0	60.0	90.0
	3	0.107	0.91	88.4	91.6	1.8
S	1	0.070	0.39	30.0	150.0	86.1
	2	0.094	0.69	60.0	60.0	90.0
	3	0.103	0.84	93.4	86.6	3.9

Standard deviations were not calculated for these measurements.

* A,B,C are the angles between the ellipsoid axes 1,2,3, and the crystallographic lattice axes x,y,z , respectively.

Table IV.1.5. Millerite: Interatomic distances and interbond angles.

<u>Equivalent Position Code</u>			<u>Interatomic Distances</u>				
x	y	z		<u>Distance, Å</u>	<u>Multi- plicity</u>	<u>Mean</u>	
a	$1-2x$	$-x$	z	Ni-S(a,e)	2.264(3)	2	2.306(2)
b	$1-2x$	$-x$	$1+z$	Ni-S(b,d)	2.369(3)	2	
c	$2/3+x$	$1/3-x$	$1/3+z$	Ni-S(c)	2.263(2)	1	
d	$1+x$	$2x$	$1+z$				
e	$1+x$	$2x$	z	Ni-Ni(f,h)	2.529(1)	2	2.529(1)
f	x	$2x-2$	z				
g	$3-2x$	$1-x$	z	S-S	3.143(4)	1	3.143(4)
h	$2x-2$	x	z				

Interbond Angles

	<u>Angle</u>
S(a)-Ni-S(b)	85.41(06)°
S(a)-Ni-S(c)	95.60(08)°
S(a)-Ni-S(e)	91.18(12)°
S(a)-Ni-S(d)	153.58(06)°
S(b)-Ni-S(c)	111.80(07)°
S(b)-Ni-S(d)	86.12(12)°
S(a)-Ni-Ni(f)	56.05(04)°
S(a)-Ni-Ni(g)	98.97(02)°
S(b)-Ni-Ni(f)	57.74(04)°
S(b)-Ni-Ni(g)	98.57(02)°
S(c)-Ni-Ni(f)	148.10(04)°
Ni(f)-Ni-Ni(g)	60°

S atoms in another. The stacking could be thought of as six stepped overlapping layers within each c repeat period, with three Ni atoms at each of heights 14, 48 and 81 (hundredths of c) and three S atoms at each of heights 0, 33 and 67. Figure IV.2.1 is a projection along the y -axis and can be used to see this layering.

The bond distances and interbond angles shown in Table IV.1.5 confirm the co-ordination of S atoms around Ni given by Kolkmeijer and Moesveld (1931), namely that each Ni atom is surrounded by five S atoms in the form of a distorted tetragonal pyramid at distances of 2.26 Å to 2.37 Å. Kolkmeijer and Moesveld quote Ni-S distances of 2.17 Å and 2.36 Å. However, Figure IV.1.1 shows that each Ni atom has, besides five S atoms, two other Ni atoms at the same height as itself and at a distance of 2.53 Å. This suggests that the co-ordination around each Ni should be considered as seven-fold and not five-fold as previously believed. The co-ordination around S is, however, restricted to five Ni atoms at distances of 2.26 Å to 2.37 Å in a distorted tetragonal pyramidal configuration as found by Kolkmeijer and Moesveld (1931). There are no S-S distances small enough to suggest any S-S interaction, the smallest distances being 3.14 Å.

IV.2.b Discussion of the Millerite Structure

(i) Layering and Anisotropism of the Atoms

The stepped-layering in the millerite structure, which was discussed in the previous section, is reflected in the magnitudes of the root mean square amplitudes of the thermal ellipsoids. It can be readily seen in Table IV.1.3b that for both the Ni and S atoms the magnitudes of the r.m.s. amplitudes nearly parallel to the z -axis (i.e., along ellipsoids axes 3) are considerably larger than they are in the two directions parallel and perpendicular to the vertical mirror-planes, (i.e., along ellipsoid axes 1 and 2, respectively). The reason for this might be that the density of atoms in the z -direction is less than in either of the other two directions, and thus a larger amplitude of vibration is possible parallel to z . In the horizontal plane (perpendicular to the z -axis) there are two vibrational directions and for both directions the r.m.s. amplitude of the S atom is greater than that for the Ni atom. A possible reason for this is that the S-S distance is considerably larger than the Ni-Ni distance (3.14 \AA as opposed to 2.53 \AA) and thus allows a greater vibrational freedom for S atoms than for Ni atoms. One final comment concerning the amplitudes of vibrations; on viewing Figure IV.1.1 it is evident for both the Ni and S atoms that the r.m.s. amplitudes that parallel the mirror planes

(ellipsoid axes 1) are smaller than those (ellipsoid axes 2) which are perpendicular to the mirror planes. The most likely reason for this difference is that the relative distances of Ni-Ni or S-S atoms is greater perpendicular to the mirror plane than parallel to it thus allowing a greater degree of vibration along ellipsoid axes 2.

(ii) Interatomic Bonding

In this section the co-ordination and bond lengths observed in the millerite structure are discussed. In an attempt to explain the observed interatomic bonding, the simpler less sophisticated arguments are given first, and in the latter part of the discussion molecular orbital theory is applied to the structure.

In section (a) of this chapter the co-ordination of atoms about Ni was discussed. Each Ni atom is surrounded by five S atoms in a distorted tetragonal pyramid configuration having pseudo-symmetry of C_{4v} ($= 4mm$). The Ni-S bond distances vary from 2.26 Å to 2.37 Å as shown in Table IV.1.5. Taking Ahrens' (1952) ionic radii of 0.69 Å for Ni^{2+} in six-fold co-ordination, and 1.84 Å for S^{2-} , the Ni-S bond distance would be 2.53 Å. The actual Ni-S bond length in millerite is thus considerably shorter, and this shortening could reasonably be attributed to extensive covalent bonding. The single covalent bond distance, d_{AB} , may be calculated using the Schomaker-Stevenson (1941) formula which was

revised by Pauling (1960) to the form:

$$d_{AB} = r_A + r_B - 0.06 |x_A - x_B|$$

where r is the covalent radius and x the electronegativity of the element A or B. Using Pauling's (1960) covalent radii and electronegativities, and following his method of calculation given in his 1970 paper, the Ni-S covalent bond length calculates to 2.25 Å using covalent radii of 1.154 Å for Ni and 1.10 Å for transargononic S and electronegativities of 2.2 and 2.1 for Ni²⁺ and S²⁻, respectively. This value of 2.25 Å is close to the minimal Ni-S bond length observed in millerite, and this further substantiates the idea of covalent bonding in this mineral. With Pauling's (1960) formula for the calculation of per cent ionic character in this bond and using the electronegativities quoted above, the per cent ionic character calculates to only 0.05 per cent.

It has already been shown that each Ni atom has, besides five S atoms, two other Ni atoms at a distance of 2.53 Å (Table IV.1.5). In metallic Ni with twelve-fold coordination the Ni-Ni distance is 2.48 Å (Zhdanov, 1965). Thus, it is probably safe to assume there is some Ni-Ni bond interaction in millerite. This seven-fold co-ordinate complex around each nickel with an eight-sided polyhedral configuration that is difficult to name, has pseudo-symmetry of C_{2v} (= mm2) but a true symmetry of C_v (= m) because of the slight variations in the Ni-S bond lengths and angles.

The above discussion offers an explanation for the observed bond lengths in millerite, and it remains to find some explanation for the observed co-ordination. In the first instance it is constructive to look at other Ni sulphide structures. The known structures in the Ni-S system are listed in Table IV.2.1 with the co-ordination, interatomic distances and the appropriate reference for each phase. Vaesite, NiS_2 , has the pyrite structure and Elliot (1960) has refined the structure using intensity data on a powdered, synthetic phase. Polydymite, Ni_3S_4 , and high temperature NiS are believed to have the spinel and niccolite structures, respectively. Millerite, low temperature NiS, and heazlewoodite, Ni_3S_2 , are isotypical structures. The data for millerite is from this work and that of heazlewoodite is from Peacock's (1947) structure refinement of the synthetic phase Ni_3S_2 using powder data. From Table IV.2.1 it is evident that as the Ni:S ratio increases the co-ordination number of Ni by S atoms decreases. Regarding possible S-S interaction, the S-S distances suggest that there is such interaction for NiS_2 and for Ni_3S_2 but none for Ni_3S_4 , αNiS and βNiS . However, the Ni-Ni distances suggest that there is likely Ni-Ni interaction in αNiS , βNiS and in Ni_3S_2 but not in the two sulphides with the lowest Ni content. Within these structures there is no consistent trend in the Ni-S interatomic distances in relation to the Ni:S ratios, but the range of distances between 2.13 Å and 2.40 Å mainly

Table IV.2.1. Co-ordinations and bond lengths in the Ni-Sulphide structures.

<u>Phase</u>	<u>Co-ordination about Ni</u>		<u>Ni-S Dist., Å</u>	<u>Ni-Ni Dist., Å*</u>	<u>S-S Dist., Å*</u>	<u>Reference</u>
NiS ₂ Vaesite (Pyrite Type)	6 S's	pseudo- octahedral	2.40	4.01	2.06	Elliot (1960)
Ni ₃ S ₄ Polydymite (Spinel Type)	4 S	tetrahedral	2.13	3.33	3.33	Berry & Thompson (1962)
	6 S	octahedral	2.37			
αNiS Synthetic (Niccolite Type)	6 S's	distorted	2.43	2.67	3.44	Wyckoff (1963)
	2 Ni's	rhomboidal				
βNiS Millerite	5 S's	8-plane	2.26 to	2.53	3.14	Present Work
	2 Ni's	polyhedral	2.37			
Ni ₃ S ₂ Heazlewoodite	4 S's		2.28 to	2.45	2.38	Peacock (1947)
	2 Ni's		2.38			

* Minimum distance quoted

reflects the co-ordination number. The Ni-Ni distances decrease as the Ni:S ratio increases and this change coincides with the changes in the observed co-ordination and there thus appears to be some control over the observed configurations around each Ni by the Ni:S ratio.

In an attempt to arrive at a possible explanation for the observed coordinations in these minerals, we can note first that nickel and sulfur have the following electronic configurations in their ground states:

<u>element</u>	<u>Z</u>	<u>configuration</u>
Ni ^o	28	1s ² 2s ² 2p ⁶ 3s ² 3p ⁶ 3d ⁸ 4s ²
S ^o	16	1s ² 2s ² 2p ⁶ 3s ² 3p ⁴

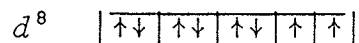
The most common ions for these elements are Ni²⁺ and S²⁻.

The co-ordination of five S atoms around each Ni might be explained at least in a superficial way, simply by the inert gas law for transition elements. The effective atomic number for Ni²⁺ is 26. The closest complete shell configuration is that of the inert gas Kr with atomic number 36. To "fill" Ni²⁺ to 36 electrons one would need five divalent S atoms which is what is observed. This would not necessarily negate any Ni-Ni interaction since no electron transfer need be postulated for such a metallic bond.

For transition metal complexes the bonding is largely determined by the electrons in the partially filled

d sub-shell. The five *d* orbitals all have identical energies for an element or ion which is free from all other species, and these orbitals are therefore called degenerate orbitals. It should be emphasized that orbitals are energy levels and thus are of significance even in the absence of electrons. As other ions approach the free ion being considered, a ligand field is established, and the energy levels in the *d* orbitals split. When covalent bonding is involved in the complex, the splitting of the energy levels is best discussed in terms of the molecular orbital theory. Using this theory one places the bare nuclei at the equilibrium positions and then computes the energy levels present. Once this has been done the electrons are added one by one until up to the number representing the chemical system. In the remainder of this section an attempt at applying molecular orbital theory to the millerite structure is given. The arguments and applications of the theory can be followed in texts such as Burns (1970), Cotton (1971), Orchin and Jaffe (1971) Orgel (1966), and Wilson, Decius and Cross (1955).

The electronic configuration of the *d* sub-shell for the free Ni²⁺ ion can be represented in the following way:



Hund's rule necessitates placing the electrons in each of the five orbitals one by one with parallel spins; there is

no spin pairing until each orbital contains one electron, so that the sixth to the eighth electrons are paired, leaving two electrons unpaired. The effect of unpaired electrons is to give the phase a paramagnetic moment. It has already been pointed out that the energy levels for the d orbitals split in the presence of ligands. Figure IV.2.2 represents the splittings of the energy levels in ligand fields with the symmetries indicated. The degree to which the energy levels split depends on the interatomic forces. These qualitative energy level diagrams are derived by the method of descending symmetries where the group of lower symmetry is correlated with O_h symmetry (Wilson, Decuis and Cross, 1955, Table X-14). Having correlated the appropriate terms, the Mulliken symbol may be used to derive the appropriate d orbital from the character table for the group (Wilson *et al.*, Table X-4). When a particular degenerate state splits into more than one state in a lower symmetry, the placement of the relative energy level is dependent on the ligand interaction. In many cases this interaction can be deduced from an inspection of the configuration involved. The higher energy level is the one with the greatest ligand field and hence the more difficult to place electrons in.

Having seen how the various symmetries affect the splitting of the d energy levels, one can proceed to construct a molecular orbital energy level diagram. The important rule governing the combination of ligand and

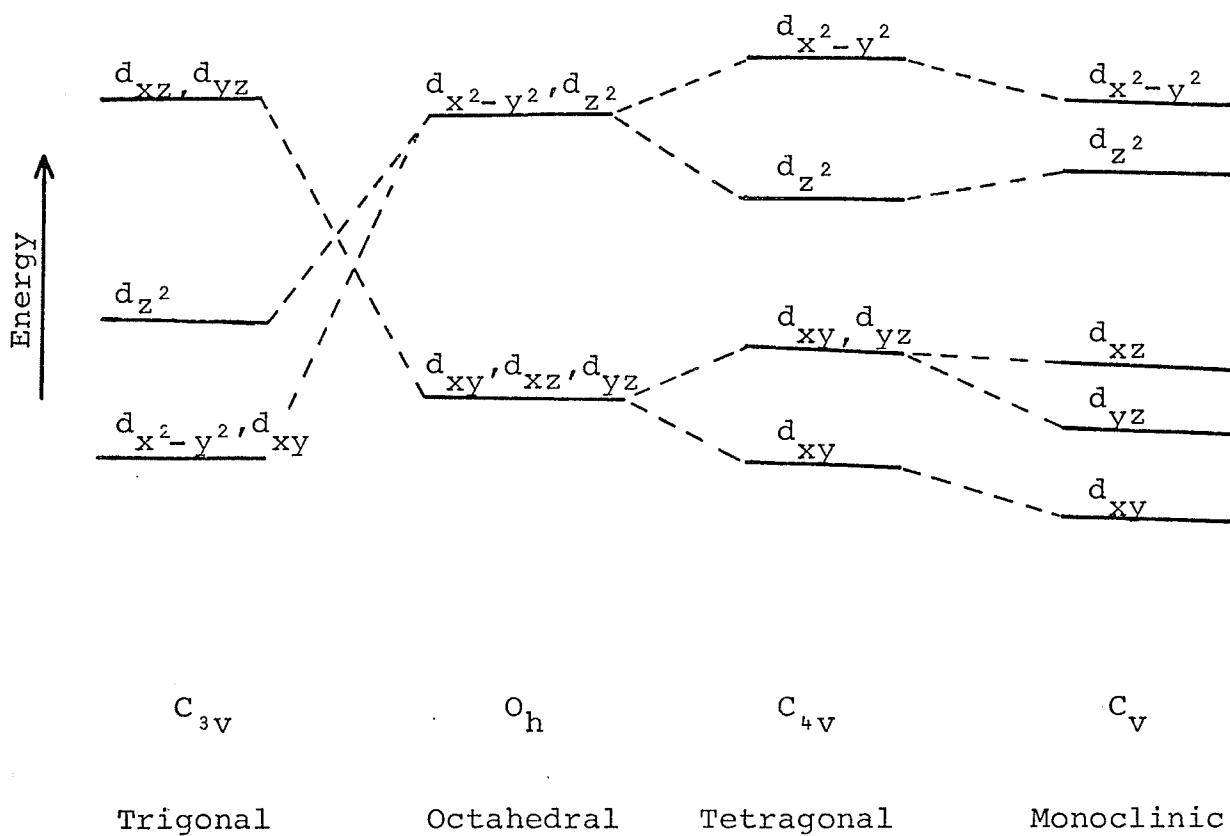


Figure IV.2.2 Splitting of energy levels for d orbitals in various symmetries.

atomic orbitals is to keep the same symmetry with respect to the molecular framework, and the molecular orbitals formed must also have this symmetry. In the construction of molecular orbital diagrams shown here in Figures IV.2.3a and b, both σ and π bondings have been taken into consideration. The reason for including π bond formation is because of the favorable formation of three π orbitals for the Ni^{2+} ion (Burns, 1970). The ligand, S^{2-} ions, are considered to be bonded through p orbitals directed along the ligand-central metal ion line in the case of σ bonding and directed perpendicular to this line for π bonding. In order to construct a set of ligand orbitals one follows the standard procedure of applying the symmetry operations to the ligand vector set to obtain the reducible representation. The irreducible representation may then be resolved through the use of the reduction formula. With the irreducible representation the atomic orbitals appropriate to the type of bonding (σ or π) being constructed may be taken from the character table. Examples of these calculations are given in Cotton (1971).

If this process is carried out for O_h symmetry and the representations reduced (Γ), one obtains;

$$\Gamma_{\sigma} = A_{1g} + E_g + T_{1u}$$

$$\Gamma_{\pi} = T_{1g} + T_{1u} + T_{2g} + T_{2u}$$

From the character tables the following orbitals are in the required symmetry classes:

A_{1g}	E_g	T_{1g}	T_{2g}	T_{1u}	T_{2u}
s	d_z^2	none	d_{xz}	p_x	none
	$d_{x^2-y^2}$		d_{yz}	p_y	
			d_{xy}	p_z	

With this information a qualitative molecular orbital energy level diagram can be drawn. Figure IV.2.3a is such a diagram and the ligand sulfur and metal nickel electrons have been placed in what would appear a logical fashion. The ligand electrons fill the s, p_x , p_y , p_z , $d_{x^2-y^2}$ and d_z^2 σ bonding energy levels. For the metal electrons there are three sets of paired electrons involved in the d_{xy} , d_{xz} , and d_{yz} π bonding orbitals. The other two electrons of Ni^{2+} remained unpaired in the anti-bonding orbitals. These unpaired electrons should make nickel sulfide compounds with octahedral co-ordination paramagnetic. Benoit (1955) measured the paramagnetic susceptibility of vaesite (NiS_2) and α NiS and found vaesite to have a large paramagnetic measurement as expected but α NiS has only a small but not negligible susceptibility. The reason for the low paramagnetic susceptibility in α NiS is probably due to the involvement of the unpaired electrons in a Ni-Ni interaction

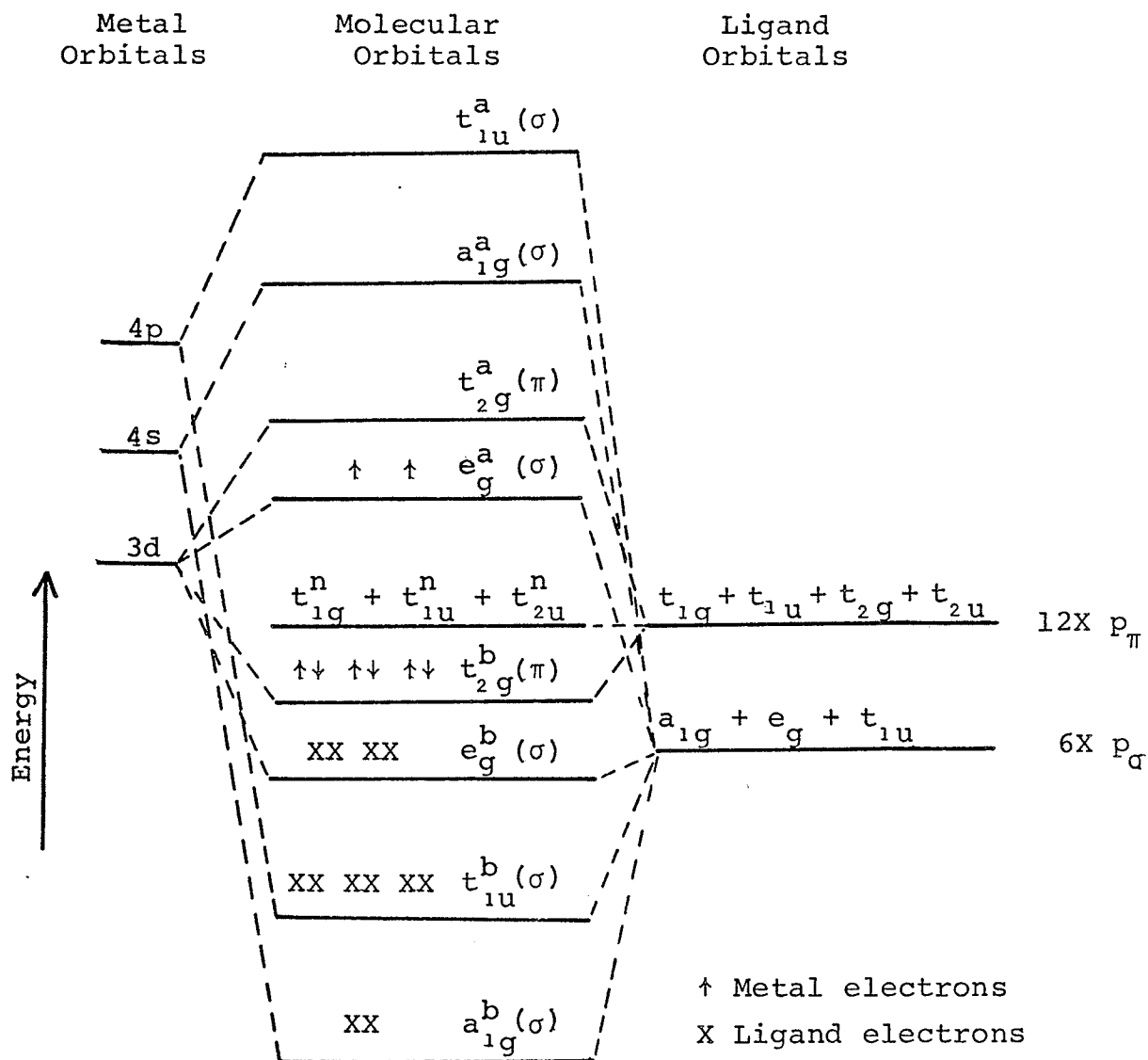


Figure IV.2.3a. Molecular orbital energy level diagram for an NiS_6 configuration with O_h symmetry. This diagram is only schematic and the members of σ and π bond sets may not lie in the order given.

which would greatly suppress the paramagnetic measurement.

As mentioned previously the NiS_5 configuration in millerite has C_{4v} pseudo-symmetry. Although the true symmetry is C_v , the arguments presented here would not change, but the calculations are simplified somewhat when C_{4v} symmetry is assumed. The irreducible representations for five-fold co-ordination in C_{4v} are:

$$\Gamma_{\sigma} = 2A_1 + B_1 + E$$

$$\Gamma_{\pi} = 2A_2 + 2B_2 + 2E$$

Referring again to the character tables, the following orbitals are in the required symmetry classes:

A_1	A_2	B_1	B_2	E
s	none	$d_{x^2-y^2}$	d_{xy}	p_x
p_z				p_y
d_{z^2}				d_{xz}
				d_{yz}

The qualitative molecular orbital energy level diagram for pentavalent co-ordination of sulfurs about nickel in C_{4v} symmetry is shown in Figure IV.2.3b. The five ligand sulfurs are involved in the s, p_x , p_y , p_z and $d_{x^2-y^2}$ bond energy levels. Six of the d electrons of

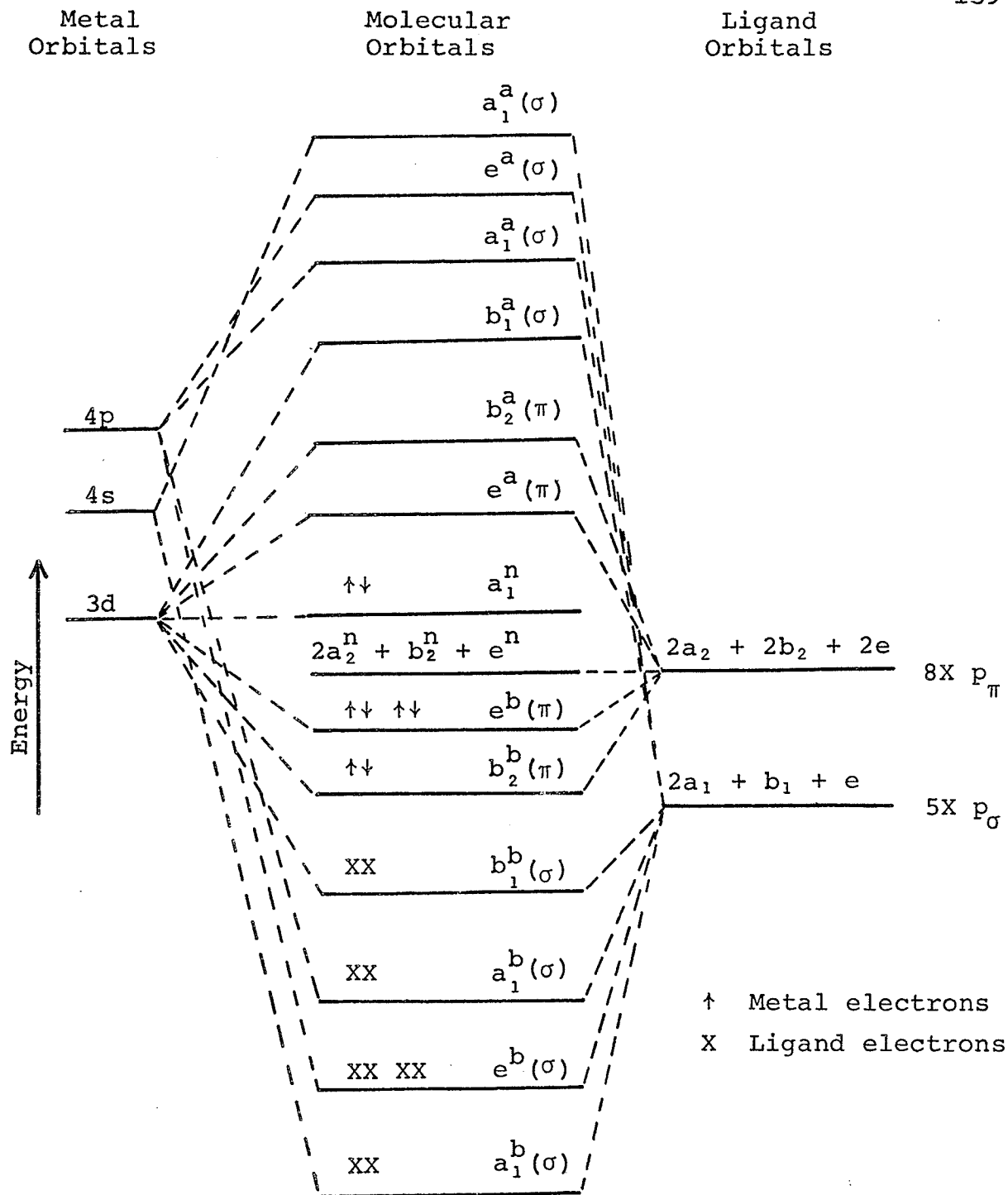


Figure IV.2.3b. Molecular orbital energy level diagram for millerite assuming C_{4v} symmetry. The energy level diagram is for S^{2-} in five-fold co-ordination around Ni^{2+} . The diagram is schematic and the members of σ and π bond sets may not lie in the order given.

nickel are in the d_{xy} , d_{yz} and d_{xz} bonding energy levels, and the remaining two of the eight electrons form a non-bonding pair in d_{z^2} . The d_{z^2} electrons may in fact be incorporated in the bonding of the Ni to two other Ni's which is symmetrical about the ligand-metal z axis. One might even think of the configuration about Ni as still maintaining a distorted octahedral co-ordination; the six ligands being five sulfurs and one non-bonding pair of electrons or the Ni-Ni interaction as the sixth. The pairing of the d_{z^2} electrons or their involvement in Ni-Ni bonding is supported by the negligible paramagnetic susceptibility measurement. Dr. Maartence, Department of Physics, University of Manitoba, made a semi-quantitative measurement of the magnetic susceptibility of a millerite sample. He found only a very low magnetic susceptibility, and this was probably due to minor amounts of Fe substituting for Ni. Thus, millerite can probably be considered as diamagnetic.

A final comment should be made concerning the two NiS polymorphs. The structures of the two polymorphs are quite different and because the phase transition from the high temperature form (α NiS) to the low temperature form (β NiS) is of the first-order type a major structural dislocation must occur and one would expect a considerable difference in the stabilization energy between the two crystal structures. In nature the low-temperature polymorph, millerite (β NiS) appears to be the only stable phase. The

reason for the increased stability of the millerite structure over the niccolite structure in αNiS can be accounted for by the lowering of the molecular orbital energy level attained in bonding within millerite as opposed to αNiS . Comparing Figure IV.2.3a to Figure IV.2.3b it is evident that the filling of the necessary orbitals for five-fold co-ordination of S about Ni in millerite requires less energy than the six-fold co-ordination in αNiS , and one would thus expect millerite to be the low temperature stable phase as is observed. Consideration of the Ni-Ni interaction in the two phases would not change these arguments. This increased stability of the millerite structure over the niccolite structure is further evidenced by an appreciable shortening of the Ni-S and Ni-Ni bond lengths in millerite relative to those in αNiS (Table IV.2.1). This shortening is presumably due to an increase in the bond strength within millerite.

REFERENCES CITED

- Alsén, N. (1925): Röntgenographische Untersuchung der Kristallstrukturen von Magnetkies, Breilhauptit, Pentlandit, Millerit und verwandten Verbindungen, *Geol. For. Forh. Stockholm*, 47, 19-72.
- Ahrens, L.H. (1952): The use of ionization potentials, *Geochimica et Cosmochimica Acta*, 155-169.
- Baird, D.C. (1962): *Experimentation: An Introduction to Measurement Theory and Experiment Design*, Englewood Cliffs, N.J.: Prentice-Hall, 64-66.
- Benoit, R. (1955): Etude paramagnetique des composés binaires, *Jour. Chim. Phys.*, 52, 119-132.
- Berry, L.G., and Thompson, R.M. (1962): X-ray powder data for ore minerals: The Peacock Atlas, *Geol. Soc. of Am., Memoir 85*.
- Buchan, R, and Blowes, J.H. (1968): Geology and mineralogy of a millerite nickel ore deposit, *C.I.M. Bulletin*, 524-534.
- Burns, R.G. (1970): *Mineralogical Applications of Crystal Field Theory*, Cambridge University Press.
- Černý, P. and Turnock, A.C. (1971): Niobium-tantalum minerals from granitic pegmatites at Greer Lake, southeastern Manitoba, *Canad. Mineral.* 10, 775-772.
- Clark, L.A. (1965): Geology and geothermometry of the Marbridge nickel deposit, Malartic, Quebec, *Econ. Geol.* 60, 792-811.
- Cotton, F.A. (1971): *Chemical Application of Group Theory*, 2nd Edition, John Wiley and Sons.
- Cromer, D.T. and Mann, J.B. (1968): X-ray scattering factors computed from numerical Hartree-Fock wave functions, *Acta Cryst.* A24, 321-324.

- Crouse, R.A. and Cerny, P. (1972): Geology of the Tanco pegmatite at Bernic Lake, Manitoba, I. Geology and paragneiss, *Canad. Mineral.* 11, 591-608.
- Elliot, N. (1960): Interatomic distance in FeS_2 , CoS_2 , and NiS_2 , *Jour. Chem. Phys.*, 33, 903-905.
- Elphick, P.M. (1972): Crystal structure analysis of wodginite from Bernic Lake, Manitoba, Unpubl. M.Sc. thesis, Univ. of Manitoba, Winnipeg.
- Evans, R.C. (1966): *An Introduction to Crystal Chemistry* 2nd Edition, Cambridge Univ. Press, 180.
- Gait, R.I. (1967): Computer calculated electrostatic charge distributions in the structures of the feldspars low albite, high albite, and anorthite, Unpubl. Ph.D. thesis, Univ. of Manitoba, Winnipeg.
- Gait, R.I., Ferguson, R.B. and Coish, H.R. (1970): Electrostatic charge distributions in the structure of low albite, $\text{NaAlSi}_3\text{O}_8$, *Acta Cryst.*, B26, 68-77.
- Graterol, M. and Naldrett, A.J. (1969): The mineralogy of the Marbridge No. 3 and No. 4 nickel-iron sulphide deposits, Preprint, MAC/GAC meeting.
- Grice, J.D. (1970): The nature and distribution of the tantalum minerals in the Tanco (Chemalloy) mine pegmatite at Bernic Lake, Manitoba, Unpubl. M.Sc. thesis, Univ. of Manitoba, Winnipeg.
- Grice, J.D., Cerny, P. and Ferguson, R.B. (1972): The Tanco pegmatite at Bernic Lake, Manitoba, II. Wodginite, tantalite, pseudo-ixiolite and related minerals, *Canad. Mineral.*, 11, 609-642.
- Jahns, R.H. and Burnham, C.W. (1969): Experimental studies of pegmatite genesis: I. A model for the observation and crystallization of granitic pegmatites, *Econ. Geol.*, 64, 843-864.
- Johnson, C.K. (1970): ORTEP: A FORTRAN thermal-ellipsoid plot program for crystal structure illustrations, Report ORNL-3794, 2nd Revision, ORTER-II addition 1971, Oak Ridge National Laboratory, Oak Ridge, Tennessee.
- International Tables for X-ray Crystallography*, C.H. Macgillivray and G.D. Rieck, eds., Kynock Press, Birmingham, England, 1962.

- Kerr, K.A. (1970): Personnel Manual for LASL Programs, University of Calgary.
- Kolkmeijer, N.H. and Moesveld, A.L.Th. (1931): Uber die Dichte und Struktur des Millerits (rhomboedrischen Nickelsulfids), *Zeit. Krist.*, 80, 91-102.
- Knorring, O. von (1968): On the geochemistry of some niobium-tantalum minerals from African pegmatites, 12th Ann. Rept., Univ. of Leeds Res Inst. of Afr. Geology, 50-53.
- Knorring, O.von, Sahama, Th.G., and Lehtinen, M. (1969): Scandian ixiolite from Mozambique and Madagascar, *Bull. Geol. Soc. Finland*, 41, 75-77.
- Kullerud, G. and Yund, R.A. (1962): The Ni-S system and related minerals, *Jour. Pet.*, 3, 126-175.
- Larson, A.C. (1971): The LASL crystal structure program library, Los Alamos Scientific Laboratory, University of California, Los Alamos, New Mexico.
- Nickel, E.H., Rowland, J.F. and McAdam, R.C. (1963a): Wodginite - a new tin-manganese tantalite from wodginia, Australia and Bernic Lake, Manitoba *Canad. Mineral.*, 7, 390-402.
- Nickel, E.H., Rowland, J.F. and McAdam, R.C. (1963b): Ixiolite - a columbite substructure, *Amer. Mineral.*, 48, 961-979.
- Orchin, M. and Jaffe, H.H. (1971): *Symmetry, Orbital, and Spectra*, John Wiley and Sons, Inc.
- Orgel, L.E. (1966): *An Introduction to Transition Metal Chemistry: Ligand-field Theory*, 2nd Edition, Methuen, London.
- Palache, C. Berman, H. and Frondel, C. (1944): *The System of Mineralogy*, 7th Edition, John Wiley and Sons, Inc., 239-242.
- Pauling, L. (1960): *The Nature of the Chemical Bond* 3rd Ed., Cornell Univ. Press.
- Pauling, L. (1970): Crystallography and chemical bonding of sulphide minerals, *Mineral. Soc. Amer. Spec. Pap.* 3, 125-131.
- Peacock, M.A. (1947): On heazlewoodite and the artificial compound Ni_3S_2 , *Contr. to Canad. Min.* 51, 59-69.

- Rucklidge, J.C. and Gasparrini, E.L. (1969): EMPADR VII a computer program for processing electron microprobe analytical data, Univ. of Toronto.
- Schomaker, V., and Stevenson, D.F. (1941): Some revisions of the covalent radii and the additivity rule for the lengths of partially ionic single covalent bonds, *Jour. Am. Chem. Soc.*, 37-40.
- Shannon, V. and Prewitt, C.T. (1969): Effective ionic radii in oxides and fluorides, *Acta. Cryst.*, 925-946.
- Stout, G.H. and Jensen, L.H. (1968): *X-ray Structure Determination*, Macmillan Company, London.
- Strunz, H. and Tennyson, Chr. (1970): *Mineralogische Tabellen*, 4th ed., Leipzig.
- Sturdivant, J.H. (1930): The crystal structure of columbite, *Zeits. Krist.*, 75, 88-108.
- Turnock, A.C. (1966): Synthetic wodginite, tapiolite, and tantalite, *Canad. Mineral.*, 8, 461-470.
- Wilson, E.B., Decius, J.C. and Cross, P.C. (1955): *Molecular Vibrations*, McGraw-Hill Book Company, New York.
- Wyckoff, R.W.G. (1935): *Crystal Structures*, 2nd Edition, 1, 122-126.
- Zhdanov, G.S. (1965): *Crystal Physics*. (A.F. Brown, translator) New York: Academic Press.

APPENDICES

APPENDIX A

Some Job Control Language (JCL) and 'De-bugging' Procedures Used with the Computer Programs

(a) Introduction

This brief section on JCL is not intended as a short course in Job Control Language. However, since Larson's programs used here (GENLES, FOURIER, DISAGL and BIJCAL) were not originally written for an IBM computer, some rather special JCL was found to be necessary, and the writer hopes that this appendix will aid users of these programs. With programs as complex as these, troubles ('bugs') inevitably occur, and a few suggestions on 'de-bugging' are also given in this appendix. Parts of this appendix will become outdated very quickly, but it is hoped that in the future users will maintain similar accounts in order to save subsequent users time, effort and money. At the time of writing, the University of Manitoba was using an IBM 360/65 computer HASP-II system.

(b) Storage

Once the programs were working, disk proved to be the cheapest and most accessible method for storage. Tapes

were used only for a permanent record of programs. The larger and most frequently used programs GENLES and FOURIER were stored on a permanent, free disk (UM1410). Since this disk was not directly accessible it was best to move the programs to the one month pack (UM1405) where they were directly accessible and kept for one month with no charge.

In the following description, it is assumed that the reader has some knowledge of JCL and FORTRAN, and consequently explanations are not given for a number of the symbols and parameters used. Some of the following information on JCL is contained in the mimeographed report "Creating and Maintaining Disk Data Sets" put out by the University of Manitoba Computer Center in 1970.

(i) Creating a Program Library

The following JCL was used to load GENLES on disk. To load a large program (partitioned data set) it is necessary to use a core size (CSIZE) definition in the EXEC statement, otherwise 104K size will be used in default.

```
//PROG JOB '3088,XXXX,,R=260K,I=20,T=3M,L=9','GRICE',  
        MSGLEVEL=(1,1)  
  
// EXEC FORTGCL,PARM.FORT='BCD',CSIZE=230K  
  
//FORT.SYSIN DD *
```

FORTRAN Source Program:

```
/*  
//LKED.SYSLMOD DD VOL=REF=ONE.MONTH,  
           DSNAME=GRICE.J0388.FEB72(GENLES),  
//DISP=(NEW,KEEP),SPACE=(TRK,(20,20,1))  
/*
```

(ii) Copying Partitioned Data Sets

As described above in the Introduction to this appendix, one may wish to move a program from one disk volume to another, or to move the data set from disk to tape. For a partitioned data set this may be done simply by using IBM's library routine called IEBCOPY. This moves the program and keeps it on both units. In the following example the program named GRICE.GO388.GENLES is being moved from disk volume UM1410 to disc volume UM1405 where it is named GENLES.J0523.JUL5. Sequential data sets can not be moved in this manner and must be re-created by a re-run of the program or by a simple READ-WRITE program.

```
//COPY JOB '0388,XXXX,,R=260K,I=20,T=20,L=1',  
          'GRICE',MSGLEVEL=(1,1)  
  
/*DISK          UM1410
```

```
// EXEC IEBCOPY,REGION=230K
//INOUT5 DD DSNAME=GRICE.G0388.GENLES,UNIT=2314,
// VOL=SER=UM1410,DISP=OLD
//INOUT4 DD DSNAME=GENLES.J0523.JUL5,UNIT=2314,
// VOL=REF=ONE.MONTH,DISP=(NEW,KEEP),SPACE=(TRK,25,1,1))
//SYSIN DD *
COPYOPER COPY OUTDD=INOUT4,INDD=INOUT5

/*
```

(iii) Creating a Data Set

Data sets generated during a program may be stored on disk for future use. A reference number must be used in the FORTRAN program (i.e. WRITE (15) list) to denote the location under which the data are to be stored. A more satisfactory method is to use a variable name, WRITE(NTI) and input NTI in the data deck. This leads to less confusion when several data sets are being created and aids in avoiding computer system incompatibilities, (for example, University of Manitoba reference numbers 5, 6 and 7 are reserved for system operations whereas at other computer centers other numbers may be reserved for system operations).

In the following example, reference number 15 is being used to store data under the name MDATA.J0388.NOV16. The DELETE command in the disposition statement has the effect of automatically erasing the data set should an error occur in the program. Reference number 8 is being

used for temporary storage and is deleted after the program has finished.

```
//DATA JOB '0388,XX,,R=200K,I=20,
      T=2M,L=5','GRICE',MSGLEVEL=(1,1)
// EXEC FORTGCLG,PARM.FORT='BCD,
      NOSOURCE,NOMAP',REGION=200K
//FORT.SYSIN DD *
```

FORTTRAN Source Program:

```
//GO.FT15F001 DD UNIT=DISK,VOLUME=REF=ONE.MONTH,
// DSNAME=MDATA.J0388.NOV16,
// SPACE=(TRK,(06,1),RLSE),DISP=(NEW,KEEP,DELETE),
// DCB=(LRECL=130,RECFM=FB,BLKSIZE=3094)
//GO.FT08F001 DD UNIT=SYSDA,
      SPACE=(TRK,(10,10)),DISP=(NEW,DELETE)
//GO.SYSIN DD *
```

data deck

/*

(iv) Executing a Program Library and Accessing
a Data Set

When a disk data set is created the physical characteristics are recorded with it. Thus, if SPACE and DCB parameters are specified when accessing the disk they must agree with the specifications used in creating the data set. Only the data set name, location and disposition

are mandatory.

In the following example, data stored on disk reference number 15 named MDATA.J0388.NOV16 is being used in the program named GENLES which is stored on the ONE.MONTH disk under the name GRICE.J0388.FEB72. Reference number 8 is for temporary storage.

The JCL for Larson's programs in this example is necessarily more complex than programs that were originally used on an IBM computer. This requires "over-writing" the standard disk reference numbers for the reader, printer and card punch. Thus, for the printer 9 over writes 6, and for the reader 10 over-writes 5.

```
//LEAST JOB '0388,XXXX,,R=265K,I=20,
           T=3M,L=5','GRICE',MSGLEVEL(1,1)
//JOB LIB DD UNIT=DISK,VOLUME=REF=ONE.MONTH,
// DSNAME=GRICE.J0388.FEB72,DISP=SHR
// EXEC PGM=GENLES,REGION=265K
//FT06F001 DD SYSOUT=A
//GO.FT15F001 DD UNIT=DISK,VOLUME=REF=ONE.MONTH,
// DSNAME=MDATA.J0388.NOV16,DISP=(OLD,KEEP)
//GO.FT07F001 DD SYSOUT=B
//GO.FT09F001 DD SYSOUT=A
//GO.FT08F001 DD SPACE=(TRK,(10,10)),
           DISP=(NEW,DELETE),UNIT=SYSDA
//GO.FT10F001 DD DDNAME=SYSIN
//GO.SYSIN DD *
```

data deck

/*

(c) 'De-bugging' Computer Programs

Each user develops his own methods for finding sources of trouble in a program. The most common way is to use the WATFIV compiler which gives explicit and comprehensible error messages. Unfortunately it is not always possible to use this compiler. In Larson's programs, as was indicated in the previous section, certain standard reference numbers are over-written and this necessitates the use of the FORTRAN G or H compiler, neither of which gives very good error messages. In these programs if the error message is not sufficiently helpful, the following two IBM programs used in conjunction with each other may solve the problem.

(i) DUMP - Part of the IBM Computer Program Library

The source program continues executing until the error is encountered. At the termination of the source program, the program DUMP ejects all the addresses in each register for the whole program. Knowing the entry address of the error message one can determine the hexadecimal length of program which has passed until the error is met. This information is then used in conjunction with LIST. The JCL necessary for DUMP is given in an example below for the program GENLES.

```
//JDG JOB '0388,XXXX,,R=260K,I=20,T=3M,L=9',
      'GRICE',MSGLEVEL=(1,1)
// EXEC FORTGCLG,PARM.FORT='BCD,NOSOURCE',
      SIZE=260K,CSIZE=230K
//FORT.SYSIN DD *
```

FORTRAN Source Program:

```
//GO.FT050001 DD DSNAME=XX SCRATCH,UNIT=2314,
      VOL=REF=ONE.MONTH,DISP=(NEW,DELETE),
// DCB=(RECFM=VBS,LRECL=624,BLKSIZE=3124),SPACE=(TRK,(100,20))
//GO.FT09F001 DD SYSOUT=A
//GO.FT11F001 DD SPACE=(TRK,(10,10)),
      DISP=(NEW,DELETE),UNIT=SYSDA
//GO.FT02F001 DD SPACE=(TRK,(10,10)),
      DISP=(NEW,DELETE),UNIT=SYSDA
//GO.FT10F001 DD DDNAME=DYDIN
//GO.SYSUDUMP DD SYSOUT=A
//GO.SYSIN DD *
```

data deck

/*

(ii) LIST - Part of the IBM Computer Library

The program LIST tabulates each operation taking place within the program, the variable name being operated on, and its location address within the program. From DUMP the location of the error is determined, and then one merely finds the correct hexadecimal location and sees which operation is taking place. At this point the error should be easily corrected. To get a listing one

merely adds the following parameter to the EXEC statement
in the JCL: PARM.FORT = 'LIST'.

APPENDIX B

Computer Program DATAP5 (Data Processing) - Reduction of Intensities to Relative F_0 Values

See Section II.3.b

(a) Input

As an example of the input format the data for tantalite are given here.

Card 1 (Title card)

2-80 TANTALITE HEATED G69-58

Card 2 (Reciprocal cell dimensions)

1- 9 0.069381 (a^*)
10-18 0.173611 (b^*)
19-27 0.196696 (c^*)
28-36 0.0 ($\cos \alpha^*$)
37-45 0.0 ($\cos \beta^*$)
46-54 0.0 ($\cos \gamma^*$)

Card 3 (Transformation matrix from cell axes to internal axes)

These cards, of which there are three, are not critical for diffractometer data and any values will do. They are, however, critical for Weissenberg data and precession data.

Card 8 (Reflection batch card)

1- 2	1	(If > 0 then format of reflection cards is not that of Card 10 but is changeable on Program Card 293.)
3- 5	1	(Index number of level)
6-15	0.71069	(Wavelength in Å units of radiation which is MoK α here)
36-45	1.0	(Overall scale factor. All F _o 's are multiplied by this number)

Card 9 (Absorption correction for a sphere)

Values of μ_R from International Tables for X-ray Crystallography, Volume II (1959)

Card 10 (Reflection data cards)

1- 4	0	(h)
5- 7	0	(k)
6-10	2	(l)
11-18	359.88	(χ)
19-25	58.86	(ϕ)
33-40	56.86	(Time in sec. on peak)
41-48	368605	(Total counts over peak)
49-53	825	(Background 1)
54-59	355	(Background 2)
68-75	0.04	(Weight)

(b) Output

The printed output of DATAP5, an example of which is given in Table B.1, is largely self-explanatory. Some of the printed output is not needed in a least-squares refinement, and need not be stored on disk for GENLES. The first page of the output contains the title, cell data,

Table B.1. Example of output for program DATAP5: Tantalite

TANTALITE HEATED G69-58
A**#06938100 B**#17361099 C**#19669598 COSA**#0.0 COSB**#0.0 COSC**#0.0
A # 14.41325 B # 5.76000 C # 5.08399 COSA #0.0 COSB #0.0 COSC #0.0

TRANSFORMATION MATRIX

1.	2.	0.
0.	0.	1.
1.	3.	0.

SCALE FACTOR NO.	1
WAVE LENGTH	0.71069
ABSORPTION COEFFICIENT	0.0
EXTINCTION COEFFICIENT	0.0
OVERALL SCALE FACTOR	1.00000
THRESHOLD VALUE	0.0

Table B.1. (Continued)

H	K	L	I	IXOPPK	SPOT	ARS	SZABSC	FXNBSK	WEIGHT	SINT	SCNO.
0.	0.	2.	365260.88	365260.88	1.0000	1.0000	0.0	324.408	24.9999	0.13979	1
0.	0.	4.	111776.44	111776.44	1.0000	1.0000	0.0	265.294	24.9375	0.27958	1
0.	0.	6.	54787.95	54787.95	1.0000	1.0000	0.0	243.505	24.8139	0.41937	1
0.	2.	0.	124527.88	124527.88	1.0000	1.0000	0.0	177.367	24.9376	0.12338	1
0.	2.	1.	174217.25	174217.25	1.0000	1.0000	0.0	225.753	24.9377	0.14181	1
0.	2.	1.	138168.88	138168.88	1.0000	1.0000	0.0	233.132	24.9376	0.18645	1
0.	2.	3.	201358.69	201358.69	1.0000	1.0000	0.0	327.490	24.9375	0.24329	1
0.	2.	4.	44422.53	44422.53	1.0000	1.0000	0.0	176.822	24.8139	0.30559	1
0.	2.	5.	34124.40	34124.40	1.0000	1.0000	0.0	176.089	24.7525	0.37061	1
0.	2.	6.	14748.04	14748.04	1.0000	1.0000	0.0	130.224	24.3902	0.43714	1
0.	4.	0.	45485.47	45485.47	1.0000	1.0000	0.0	156.958	24.8139	0.24677	1
0.	4.	1.	198482.56	198482.56	1.0000	1.0000	0.0	335.489	24.9376	0.25647	1
0.	4.	2.	4962.90	4962.90	1.0000	1.0000	0.0	56.397	22.9358	0.28361	1
0.	4.	3.	93196.63	93196.63	1.0000	1.0000	0.0	265.847	24.9375	0.32382	1
0.	4.	4.	2550.30	2550.30	1.0000	1.0000	0.0	48.344	20.9205	0.37291	1
0.	4.	5.	46414.00	46414.00	1.0000	1.0000	0.0	227.399	24.8139	0.42781	1
0.	4.	6.	4454.40	4454.40	1.0000	1.0000	0.0	77.508	22.8832	0.48658	1
0.	6.	0.	85326.00	85326.00	1.0000	1.0000	0.0	278.205	24.8755	0.37015	1
0.	6.	1.	23141.10	23141.10	1.0000	1.0000	0.0	146.648	24.6305	0.37669	1
0.	6.	2.	87481.75	87481.75	1.0000	1.0000	0.0	295.130	24.8755	0.39567	1
0.	6.	3.	4467.16	4467.16	1.0000	1.0000	0.0	70.258	22.7790	0.42542	1
0.	6.	4.	42030.92	42030.92	1.0000	1.0000	0.0	229.723	24.8139	0.46387	1
0.	8.	0.	33735.72	33735.72	1.0000	1.0000	0.0	215.582	24.7525	0.49353	1
0.	8.	1.	17553.52	17553.52	1.0000	1.0000	0.0	156.657	24.4499	0.49846	1
1.	8.	1.	340.09	340.09	1.0000	1.0000	0.0	21.827	7.2202	0.49907	1
1.	7.	0.	28.96	28.96	1.0000	1.0000	0.0	5.726	0.6648	0.43255	1
1.	7.	1.	8530.12	8530.12	1.0000	1.0000	0.0	99.207	23.8663	0.43816	1
1.	7.	2.	221.02	221.02	1.0000	1.0000	0.0	16.409	5.2219	0.45458	1
1.	7.	3.	5914.55	5914.55	1.0000	1.0000	0.0	88.502	23.2558	0.48069	1
1.	6.	4.	3503.50	3503.50	1.0000	1.0000	0.0	66.354	22.1238	0.46453	1
1.	6.	3.	273.88	273.88	1.0000	1.0000	0.0	17.418	5.9701	0.42613	1
1.	6.	2.	786.17	786.17	1.0000	1.0000	0.0	28.016	13.1233	0.39643	1
1.	6.	1.	39.48	39.48	1.0000	1.0000	0.0	6.066	0.8934	0.37750	1
1.	5.	0.	8129.38	8129.38	1.0000	1.0000	0.0	76.248	23.7529	0.30944	1
1.	5.	1.	7421.48	7421.48	1.0000	1.0000	0.0	74.027	23.6406	0.31724	1
1.	5.	2.	7903.45	7903.45	1.0000	1.0000	0.0	79.870	23.7529	0.33955	1
1.	5.	3.	2987.83	2987.83	1.0000	1.0000	0.0	52.413	21.4132	0.37379	1
1.	5.	4.	2390.92	2390.92	1.0000	1.0000	0.0	50.663	20.6611	0.41703	1
1.	5.	5.	1867.76	1867.76	1.0000	1.0000	0.0	48.653	19.6078	0.46678	1
1.	4.	6.	473.74	473.74	1.0000	1.0000	0.0	25.301	9.4787	0.48721	1
1.	4.	5.	4667.17	4667.17	1.0000	1.0000	0.0	72.156	22.8832	0.42852	1
1.	4.	4.	311.74	311.74	1.0000	1.0000	0.0	16.928	6.9686	0.37372	1
1.	4.	3.	3607.52	3607.52	1.0000	1.0000	0.0	52.403	22.1729	0.32476	1
1.	4.	2.	0.10	0.10	1.0000	1.0000	0.0	0.254	0.6978	0.28468	1
1.	4.	1.	1865.45	1865.45	1.0000	1.0000	0.0	32.614	18.6567	0.25766	1
1.	3.	0.	18469.80	18469.80	1.0000	1.0000	0.0	85.202	24.5098	0.18671	1
1.	3.	1.	598.75	598.75	1.0000	1.0000	0.0	15.930	9.4607	0.19936	1
1.	3.	2.	17791.12	17791.12	1.0000	1.0000	0.0	94.970	24.5097	0.23324	1
1.	3.	3.	423.01	423.01	1.0000	1.0000	0.0	16.363	7.7160	0.28076	1
1.	3.	4.	10114.08	10114.08	1.0000	1.0000	0.0	89.759	24.0384	0.33619	1
1.	3.	5.	612.02	612.02	1.0000	1.0000	0.0	74.710	11.9474	0.39622	1
1.	3.	6.	2803.43	2803.43	1.0000	1.0000	0.0	58.869	21.3219	0.45905	1
1.	2.	6.	2200.70	2200.70	1.0000	1.0000	0.0	50.363	20.4498	0.43784	1
1.	2.	5.	3982.07	3982.07	1.0000	1.0000	0.0	60.244	22.6244	0.37143	1
1.	2.	4.	3478.25	3478.25	1.0000	1.0000	0.0	49.581	21.9780	0.30659	1
1.	2.	3.	6224.76	6224.76	1.0000	1.0000	0.0	57.754	23.4192	0.24454	1
1.	2.	2.	1172.72	1172.72	1.0000	1.0000	0.0	21.581	15.2206	0.18808	1
1.	2.	1.	803.28	803.28	1.0000	1.0000	0.0	15.451	10.6952	0.14393	1

transformation matrix and a few other input parameters. For each reflection the main output lists the indices HKL; the net intensity I, the intensity corrected for absorption, I%CORR (there was no absorption correction made in this program for tantalite), the spot extension correction for Weissenberg data, SPOT; the absorption correction, ABS; relative observed F%OBS; weighting factor WEIGHT (input based on counting statistics); $\sin \theta$ SINT; and data reference number, SCNO.

(c) Polarization Correction for a Single-Crystal Monochromator

The polarization factor for the single-crystal monochromator is a simple function of 2θ and is independent of the method of data collection. Normally the X-ray beam is unpolarized before it enters the sample and the polarization factor (p) within the specimen is given by: $p = (1 + \cos^2 2\theta) / 2$. When a crystal monochromator is used, the X-ray beam suffers partial polarization before it enters the sample and this must be taken into consideration since it will affect the subsequent reflections from the crystal being irradiated. Assuming the monochromator is an ideally imperfect crystal, the combined polarization factor (p') becomes:

$$p' = (\cos^2 2\theta_m + \cos^2 2\theta_s) / (1 + \cos^2 2\theta_m)$$

where subscripts m and s denote the contribution to the polarization factor by the monochromator and sample, respectively. Union Carbide gives a $2d$ value of 6.708 \AA for their graphite crystal monochromator, and these monochromators are used on most single-crystal diffractometers.

(d) Subroutine Added to DATAP5 for Spherical Absorption Correction

The subroutine ABCALC was added by the writer to the data reduction program DATAP5 in order to correct for absorption in crystals approximating a spherical shape. The 19 values of μ_R from the International Tables for X-ray Crystallography, Volume II (1959), p. 295, for spherical absorption correction are read in on Card 9 in the MAIN program. The necessary variable names used in the subroutine are:

TUR = 19 values of μ_R
TSIN = $\sin \theta$
BA = transmission factor

These three variables are carried between the MAIN and the subroutine as arguments of the function ABCALC.

```
SUBROUTINE ABCALC(BA,TSIN,TUR)
DIMENSION TUR(19)
DO 7701 J=1,19
AJ=J
TET=AJ*5.-5.
THEL=ATSIN(TSIN)*57.2957795
THET=TET-THEL
IF (THET) 7701, 7703, 7704
7703 BA=1.0/TUR(J)
GO TO 7710
7704 BA=1./(((TUR(J-1)-TUR(J))*(THET/5.))+TUR(J))
GO TO 7710
7701 CONTINUE
7710 CONTINUE
RETURN
END
```

APPENDIX C

Computer Program GON09 (Goniostat)

Absorption Correction for a Polyhedron

See Section II.3.c

(a) Example of Crystal Description Necessary for GON09

Figure C.1 is a simplified sketch of the tantalite crystal used for the data collection. The major bounding planes are shown with approximately the correct dimensions on the crystal. Within the crystal an origin is chosen, and all dimensions are measured from it, perpendicular to each face. In GON09 these distances constitute, with the appropriate functions of χ and ϕ of the bounding planes, the input to define the orientation matrix of the crystal.

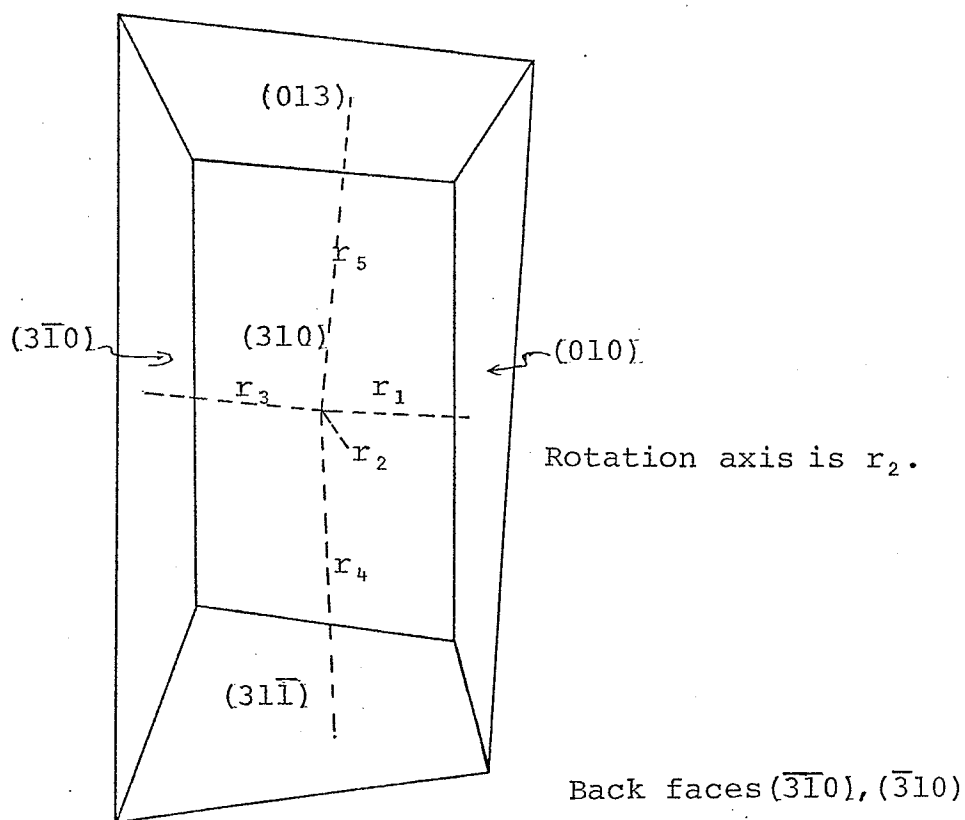
(b) Input

As an example of the input format, the data used for the tantalite crystal described above is given.

Card 1 (Title card)

1-72

TANT ABS.2



<u>hkl</u>	<u>χ</u>	<u>ϕ</u>	<u>Distance, cm</u>
010	40.01°	328.97°	0.006, r_1
310	89.78°	113.89°	0.0085, r_2
$\bar{3}10$	349.81°	329.14°	0.008
$\bar{3}\bar{1}0$	270.21°	294.62°	0.0085
$3\bar{1}0$	10.16°	148.84°	0.008, r_3
$31\bar{1}$	54.15°	238.62°	0.012, r_4
013	10.33°	46.17°	0.017, r_5

Figure C.1. Tantalite crystal as an example of input into GON09 for absorption correction

Card 2 (Indicator card)

7- 9 1.0 (always)
 10-12 1.0 (top ϕ scale used on Picker)
 13-15 1. (scale factor)
 16-18 0 (No extinction correction)

Card 3

1-10 0.0 (omega value for data)
 11-20 12.16 (Monochromator 2θ angle)

Card 4 (Guide card)

1- 5 7 (number of bounding planes)
 6-10 16 (number of grid slices)
 11-20 .0021 (interval in cm between slices)
 21-30 -.0165 (minimum value of slice co-ordinate)

Card 5 (Crystal orientation matrix)

One card of this type for each plane. Four parameters of each card A_i .

$$A_1 = -(\sin(\phi) * |\cos(\chi)|)$$

$$A_2 = -(\cos(\phi) * |\cos(\chi)|)$$

$$A_3 = -(\sin(\chi))$$

$$A_4 = -(\text{perpendicular distance from origin to plane, in cm})$$

1-15 0.0 (the (310) plane is given as an example here)
 16-30 0.0
 31-45 -1.0
 46-60 - .0085

Card 6

1-10 390.2 (linear absorption coefficient, cm^{-1})
 11-20 0.10 (approximation interval of μ)
 21-30 8.0 (No. of grid lines cutting crystal section)

Card 7 (Data cards)

There is no limit to the number of data cards.

1- 3	0.0	(h)
4- 6	0.0	(k)
7- 9	2.0	(l)
10-17	16.07	(2 θ)
18-25	359.88	(χ)
26-33	58.86	(ϕ)
34-43	105241.75	(F_o^2)
44-53	302.68	(σF)

(c) Output

An example of the output from GON09 using tantalite is shown in Table C.1. The first page of printed output gives all the input data except for the reflection cards. After this page the relevant figures for each reflection are listed as shown on the second page of Table C.1. The headings on this page are self-explanatory except for the following: F(CORR) is the relative F_o corrected for absorption (and extinction); F**2(CORR) is F(CORR) squared; F**2(OBS) is F_o squared; A stands for the absorption correction but it is actually the reciprocal of absorption, namely transmission; EXT1 and EXT2 are primary and secondary extinction correction, respectively.

Table C.1. Example of output for program GONO9: Tantalite

TANT ABS. 2
 CARD TWO CONTROL DIGITS 0 0 1. 1. 1 0

ABSORPTION CORRECTIONS ONLY

MEGA= 0.0 MONOCHROMATOR 2-THETA= 12.1600

EXTINCTION AND ABSORPTION CORRECTIONS FOR GONICSTAT DATA

KP= 7	NZ=16	DELTAZ= 0.2100E-02	ZMIN= -0.1650E-01	A(1,I)	A(2,I)	A(3,I)	A(4,I)
				0.0	0.0	-0.1000E 01	-0.8500E-02
				0.0	0.0	0.1000E 01	-0.8500E-02
				-0.5097E 00	0.8421E 00	-0.1762E 00	-0.1000E-01
				-0.7097E 00	0.6813E 00	-0.1794E 00	-0.1600E-01
				0.3050E 00	0.5000E 00	-0.8105E 00	-0.1000E-01
				0.5047E 00	-0.8450E 00	0.1768E 00	-0.1000E-01
				0.3944E 00	-0.6565E 00	-0.6430E 00	-0.7500E-02

MU= 0.3902E 03 DMU= 0.1000E 00 GRID= 8.

Table C.1 (Continued)

H	K	L	F(CORR)	SIGMA(F)	F**2(CORR)	A	F**2(OBS)	OMEGA	CHI	PHI	ZTHETA	EXT1	EXT2
0	0	2	4454.46	343.27	19842176.00	C.015364	105241.75	0.0	359.88	58.86	16.07	C.0	C.0
0	0	4	3200.84	300.91	17245405.00	C.006869	70378.63	0.0	359.88	58.86	32.47	0.0	C.0
0	0	6	1625.07	155.58	2640851.00	C.022452	59292.25	0.0	359.88	58.86	49.55	0.0	C.0
0	2	0	1382.97	174.33	1510122.00	C.016470	31462.11	0.0	40.01	328.97	14.17	0.0	C.0
0	2	1	2164.37	232.48	4429358.00	C.011508	50963.36	0.0	33.54	5.42	16.30	0.0	0.0
0	2	2	2144.99	229.46	4600574.00	C.011814	54349.59	0.0	25.07	24.83	21.49	0.0	0.0
0	2	3	2795.87	212.02	7816506.00	C.013720	107249.69	0.0	18.92	34.62	28.16	0.0	0.0
0	2	4	1407.75	197.52	1981757.00	C.015777	31265.31	0.0	14.93	40.20	35.59	0.0	0.0
0	2	5	1159.70	163.00	1344859.00	C.023056	31017.68	0.0	12.74	43.74	43.51	0.0	0.0
0	2	6	901.76	168.90	913163.00	C.020853	16957.24	0.0	10.33	46.17	51.84	0.0	0.0
0	4	0	892.43	141.22	798209.13	C.030865	24636.44	0.0	40.01	328.97	28.57	0.0	C.0
0	4	1	2257.24	167.80	5055146.00	C.022090	112553.57	0.0	38.17	349.25	29.72	0.0	C.0
0	4	2	345.04	156.61	148254.50	C.021456	3182.96	0.0	33.54	5.42	32.95	0.0	0.0
0	4	3	1773.24	156.35	3144376.00	C.022477	70676.13	0.0	29.24	16.88	37.79	0.0	C.0
0	4	4	316.07	136.79	59502.06	C.023390	2336.76	0.0	25.07	24.83	43.79	0.0	0.0
0	4	5	1488.88	142.44	2216750.00	C.023327	51710.75	0.0	21.66	30.48	50.66	0.0	0.0
0	4	6	496.33	143.55	236517.70	C.025401	6007.80	0.0	18.92	34.62	58.23	0.0	C.0
0	6	0	1285.76	114.99	1553189.00	C.046816	77355.19	0.0	40.01	328.97	43.45	0.0	C.0
0	6	1	733.09	131.52	613229.00	C.035071	21566.22	0.0	39.15	342.81	44.26	0.0	C.0
0	6	2	1659.95	139.93	2755093.00	C.031615	87101.63	0.0	36.92	355.19	46.62	0.0	C.0
0	6	3	390.99	146.77	152870.25	C.032292	4936.46	0.0	33.94	5.42	50.35	0.0	0.0
0	6	4	1765.32	136.66	1601380.00	C.032961	52771.27	0.0	30.78	13.52	55.27	0.0	C.0
0	8	0	845.78	171.69	784614.00	C.059233	46474.73	0.0	40.01	328.97	59.15	0.0	0.0
0	8	1	683.49	136.67	467154.25	C.052543	24545.49	0.0	39.51	339.44	59.80	0.0	C.0
1	8	1	96.64	31.95	9339.46	C.051025	476.55	0.0	42.32	339.90	59.88	0.0	C.0
1	7	0	24.87	2.96	618.67	C.051070	32.83	0.0	43.27	328.98	51.26	0.0	C.0
1	7	1	470.77	113.27	221623.63	C.044411	9842.62	0.0	42.56	341.40	51.97	0.0	0.0
1	7	2	82.95	26.36	6864.55	C.039229	269.29	0.0	40.66	352.90	54.08	0.0	C.0
1	7	3	459.80	120.85	211415.94	C.037047	7832.25	0.0	38.02	2.60	57.46	0.0	C.0
1	6	4	365.76	121.87	133783.25	C.032946	4407.63	0.0	33.48	15.17	55.36	0.0	0.0
1	6	3	94.00	32.71	8825.33	C.034346	373.46	0.0	36.99	7.01	50.44	0.0	C.0
1	6	2	156.03	72.59	24934.76	C.032666	785.12	0.0	40.33	356.53	46.71	0.0	0.0
1	6	1	32.34	4.74	1945.67	C.035236	36.84	0.0	42.84	343.61	44.36	0.0	0.0
1	5	0	338.01	120.86	150551.00	C.038619	5814.06	0.0	44.58	328.98	36.05	0.0	0.0
1	5	1	424.12	136.07	181578.38	C.030182	5480.44	0.0	43.17	346.57	36.99	0.0	0.0
1	5	2	470.31	139.95	221187.44	C.028841	6379.21	0.0	39.70	1.33	39.70	0.0	C.0
1	5	3	314.96	128.66	99157.91	C.027690	2746.81	0.0	35.44	12.50	43.90	0.0	0.0
1	5	4	302.94	123.54	91773.31	C.027965	2566.43	0.0	31.29	20.66	49.30	0.0	0.0
1	5	5	283.69	114.35	80482.38	C.029408	2366.82	0.0	27.62	26.66	55.65	0.0	C.0
1	4	6	157.05	58.85	24663.82	C.025953	640.05	0.0	21.25	36.45	58.31	0.0	0.0
1	4	5	451.18	142.93	203564.63	C.025608	5212.84	0.0	24.36	32.53	50.75	0.0	0.0
1	4	4	198.96	44.86	11871.27	C.024144	296.62	0.0	28.26	27.13	43.89	0.0	0.0
1	4	3	348.99	147.65	121793.31	C.022544	2745.76	0.0	33.04	19.36	37.90	0.0	0.0
1	4	2	1.68	4.70	2.82	C.022159	0.06	0.0	38.50	7.85	33.08	0.0	C.0
1	4	1	207.73	116.87	43153.16	C.024643	1063.41	0.0	43.50	350.95	29.86	0.0	0.0
1	3	0	558.91	162.47	323659.38	C.022481	7276.09	0.0	47.55	329.00	21.52	0.0	C.0
1	3	1	115.48	58.58	13335.70	C.019029	253.76	0.0	43.69	358.00	23.00	0.0	C.0
1	3	2	712.09	183.78	507068.25	C.017787	9019.30	0.0	36.14	16.91	26.98	0.0	0.0
1	3	3	119.96	56.61	14390.15	C.018599	267.55	0.0	29.30	27.92	32.61	0.0	0.0
1	3	4	644.82	172.70	415795.00	C.019377	8056.86	0.0	24.10	34.64	39.09	0.0	C.0
1	3	5	170.55	82.43	28087.97	C.020991	610.58	0.0	20.25	39.07	46.68	0.0	0.0
1	3	6	379.38	137.39	143931.38	C.024779	3465.58	0.0	17.36	42.16	54.65	0.0	0.0
1	2	6	340.95	138.45	116248.25	C.021816	2536.13	0.0	12.84	48.25	51.93	0.0	0.0
1	2	5	427.13	160.39	182437.63	C.019891	3628.86	0.0	15.21	46.19	43.61	0.0	0.0
1	2	4	347.48	171.78	150144.31	C.016372	2458.18	0.0	18.56	43.16	35.71	0.0	C.0
1	2	3	480.17	174.73	230563.56	C.014465	3335.06	0.0	23.56	38.32	28.31	0.0	0.0
1	2	2	188.63	133.04	35582.76	C.013088	465.70	0.0	31.37	29.53	21.68	0.0	C.0
1	2	1	134.99	93.49	18222.80	C.013099	238.70	0.0	42.94	10.57	16.55	0.0	C.0

APPENDIX D

Computer Program GENLES (General Least Squares)

Calculating of Structure Factors and Least Squares Refining of Parameters

See Section II.3.d

(a) Input

The example used here for the general least squares program is the data used in one of the final runs of the tantalite structure. Some of the options may not be clear to the reader without the manual (Larson, 1971).

Card 1 (Title card)

1-72 TANTALITE G69-58 L-S

Card 2 (Run control card)

1- 4	5	(No. of atomic positions to be read)
5- 8	0	(No. of $\Delta f'$ to be least squared)
9-12	0	(No. of $\Delta f''$ to be least squared)
13-16	1	(non-standard data tape, read card 5)
17-20	1	(read cell card 3)
21-24	1	(read space group card 4)
25-28	4	(No. of form factor cards to be read)
29-32	0	(No. of secondary data tapes)
33-36	0	(No. of constraints on inter atomic distances)
37-40	3	(weighting scheme used) $w=(F_0+.02F_0^2)^{-\frac{1}{2}}$
41-44	0	(do not prepare a new standard data tape)

45-48	0	(use weights as specified in col. 37-40)
49-52	0	(allow only positive definite values for β_{ij})
53-56	1	(compute secondary extinction)
57-60	1	(assume extinction not present)
61-64	0	(minimize $\sum \omega_i F_o - F_c ^2$)
65-68	0	(least square on all scale factors)
69-72	-2	(convergence criterion)
73-76	0	(all data used)
77-80	-1	(output de-bugging information)

Card 3 (Unit cell and X-ray Wavelength)

1-10	14.4134	($a, \text{\AA}$)
11-20	5.7600	($b, \text{\AA}$)
21-30	5.0838	($c, \text{\AA}$)
31-40	0.0	($\cos \alpha$)
41-50	0.0	($\cos \beta$)
51-60	0.0	($\cos \gamma$)
61-70	.71069	($\lambda, \text{\AA}$)

Card 4 (Space group symbol)

1-80 P b c n

Card 5 (Non-standard data tape control)

1- 4	1	(BCD data tape. Read card 6)
5- 8	0	(No. of initial records to be skipped)
9-12	0	(hkl are floating point numbers)
13-16	1	(serial number of h in record)
17-20	2	(serial number of k in record)
21-24	3	(serial number of l in record)
33-36	4	(serial number of F_o in record)
37-40	5	(serial number of F_o^2 in record)
41-44	-6	(serial number of σF in record)
53-56	20	(h for last reflection on tape)
57-60	0	(k for last reflection on tape)

61-64	0	(1 for last reflection on tape)
65-68	6	(total number of items in record)
73-76	780	(F ₀₀₀)
77-80	15	(Fortran reference number for tape)

Card 6 (Format for non-standard data tape)

1-72 % 3F5.0, 3F15.6 <

Card 7 (Form factor cards)

Form factor cards are taken from tables in Acta Crystal. A24,321,1968 and one card for each atom type is needed. Mn⁺² is used as an example here.

2- 7	Mn ⁺²
10-16	9.78094
17-23	4.98303
24-30	7.79153
31-37	0.30421
38-44	4.18544
45-51	11.4399
52-58	0.72736
59-65	27.7750
65-72	0.51454

Card 8 (Anomalous dispersion correction cards)

Blank

Card 9 (Atomic parameter card)

There are two types of card 9. The first gives atomic co-ordinates and signals optioned refinements. The second lists β_{ij} if necessary. There are as many of these cards as there are atomic positions.

Card 9a

1-10	0.0	(x/a)
11-20	0.321	(y/b)
21-30	0.250	(z/c)
31-40	0.5	(B isotropic)
43	1	(serial number of form factor)
46	0	(serial number of secondary form factor)
50	1	(read anisotropic β_{ij} from card 9b)
51	0	(do not refine occupancy)
52	0	(refine x)
53	0	(refine y)
54	0	(refine z)
55	1	(hold B constant)
56-65	0.419	(occupancy parameter)

Card 9b

1-10	0.00131496	(β_{11})
11-20	0.0	(β_{22})
21-30	0.00722358	(β_{33})
31-40	0.0	(β_{12})
41-50	0.00063111	(β_{13})
51-60	0.0	(β_{23})

Cards 10 and 11

Needed only if a secondary data tape is used.

Card 12 (Scale factor card)

1-10	5.983	($k=F_O/F_C$)
------	-------	-----------------

Card 16 (Refinement cycle control card)

One of these cards is needed for each cycle of least squares. Card contains signals as to how data is to be listed and what tapes are to be generated for following programs.

(b) Output

The tantalite structure is used as an example for the GENLES output in Table D.1. Most of the output is self-explanatory. There are two essential parts to the output and these are separated by a listing of the input reflection data. The first sample page of output initially gives the input data from cards 1,2,3,7,9a,9b and 12. Also with this data are given the number of reflections input, the number observed and the number used in the least-squares. The number of space group extinct reflections is recorded and these are not used in the refinement. Next on this first page there are a number of agreement factors, and then begins the output of the first cycle of refinement. For each atomic position there are four columns of information listed for the positional and thermal parameters and the occupancy factor: (i) the amount of change; (ii) the standard deviation; (iii) the new value, and (iv) the change divided by the standard deviation which is the convergence criterion. The second part of the output is a listing of all the reflections within the $\sin \theta$ requested, and for these it gives as shown in Table D.1: h,k,l , F_o, F_c , ΔF , the A and B parts of the structure factor, the phase angle α , the weight, F_c/volume , secondary extinction (PL) and primary extinction ($y^{**-\frac{1}{2}}$).

Table D.1. Example of output for program GENLES: Tantalite

```

1 TANTALITE 669-58 L-5
OTHE J1 ARE 5 0 0 1 1 1 4 0 0 3 0 0 0 1 1 0 0 -2 0 -1
OTHE FORM FACTORS ARE
MANG 9.740939 4.383029 7.791530 0.304210 4.185439 11.439899 0.727360 27.774994 0.514540 0.0 C 0.0 0
TANT 28.175690 1.060339 14.428900 3.207840 12.641199 12.605400 3.744360 85.018295 13.982400 0.0 C 0.0 0
NB+5 19.017497 1.060339 10.759100 0.362390 1.099000 0.037650 0.484690 20.976395 4.640450 0.0 C C.0 0
OXYGEN 3.225430 18.409100 3.017170 6.656799 1.425529 0.405890 0.205250 61.188889 0.423620 0.0 C 0.0 0
LATTICE CONSTANTS ARE A # 14.4134 B # 5.7600 C # 5.7638 COSA # 0.0 COSB # 0.0 COSC # 0.0
OFORM FACTOR DESCRIPTION X Y Z H11 H22 H33 H12 H13 H23 P N FCLD
H1-P<K* <EP* < 0.0 0.32100 0.25000 0.00131 0.0 0.00722 0.0 0.00063 0.0 0.41900 4
H1-P<K* <EP* < 0.16200 0.17700 0.73700 0.00113 0.00143 0.00207-0.00029-0.00005-0.00096-C.49250 8
H1-P<K* <EP* < 0.09600 0.10300 0.08560 0.00000 0.0 0.0 0.0 0.0 0.0 0.0 8
H1-P<K* <EP* < 0.41900 0.12600 0.16830 1.60000 0.0 0.0 0.0 0.0 0.0 0.0 8
H1-P<K* <EP* < 0.75710 0.12500 0.11280 0.55000 0.0 0.0 0.0 0.0 0.0 0.0 8
OTHER WERE 622 REFLECTIONS READ IN, OF WHICH 622 WERE OBSERVED
6 SPACE GROUP EXTINCT REFLECTIONS WERE READ.
OTHER ARE 621 OBSERVED REFLECTIONS WITH SCALE 1
OSCALE FACTORS ARE 5.29300
MANG 9.781 4.933 7.792 0.304 4.185 11.440 0.727 27.775 0.515 0.0 0.0
TANT 28.176 1.060 14.429 3.208 12.641 12.505 3.744 85.018 13.982 0.0 0.0
NB+5 19.017 1.060 10.759 0.362 1.099 0.038 0.485 20.976 4.640 0.0 0.0
OXYGEN 3.226 18.409 3.017 6.657 1.426 0.406 0.905 61.189 0.424 0.0 0.0
1 TANTALITE 669-58 L-5
DATA SET
THIS IS CYCLE NO. 1 IN THIS RUN. 615 REFLECTIONS WERE USED

R # 0.1810 WEIGHTED R # 2.2477 SUMDELSD # 1.44007E 04 HAMILTONS R IS 0.7768 FOR DATA SET WITH SCALE 1
THE GOODNESS OF FIT IS 4.91551
STANDARD DEVIATION OF ELECTRON DENSITY IS 2.083F CC
O FORM FACTOR DESCRIP. NO. PARA. CHANGE STD. DEV. NEW VALUE DELTA/SIGMA
O SCALE 1 -0.08909136 0.83716780 5.89399815 1.0631E-01 19
01-PZ MANG <EPZ NB+5 < 1 X 0.0 0.0 C.0 0.0 0
SET MULTIPLICITY IS 4 Y 0.00059300 0.00090958 0.32159293 6.5195E-C1 1
Z 0.0 0.0 0.25000000 0.0 0
H11 0.0 0.0 0.00131496 0.0 0
H22 0.0 0.0 0.0 0.0 0
H33 0.0 0.0 0.00722358 0.0 0
H12 0.0 0.0 0.0 0.0 0
H13 0.0 0.0 0.00063111 0.0 0
H23 0.0 0.0 0.0 0.0 0
P -0.14425874 0.24964231 0.27474123 5.7786E-C1 2
01-PZ NB+5 <EPZ YMV < 2 X 0.00075534 0.00025486 0.16275525 2.9637E 00 3
SET MULTIPLICITY IS 8 Y 0.00015950 0.00050861 0.17715943 3.1360E-01 4
Z -0.00005568 0.00087168 0.73694426 6.3882E-C2 5
H11 0.0 0.0 0.00112985 0.0 0
H22 0.0 0.0 0.00143409 0.0 0
H33 0.0 0.0 0.00207398 0.0 0
H12 0.0 0.0 -0.00029573 0.0 0
H13 0.0 0.0 -0.00005406 0.0 0
H23 0.0 0.0 -0.00096189 0.0 0
P -0.11624932 0.20826824 -0.60374927 5.5790E-01 6
01-PZ OXYGEN <EPZ YMV < 3 X 0.00136039 0.00159035 0.00736031 8.6082E-C1 7
SET MULTIPLICITY IS 8 Y -0.01120421 0.00282772 0.09179378 3.9630F 00 8
Z -0.02653285 0.00453745 0.05904741 5.8475E 00 9
H 0.26389368 0.51475185 0.84889364 4.8352E-C1 10
01-PZ OXYGEN <EPZ YMV < 4 X -0.00244471 0.00142475 0.41655523 1.7111E 00 11
SET MULTIPLICITY IS 8 Y -0.01011376 0.00633554 0.11599421 1.5944E 00 12
Z -0.01764835 0.00737885 0.18865160 2.6628E CC 13
H 1.32945061 0.04681200 2.07465004 2.4313E 00 14
01-PZ OXYGEN <EPZ YMV < 5 X 0.00498885 0.00105614 0.75209884 4.7237E CC 15
SET MULTIPLICITY IS 3 Y -0.00197763 0.00501319 0.13302631 3.9449E-C1 16
Z -0.01257459 0.00655766 0.10022330 1.9178E 00 17
H 0.20176792 0.45755202 0.75176787 4.4097E-C1 18

```

Table D.1. (Continued)

H	K	L	FOR	FCALC	DEL-F	A-PT	P-PT	ALPHA	W	XPARD	FCALC/V	PL	Y**=1/2
0	0	2	518	282	230	-282	C	190	0.00158	C.0	0.66721	3.47923	1.00000
0	0	4	372	219	153	212	C	C	0.00219	C.0	0.51946	1.63938	1.00000
0	0	6	184	179	17	-179	C	190	0.00429	C.0	0.42365	1.08890	1.00000
0	2	C	161	194	-33	-194	C	190	0.00503	C.0	0.45949	3.96495	1.00000
0	2	1	245	216	27	216	C	0	0.00332	C.0	0.51079	3.42730	1.00000
0	2	2	249	202	47	202	C	C	0.00326	C.0	0.47978	2.55944	1.00000
0	2	3	325	275	59	-275	C	190	0.00251	C.0	0.65075	1.91234	1.00000
0	2	4	164	137	27	-137	C	190	0.00494	C.0	0.32468	1.48665	1.00000
0	2	5	135	129	-4	130	C	C	0.00597	C.0	0.32891	1.21520	1.00000
0	2	6	105	92	13	92	C	0	0.00763	C.0	0.21865	1.05449	1.00000
0	4	0	194	136	-32	-136	C	190	0.00770	C.0	0.32125	1.88261	1.00000
0	4	1	262	270	-9	-270	C	190	0.00210	C.0	0.63971	1.80381	1.00000
0	4	2	45	44	1	44	C	0	0.01728	C.0	0.10415	1.61370	1.00000
0	4	3	206	203	3	203	C	C	0.00373	C.0	0.48104	1.39640	1.00000
0	4	4	37	40	-3	-40	C	190	0.00079	C.0	0.09500	1.20795	1.00000
0	4	5	173	170	3	-170	C	190	0.00467	C.0	0.40305	1.07130	1.00000
0	4	6	57	50	7	50	C	C	0.01385	C.0	0.11802	0.99168	1.00000
0	6	0	149	191	-31	181	C	0	0.00540	C.0	0.42783	1.21672	1.00000
0	6	1	91	92	-1	92	C	0	0.00875	C.0	0.21716	1.19628	1.00000
0	6	2	193	193	-1	-193	C	190	0.00420	C.0	0.45844	1.14299	1.00000
0	6	3	45	49	-4	-49	C	190	0.01703	C.0	0.11681	1.07592	1.00000
0	6	4	147	152	-6	153	C	C	0.00548	C.0	0.36246	1.01534	1.00000
0	8	0	193	130	-27	-130	C	190	0.00777	C.0	0.30916	0.98608	1.00000
0	9	1	79	88	-9	88	C	C	0.00999	C.0	0.22912	0.98253	1.00000
1	3	1	11	6	5	6	C	C	0.05940	C.0	0.01506	0.98212	1.00000
1	7	0	3	2	1	-2	C	190	0.16385	C.C	0.00548	1.06259	1.00000
1	7	1	55	55	0	55	C	0	0.01428	C.0	0.13001	1.05279	1.00000
1	7	2	10	8	1	-8	C	190	0.06740	C.0	0.01943	1.02752	1.00000
1	7	3	53	51	3	-51	C	190	0.01460	C.0	0.12040	0.99703	1.00000
1	6	4	43	42	1	42	C	C	0.01813	C.0	0.09914	1.01454	1.00000
1	6	3	11	12	-2	-13	C	190	0.06078	C.0	0.03171	1.07454	1.00000
1	6	2	18	20	-2	-20	C	190	0.03966	C.0	0.06822	1.14102	1.00000
1	6	1	4	1	3	-1	C	190	0.13704	C.0	0.07126	1.19384	1.00000
1	5	C	45	47	-2	47	C	0	0.01715	C.C	0.11176	1.46658	1.00000
1	5	1	50	50	0	-50	C	190	0.01579	C.0	0.11826	1.42759	1.00000
1	5	2	55	55	0	-55	C	190	0.01429	C.0	0.12967	1.32801	1.00000
1	5	3	37	35	2	35	C	C	0.02086	C.0	0.08214	1.20519	1.00000
1	5	4	35	35	0	35	C	C	0.02162	C.0	0.08288	1.09290	1.00000
1	5	5	33	35	-2	-35	C	190	0.02298	C.0	0.08405	1.01183	1.00000
1	4	6	18	17	2	17	C	C	0.03921	C.C	0.03953	0.99115	1.00000
1	4	5	52	54	-3	-54	C	190	0.01487	C.0	0.13156	1.06996	1.00000
1	4	4	13	14	-1	-14	C	190	0.05373	C.C	0.03339	1.20541	1.00000
1	4	3	41	39	1	39	C	C	0.01895	C.C	0.09268	1.39209	1.00000
1	4	2	C	C	0	0	C	C	0.75420	C.0	0.00085	1.60701	1.00000
1	4	1	24	23	1	-23	C	190	0.03056	C.C	0.05474	1.79464	1.00000
1	3	C	66	67	-1	-67	C	190	0.01192	C.0	0.15940	2.55569	1.00000
1	3	1	13	12	2	-12	C	190	0.05115	C.C	0.02737	2.38013	1.00000
1	3	2	83	74	9	74	C	C	0.00960	C.0	0.17444	2.00367	1.00000
1	3	3	14	10	4	10	C	C	0.04952	C.0	0.02371	1.63177	1.00000
1	3	4	75	68	7	-68	C	190	0.01056	C.0	0.16186	1.34190	1.00000
1	3	5	20	19	1	-19	C	190	0.03646	C.0	0.04444	1.14154	1.00000
1	3	6	44	46	-2	46	C	C	0.01752	C.C	0.10957	1.02145	1.00000
1	2	6	40	40	0	40	C	C	0.01937	C.C	0.09436	1.05330	1.00000
1	2	5	50	44	6	44	C	C	0.01566	C.0	0.10447	1.21258	1.00000
1	2	4	45	29	4	-29	C	190	0.01717	C.0	0.09345	1.48140	1.00000
1	2	3	56	46	10	-46	C	190	0.01401	C.0	0.10882	1.90156	1.00000
1	2	2	22	20	2	20	C	C	0.03333	C.0	0.04633	2.53556	1.00000
1	2	1	16	16	0	16	C	C	0.04475	C.0	0.03708	3.37396	1.00000
1	1	0	45	46	-2	46	C	0	0.01726	C.0	0.11011	7.47706	1.00000
1	1	1	147	85	57	89	C	C	0.00549	C.0	0.21203	5.11594	1.00000

APPENDIX E

Computer Program FOURIER - Calculation of Fourier Syntheses

See Section II.3.e

(a) Input

This example of input is for a ΔF synthesis for the tantalite structure.

Card 1 (Signal card)

11-15	20	(maximum h)
16-20	10	(maximum k)
21-25	10	(maximum l)
30	3	(for z-sections)
35	3	(for ΔF Fourier)
40	-1	(for data tape from GENLES)
45	8	(Fortran reference No. of input tape)

Card 2 (Space group symbol card)

Not needed unless data are from cards.

Card 3 (Title card)

1-72 TANTALITE DELTA F SYN.

Card 4 (Map description card)

1- 5	40	(No. of cell divisions in X direction)
6-10	16	(No. of cell divisions in Y direction)
11-15	8	(No. of cell divisions in Z direction)
16-20	0	(X origin)
21-25	0	(Y origin)

26-30	0	(Z origin)
31-35	22	(No. of points in X)
39-40	10	(No. of points in Y)
41-45	5	(No. of points in Z)
46-55	37.5	(Vol. of unit cell, Å ³)
70	1	(print min. and max. value of electron density on each section)

(ii) Output

The example of the output shown here as Table E.1 consists of a number of z -sections, with the x -axis horizontal and the y -axis vertical. The grid is marked by fractions along each axis, and at each point in the grid the computed electron density is printed. The map can then be contoured by hand although there is another program available called PLOTTER which enables the Calcomp plotter to draw in the contours. Note that the volume of the unit cell is used to scale the size of the numbers printed on the output. The number 37.5 above is approximately one-tenth the volume of the tantalite cell. One should keep in mind the scaling used when interpreting the sections.

Table E.1. Example of output of program FOURIER: Tantalite ΔF

1 TANTALITE 60-54 L-5		FOURIER 7 # 0.0																		
21 11 11 48% 3 0 3 9261 9261																				
1 TANTALITE	DELTA F SYM.	FOURIER 7 # 0.0																		
0Y / X #	0 250 500 750 1000 1250 1500 1750 2000 2250 2500 2750 3000 3250 3500 3750 4000 4250 4500 4750 5000 5250																			
0 0.0	3 -2 -1 -9 -9 0 2 1 8 -2 -1 6 4 6 6 6 5 -4 8 16 11 16																			
0 0.0625	2 6 3 -24 -23 -3 7 9 6 -9 -16 -4 1 4 7 11 8 -6 0 9 4 6																			
0 0.1250	-3 10 -1 -79 -16 -12 -5 -11 -25 -14 -6 2 6 1 2 4 -2 -12 -12 0 -2 -7																			
0 0.1875	-4 6 -4 -20 -17 -24 -15 -29 -36 -1 2 -8 -5 0 3 -4 -17 -17 -17 -9 -12 -21																			
0 0.2500	3 -8 -6 -5 -1 -12 1 -1 -5 -4 -6 -10 -11 6 1 -16 -8 4 0 4 3 -8																			
0 0.3125	-12 -21 -11 -4 3 -11 -10 -1 1 -22 -18 -12 -32 -21 -27 -36 -7 3 -4 -9 -4 6																			
0 0.3750	-2 -7 -7 -8 3 6 4 -1 3 -13 -20 -11 -11 -6 -15 -22 -12 -15 1 1 -3 10																			
0 0.4375	4 6 1 -9 -6 -3 3 4 9 6 -11 -13 5 10 6 2 -9 -26 -14 -2 2 6																			
0 0.5000	11 16 8 -4 5 6 6 6 4 6 -1 -2 8 1 2 0 -9 -9 -1 -2 3 -2																			
0 0.5625	4 9 0 -6 8 11 7 4 1 -4 -16 -9 6 9 7 -3 -23 -24 3 6 2 -2																			
RHO MAX # 1.637E 01, RHO MIN # -3.566E 01 IN SECTION NO. 1																				
0		FOURIER 7 # 0.1250																		
1 TANTALITE	DELTA F SYM.	FOURIER 7 # 0.1250																		
0Y / X #	0 250 500 750 1000 1250 1500 1750 2000 2250 2500 2750 3000 3250 3500 3750 4000 4250 4500 4750 5000 5250																			
0 0.0	0 -5 3 -5 -7 -4 -9 3 12 1 -1 1 -9 -13 -4 2 -8 -17 -6 -2 -8 -1																			
0 0.0625	-9 -8 1 -19 -23 -7 -7 -2 3 -8 -11 -8 0 -8 -8 10 -2 -20 -8 0 -11 -3																			
0 0.1250	-8 -4 -5 -12 -6 -20 -18 -18 -31 -20 -12 -8 7 5 -3 -2 -15 -7 1 2 0 -12																			
0 0.1875	-10 -3 -11 -17 -17 -37 -29 -28 -32 -6 -3 -1 -8 -10 -4 3 -18 -19 -7 -13 -8 -15																			
0 0.2500	-19 -21 -10 -12 -17 -22 -13 -11 -14 -6 -6 11 -15 -24 -25 1 13 -3 4 -7 2 -7																			
0 0.3125	-39 -34 -22 -23 -19 -17 -16 -7 -9 -12 -12 9 -32 -33 -34 -27 -3 -9 -2 -18 1 -7																			
0 0.3750	-21 -26 -18 -16 -14 -14 -19 -14 -13 -11 -6 20 -20 -22 -10 -9 5 -5 0 -16 -4 -8																			
0 0.4375	-9 -20 -9 -1 -9 -17 -15 -15 -12 -3 -8 -1 -13 -11 -8 2 17 1 -2 -7 -1 -15																			
0 0.5000	-6 -2 -6 -17 -8 2 -4 -13 -9 1 -1 1 12 3 -9 -4 -7 -5 3 -5 0 -10																			
0 0.5625	-11 0 -8 -20 -2 10 -8 -8 0 -8 -11 -8 3 -2 -7 -7 -23 -18 1 -8 -9 -4																			
RHO MAX # 1.976E 01, RHO MIN # -3.887E 01 IN SECTION NO. 2																				
0		FOURIER 7 # 0.2500																		
1 TANTALITE	DELTA F SYM.	FOURIER 7 # 0.2500																		
0Y / X #	0 250 500 750 1000 1250 1500 1750 2000 2250 2500 2750 3000 3250 3500 3750 4000 4250 4500 4750 5000 5250																			
0 0.0	9 8 19 22 19 7 24 23 7 11 23 14 8 -3 -3 12 17 20 17 25 21 25																			
0 0.0625	4 13 19 2 7 8 6 3 10 9 13 8 15 2 2 14 9 11 19 27 18 27																			
0 0.1250	14 22 19 4 7 0 9 11 2 13 14 3 19 22 17 0 1 22 24 24 29 24																			
0 0.1875	24 22 24 13 12 -6 -9 -8 -10 23 24 23 24 42 40 21 33 31 23 15 26 15																			
0 0.2500	-1 27 41 23 0 5 5 9 4 20 22 69 67 75 57 60 78 30 25 16 27 16																			
0 0.3125	-8 -7 31 22 10 9 8 16 12 15 10 80 77 57 35 62 74 15 28 13 20 13																			

APPENDIX F

Computer Program DISAGL (Distance Angle) Calculating Bond Distances and Interbond Angles

See Section II.3.f

(a) Input

The input into DISAGL can be from tape or entirely from cards. In the example given here for tantalite, all the data for tantalite were from cards.

Card 1 (Signal card)

11-20	3.0	(largest distance to be printed, Å)
21-30	3.0	(maximum length of vector for angle calculation)
36-40	0	(No. of atoms for special angle calculation)
41-45	2	(read all data from cards)

Card 2 (Standard deviations of unit cell dimensions)

1-10	0.0034	($\sigma(a)$ in Å)
11-20	0.0014	($\sigma(b)$ in Å)
21-30	0.0013	($\sigma(c)$ in Å)
31-40	0.0	($\sigma(\cos\alpha)$)
41-50	0.0	($\sigma(\cos\beta)$)
51-60	0.0	($\sigma(\cos\gamma)$)

Card 3 (Space group symbol)

1-80 P b c n

Card 4 (Unit cell dimensions)

1-10	14.4134	($a, \overset{\circ}{\text{Å}}$)
11-20	5.7600	($b, \overset{\circ}{\text{Å}}$)
21-30	5.0838	($c, \overset{\circ}{\text{Å}}$)

Card 5 (No. of atoms per scattering type)

5	5	(No. of atom types)
10	1	(No. of atoms type 1)
15	1	(No. of atoms type 2)
20	1	(No. of atoms of type 3)
25	1	(No. of atoms of type 4)
30	1	(No. of atoms of type 5)
40	5	(Total No. of atoms input)

Card 6 (Atom names card)

9-12	MN	(name of each atom type)
21-24	TA	
33-36	OXI	
45-48	OX2	
57-60	OX3	

Card 7 (Atomic co-ordinate card for first atom)

1-10	0.0	($x/a, \overset{\circ}{\text{Å}}$)
11-20	0.32307714	($y/b, \overset{\circ}{\text{Å}}$)
21-30	0.25	($z/c, \overset{\circ}{\text{Å}}$)

Card 8 (Standard deviation of atomic co-ordinates)

1-10	0.0	($\sigma(x), \overset{\circ}{\text{Å}}$)
11-20	0.00058714	($\sigma(y), \overset{\circ}{\text{Å}}$)
21-30	0.0	($\sigma(z), \overset{\circ}{\text{Å}}$)

There should be as many cards 7 and 8 as there are atomic positions.

Card 9 (Title card)

1-72 TANTALITE BOND DISTANCES AND ANGLES

(b) Output

An example of the output of DISAGL using tantalite is shown in Table F.1 where it may be seen that the input data are listed first (atomic co-ordinates and their standard deviations for each atomic site). Next each atom is taken in sequence, and for each all the bond distances and then all the bond angles are listed for adjacent atoms within the confining distances defined in the input. The listings are easily understood. For the distances, ATOM1 is the site around which the surrounding atoms are being observed, ATOM2 defines one of the adjacent atoms, CELL is the part of the co-ordinate systems within which ATOM2 lies, and then follow the distance, the standard deviation of the distance, X_1, Y_1, Z_1 , the co-ordinates of ATOM1, and X_2, Y_2, Z_2 , the co-ordinates of ATOM2 in the CELL designated. In the angle table, the two end atoms are named and the vertex atom which is ATOM1 in the preceding distance table; the angle and its standard deviation are given next; and then the co-ordinates of the three atoms involved are listed.

Table F.1. Example of output for program DISAGL: Tantalite

PAGE 1																
0	TANTALITE		ATOM 1	ATOM 2	CELL	DISTANCE	STD.	X1	Y1	Z1	X2	Y2	Z2			
MN	0.0	0.323076	0.250000	0.0	0.0005871	0.0										
TA	0.162492	0.176585	0.736732	0.0001032	0.0001906	0.0002602										
OX1	0.095771	0.094226	0.060477	0.0005237	0.0014883	0.0017724										
OX2	0.418324	0.114576	0.099762	0.0005131	0.0019318	0.0022166										
OX3	0.759698	0.119343	0.094048	0.0005561	0.0016451	0.0019765										
0	END ATOM 1	VERTEX ATOM	END ATOM 2	ANGLE	STD.	XYZ END ATOM 1	XYZ VERTEX ATOM	XYZ END ATOM 2								
OX1	1	MN	1	OX1	1	103.87	0.47	-0.096	0.094	0.440	0.0	0.323	0.250	0.096	0.094	0.060
OX1	1	MN	1	OX2	1	96.98	0.34	-0.096	0.094	0.440	0.0	0.323	0.250	-0.082	0.385	0.100
OX1	1	MN	1	OX2	1	88.19	0.34	-0.096	0.094	0.440	0.0	0.323	0.250	-0.082	0.615	0.400
OX1	1	MN	1	OX2	1	167.87	0.37	-0.096	0.094	0.440	0.0	0.323	0.250	0.082	0.615	0.100
OX1	1	MN	1	OX2	1	94.78	0.36	-0.096	0.094	0.440	0.0	0.323	0.250	0.082	0.385	0.600
OX1	1	MN	1	OX2	1	94.78	0.36	0.096	0.094	0.060	0.0	0.323	0.250	-0.082	0.385	0.100
OX1	1	MN	1	OX2	1	167.87	0.37	0.096	0.094	0.060	0.0	0.323	0.250	-0.082	0.615	0.400
OX1	1	MN	1	OX2	1	88.19	0.34	0.096	0.094	0.060	0.0	0.323	0.250	0.082	0.615	0.100
OX1	1	MN	1	OX2	1	96.98	0.34	0.096	0.094	0.060	0.0	0.323	0.250	0.082	0.385	0.600
OX2	1	MN	1	OX2	1	82.34	0.31	-0.082	0.385	0.100	0.0	0.323	0.250	-0.082	0.615	0.400
OX2	1	MN	1	OX2	1	83.02	0.36	-0.092	0.385	0.100	0.0	0.323	0.250	0.082	0.615	0.100
OX2	1	MN	1	OX2	1	160.88	0.61	-0.082	0.385	0.100	0.0	0.323	0.250	0.082	0.385	0.600
OX2	1	MN	1	OX2	1	79.78	0.53	-0.082	0.615	0.400	0.0	0.323	0.250	0.082	0.615	0.100
OX2	1	MN	1	OX2	1	83.02	0.36	-0.082	0.615	0.400	0.0	0.323	0.250	0.082	0.385	0.600
OX2	1	MN	1	OX2	1	82.34	0.31	0.082	0.615	0.100	0.0	0.323	0.250	0.082	0.385	0.600
1	TANTALITE	PAGE 2														
0	TANTALITE		ATOM 1	ATOM 2	CELL	DISTANCE	STD.	X1	Y1	Z1	X2	Y2	Z2			
TA	1	OX1	1	0-1	0	2.03983	0.00854	0.16249	0.17659	0.73673	0.09577	0.09577	0.56048			
TA	1	OX1	1	0	0	1.96436	0.00877	0.16249	0.17659	0.73673	0.09577	0.09423	0.06048			
TA	1	OX2	1	0	0	1.81347	0.00987	0.16249	0.17659	0.73673	0.08168	0.38542	0.59976			
TA	1	OX3	1	0-1	0	2.21435	0.00922	0.16249	0.17659	0.73673	0.24030	0.88056	0.90595			
TA	1	OX3	1	0	0	2.04801	0.00922	0.16249	0.17659	0.73673	0.24030	0.11934	0.40595			
TA	1	OX3	1	0	0	2.02108	0.00892	0.16249	0.17659	0.73673	0.25970	0.38056	0.90595			
0	END ATOM 1	VERTEX ATOM	END ATOM 2	ANGLE	STD.	XYZ END ATOM 1	XYZ VERTEX ATOM	XYZ END ATOM 2								
OX1	1	TA	1	OX1	1	87.28	0.26	0.096	-0.094	0.560	0.162	0.177	0.737	0.096	0.094	1.060
OX1	1	TA	1	OX2	1	92.05	0.41	0.096	-0.094	0.560	0.162	0.177	0.737	0.082	0.385	0.600
OX1	1	TA	1	OX3	1	79.68	0.33	0.096	-0.094	0.560	0.162	0.177	0.737	0.240	-0.119	0.906
OX1	1	TA	1	OX3	1	76.96	0.35	0.096	-0.094	0.560	0.162	0.177	0.737	0.240	0.119	0.406
OX1	1	TA	1	OX3	1	163.45	0.34	0.096	-0.094	0.560	0.162	0.177	0.737	0.260	0.381	0.906
OX1	1	TA	1	OX2	1	99.64	0.40	0.096	0.094	1.060	0.162	0.177	0.737	0.082	0.385	0.600
OX1	1	TA	1	OX3	1	74.72	0.33	0.096	0.094	1.060	0.162	0.177	0.737	0.240	-0.119	0.906
OX1	1	TA	1	OX3	1	156.52	0.37	0.096	0.094	1.060	0.162	0.177	0.737	0.240	0.119	0.406
OX1	1	TA	1	OX3	1	97.08	0.36	0.096	0.094	1.060	0.162	0.177	0.737	0.260	0.381	0.906
OX2	1	TA	1	OX3	1	170.10	0.37	0.032	0.385	0.600	0.162	0.177	0.737	0.240	-0.119	0.906
OX2	1	TA	1	OX3	1	98.24	0.42	0.032	0.385	0.600	0.162	0.177	0.737	0.240	0.119	0.406
OX2	1	TA	1	OX3	1	102.88	0.41	0.032	0.385	0.600	0.162	0.177	0.737	0.260	0.381	0.906
OX3	1	TA	1	OX3	1	85.28	0.29	0.240	-0.119	0.906	0.162	0.177	0.737	0.240	0.119	0.406
OX3	1	TA	1	OX3	1	86.06	0.22	0.240	-0.119	0.906	0.162	0.177	0.737	0.260	0.381	0.906
OX3	1	TA	1	OX3	1	93.64	0.23	0.240	0.119	0.406	0.162	0.177	0.737	0.260	0.381	0.906

APPENDIX G

Computer Program BIJCAL (B_{ij} Calculation) -
Calculation of Principal Axes of Thermal Vibration Ellipsoids

See Section II.3.g

(a) Testing β_{ij} for Non-positive Definite

Before β_{ij} 's may be used in BIJCAL they must be positive definite. The test is given below and if any of the conditions 1-7 given below should occur, then the atom is non-positive definite. Normally one uses isotropic temperature factors if this should occur.

(i) $\beta_{11} < 0$

(ii) $\beta_{22} < 0$

(iii) $\beta_{33} < 0$

(iv) $\beta_{11} * \beta_{22} - \beta_{12}^2 < 0$

(v) $\beta_{11} * \beta_{33} - \beta_{13}^2 < 0$

(vi) $\beta_{22} * \beta_{33} - \beta_{23}^2 < 0$

(vii) $\beta_{11} * D_{11} - \beta_{12} * D_{12} + \beta_{13} * D_{13} < 0$

where $D_{12} = \beta_{12} * \beta_{33} - \beta_{13} * \beta_{23}$

$D_{13} = \beta_{12} * \beta_{23} - \beta_{22} * \beta_{13}$

(b) Calculation of B_{iso} from β_{ij} 's

Often it is desirable to calculate an isotropic temperature factor equivalent from the anisotropic β_{ij} 's. This may be done simply by means of one equation which is given below for the reader's convenience.

$$B_{iso} = 4/3 [\beta_{11} * a^2 + \beta_{22} * b^2 + \beta_{33} * c^2 + 2(\beta_{12} * a*b*cos\gamma + \beta_{13} * a*c*cos\beta + \beta_{23} * b*c*cos\alpha)]$$

(c) Input

The input into BIJCAL can be from a tape generated by GENLES or from cards. In this example the data from the tantalite structure is used and is read in from cards. The standard deviations and β_{ij} correlation matrix are not used in this example.

Card 1 (Input control card)

5 1 (take all data from cards)

Card 2 (Card input control)

1- 5 5 (No. of atoms to be input)

6-10 -1 (standard deviations are set to zero)

Card 3 (Identification of run)

1-72 TANTALITE BIJ

Card 4 (Unit cell card)

1-10 14.4134 ($a, \overset{\circ}{\text{A}}$)

11-20 5.7600 ($b, \overset{\circ}{\text{A}}$)

21-30	5.0838	($a, \text{\AA}$)
31-40	0.0	($\cos\alpha$)
41-50	0.0	($\cos\beta$)
51-60	0.0	($\cos\gamma$)

Card 5 (Atom identification card for first atom)

1-72 MN (atom title)

Card 6 (β_{ij} card for first atom)

1-10	0.00279017	(β_{11})
11-20	0.01141177	(β_{22})
21-30	0.01705850	(β_{33})
31-40	0.0	(β_{12})
41-50	-0.00038056	(β_{13})
51-60	0.0	(β_{23})

There are as many pairs of cards 5 and 6 as there are atoms.

(d) Output

An example of BIJCAL using the tantalite temperature factors is given in Table G.1. The output for BIJCAL takes each atom and for each of the three principal axes in the vibrational ellipsoid it lists the root mean square amplitude, the equivalent B and the angles that the axis makes with the real axes and the corresponding directional cosines relative to the orthogonal lattice axes.

Table G.1. Example of output for program BIJCAL: Tantalite

II

ROOT				ANGLES THAT THE ELLIPSOID AXES MAKE WITH THE REAL LATTICE AXES					DIRECTION COSINES OF ELLIPSOID AXES RELATIVE TO ORTHOGONAL LATTICE AXES							
I	MEAN SQ AMPLITUDE	SD	B.I	SD	A	SD	B	SD	C	SD	A	SD	B	SD	C	SD
1	0.172	0.0	2.32	0.0	5.7	0.0	90.0	0.0	95.7	0.0	0.9951	0.0	0.0	0.0	-0.0990	0.0
2	0.138	0.0	1.51	0.0	90.0	0.0	0.0	0.0	90.0	0.0	0.0	0.0	1.0000	0.0	0.0	0.0
3	0.149	0.0	1.76	0.0	84.3	0.0	90.0	0.0	5.7	0.0	0.0990	0.0	0.0	0.0	0.9951	0.0

IA

ROOT				ANGLES THAT THE ELLIPSOID AXES MAKE WITH THE REAL LATTICE AXES					DIRECTION COSINES OF ELLIPSOID AXES RELATIVE TO ORTHOGONAL LATTICE AXES							
I	MEAN SQ AMPLITUDE	SD	B.I	SD	A	SD	B	SD	C	SD	A	SD	B	SD	C	SD
1	0.115	0.0	1.05	0.0	2.8	0.0	92.4	0.0	91.3	0.0	0.9988	0.0	-0.0423	0.0	-0.0233	0.0
2	0.075	0.0	0.44	0.0	88.1	0.0	17.6	0.0	107.5	0.0	0.0333	0.0	0.9530	0.0	-0.3013	0.0
3	0.065	0.0	0.33	0.0	88.0	0.0	72.5	0.0	17.6	0.0	0.0350	0.0	0.3001	0.0	0.9533	0.0

OII

ROOT				ANGLES THAT THE ELLIPSOID AXES MAKE WITH THE REAL LATTICE AXES					DIRECTION COSINES OF ELLIPSOID AXES RELATIVE TO ORTHOGONAL LATTICE AXES							
I	MEAN SQ AMPLITUDE	SD	B.I	SD	A	SD	B	SD	C	SD	A	SD	B	SD	C	SD
1	0.154	0.0	1.88	0.0	32.5	0.0	117.2	0.0	106.4	0.0	0.8434	0.0	-0.4574	0.0	-0.2819	0.0
2	0.224	0.0	3.95	0.0	78.6	0.0	41.2	0.0	128.9	0.0	0.1982	0.0	0.7525	0.0	-0.6281	0.0
3	0.053	0.0	-0.27	0.0	60.0	0.0	61.7	0.0	43.5	0.0	0.4994	0.0	0.4739	0.0	0.7253	0.0

APPENDIX H

Computer Program ORTEP-II (Oak Ridge Thermal Ellipsoid Plot) Plotting of Crystal Structure Illustrations

See Section II.3.h

(a) Input

This example is for the tantalite structure plot. The card numbers correspond to those used in the manual by C.K. Johnson (1970).

Card 3.2.1 (Title card)

1-72 ***** TANTALITE STRUCTURE J.D.GRICE *****

Card 3.2.2 (Cell parameter card)

1- 9	14.4134	($a, \text{\AA}$)
10-18	5.7600	($b, \text{\AA}$)
19-27	5.0838	($c, \text{\AA}$)

Card 3.2.3 (Symmetry cards)

There are as many symmetry cards as there are equivalent positions for a general atom in a space group. For space group Pbcn there are eight equivalent positions, one card of which is shown here for an atom at x, y, z . An explanation of the card is given in the manual.

15	0	(T_1)
18	1	(S_{11})
21	0	(S_{12})
24	0	(S_{13})
38	0	(T_2)
42	0	(S_{21})
45	1	(S_{22})
48	0	(S_{23})
63	0	(T_3)
66	0	(S_{31})
69	0	(S_{32})
72	1	(S_{33})

Card 3.2.4 (Atom parameter cards)

Two cards are required for each atom; the positional parameter card and the temperature factor card. One such pair is given here.

1- 6	MN	(Atom name)
28-36	0.0	(x/a)
37-45	0.3231	(y/b)
46-54	0.25	(z/c)
2- 9	(β_{11})	
10-18	(β_{22})	
19-27	(β_{33})	
28-36	(β_{12})	
37-45	(β_{13})	
46-54	(β_{23})	

For plotting purposes a dummy origin card was put in here with co-ordinates which put it in the center of the cell.

Following the "crystal structure data input cards" are a number of "instruction cards". A particular operation

may be requested of the program by an instruction number which is punched in columns 4-9. The various "instructions" available are given in the manual. The instructions, with their numbers, requested for the tantalite run are:

- 103 (Principal axes of thermal motion are calculated and listed for each atom)
- 201 (Initialize mechanical plotter)
- 301 (Size of illustration plotted)
- 404 (Amount of structure to be plotted)
- 501 (Illustration orientation)
- 604 (Scaling of ellipsoids)
- 705 (Type of illustration for atoms)
- 812 (Type of bond representation and atoms between which bonds are to be plotted)
- 202 (Amount of blank paper to be left after illustration)
- 2 (Read in next structure to be plotted)

(b) Output

The printed output for ORTEP-II is shown in Table G.1 for the tantalite structure. The actual structure plot, (some labels have been added later), is given in Figure III.2.1. The printed output is easily understood. First the input structural data is listed, then each requested instruction is listed and any pertinent information given.

Table H.1. Example of output for program ORTEP-II: Tantalite

***** TANTALITE STRUCTURE J.D.GRICE *****

DIRECT CELL PARAMETERS

A	B	C	ALPHA	BETA	GAMMA
14.413400	5.757999	5.083799	90.000	90.000	90.000
COSINE			0.0	0.0	0.0

RECIPROCAL CELL PARAMETERS

A*	B*	C*	ALPHA*	BETA*	GAMMA*
0.069380	0.173611	0.196703	90.000	90.000	90.000
COSINE			0.0	0.0	0.0

SYMMETRY TRANSFORMATIONS

NO.	TRANSFORMED X	TRANSFORMED Y	TRANSFORMED Z
1	0.0 1. X 0. Y 0. Z	0.0 0. X 1. Y 0. Z	0.0 0. X 0. Y 1. Z
2	0.500000 -1. X 0. Y 0. Z	0.500000 0. X -1. Y 0. Z	0.500000 0. X 0. Y 1. Z
3	0.500000 1. X 0. Y 0. Z	0.500000 0. X 1. Y 0. Z	0.0 0. X 0. Y -1. Z
4	0.0 -1. X 0. Y 0. Z	0.0 0. X 1. Y 0. Z	0.500000 0. X 0. Y -1. Z
5	0.0 -1. X 0. Y 0. Z	0.0 0. X -1. Y 0. Z	0.0 0. X 0. Y -1. Z
6	0.500000 1. X 0. Y 0. Z	0.500000 0. X 1. Y 0. Z	0.500000 0. X 0. Y -1. Z
7	0.500000 -1. X 0. Y 0. Z	0.500000 0. X 1. Y 0. Z	0.0 0. X 0. Y 1. Z
8	0.0 1. X 0. Y 0. Z	0.0 0. X -1. Y 0. Z	0.500000 0. X 0. Y 1. Z

NO.	ATOM	X	Y	Z	B11	B22	B33	B12	B13	B23	TYPE
1	MN	0.0	0.323100	0.250000	0.002790	0.011410	0.017060	0.0	-0.000380	0.0	1.
2	TA	0.162500	0.176600	0.736700	0.001260	0.003240	0.003290	-0.000160	-0.000120	-0.000520	1.
3	OX1	0.095800	0.094200	0.060500	1.059999	0.0	0.0	0.0	0.0	0.0	6.
4	OX2	0.418300	0.114600	0.099800	2.020000	0.0	0.0	0.0	0.0	0.0	6.
5	OX3	0.759700	0.119300	0.094000	0.840000	0.0	0.0	0.0	0.0	0.0	6.
6	ORGN	0.500000	0.500000	0.500000	0.0	0.0	0.0	0.0	0.0	0.0	0.

NO.	ATOM	X	Y	Z	RMSD 1	RMSD 2	RMSD 3
1	MN	0.0	0.323100	0.250000	0.138484	0.149221	0.171562
2	TA	0.162500	0.176600	0.736700	0.064641	0.074537	0.115239
3	OX1	0.095800	0.094200	0.060500	0.115866	0.115866	0.115866
4	OX2	0.418300	0.114600	0.099800	0.159949	0.159949	0.159949
5	OX3	0.759700	0.119300	0.094000	0.103144	0.103144	0.103144
6	ORGN	0.500000	0.500000	0.500000	0.100000	0.100000	0.100000

***** TANTALITE STRUCTURE J.D.GRICE *****

ORTHONORMAL REFERENCE VECTORS BASED ON CRYSTAL AXES

X VECTOR	Y VECTOR	Z VECTOR
0.6937987E-01	0.0	0.0
0.0	0.1736112E 00	0.0
0.0	0.0	0.1967033E 00

POST-FACTOR TRANSFORMATION MATRIX

0.1441339E 02	0.0	0.0
0.0	0.5759998E 01	0.0
0.0	0.0	0.5083797E 01

(((INSTRUCTION 103)))

0.0	0.0	0.0	0.0	0.0	0.0	0.0
-----	-----	-----	-----	-----	-----	-----

*** THERMAL VIBRATION ELLIPSOIDS *****

Table H.1. (Continued)

***** TANTALITE STRUCTURE J.D.GRICE *****

ATCM	RMS DISPLACEMENT	ROW VECTORS, BASED ON REFERENCE			PROBABILITY COVARIANCE MATRIX		
MN	0.138484	0.0	0.9999996	0.0	0.0293634	0.0	-0.0007053
	0.149221	-0.0989005	0.0	-0.9950970	0.0	0.0191779	0.0
	0.171562	-0.9950964	0.0	0.0989005	-0.0007053	0.0	0.0223370
TA	0.064641	-0.0344737	-0.2993664	-0.9535151	0.0132609	-0.0003365	-0.0002227
	0.074537	0.0329402	0.9532236	-0.2004655	-0.0003365	0.0054458	-0.0003857
	0.115239	0.9988619	-0.0417671	-0.0229999	-0.0002227	-0.0003857	0.0043077
UX1	0.115866	0.9999994	0.0	0.0	0.0134250	0.0	0.0
	0.115866	0.0	1.0000000	0.0	0.0	0.0134250	0.0
	0.115866	0.0	0.0	0.9999996	0.0	0.0	0.0134250
UX2	0.155549	0.9999994	0.0	0.0	0.0255836	0.0	0.0
	0.155549	0.0	1.0000000	0.0	0.0	0.0255836	0.0
	0.155549	0.0	0.0	0.9999996	0.0	0.0	0.0255836
UX3	0.103144	0.9999994	0.0	0.0	0.0106387	0.0	0.0
	0.103144	0.0	1.0000000	0.0	0.0	0.0106387	0.0
	0.103144	0.0	0.0	0.9999996	0.0	0.0	0.0106387
CFGN	0.100000	0.9999994	0.0	0.0	0.0100000	0.0	0.0
	0.100000	0.0	1.0000000	0.0	0.0	0.0100000	0.0
	0.100000	0.0	0.0	0.9999996	0.0	0.0	0.0100000

(((INSTRUCTION 201)))
0.0 0.0 0.0 0.0 0.0 0.0 0.0

***** INITIALIZE MECHANICAL PLOTTER *****

(((INSTRUCTION 301)))
0.1100000E 02 0.1100000E 02 0.0 0.1500000E 01 0.0 0.0 0.0

*** BOUNDARY 11X11 , MARGIN 1.50 ***

PLT LIMITS 11.00 BY 11.00 IN. INCLUDING 1.50 IN. MARGIN
VIEW DISTANCE 0.0 INCHES

(((INSTRUCTION 404)))
0.6555010E 06 0.6000000E 01 0.1000000E 01 0.5000000E 01 0.5000000E 00 0.5000000E 00 0.5000000E 00

CUBE	FROM ATOMS		TO ATOMS		WITH RADIUS OR, IF A BOX, WITH SEMIDIMENSIONS		
	(MIN)	(MAX)	(MIN)	(MAX)	A	B	C
404	655501	655501	1	5	0.500	0.500	0.500

VECTORS FROM ATCM (6,55501) TO ATOMS 1 THROUGH 5

CONTENTS OF ATOMS ARRAY									
165501.	155501.	255501.	355501.	455501.	555501.	655502.	155502.	355502.	455502.
255402.	255403.	355603.	455603.	545603.	265604.	365504.	465504.	565504.	166605.
266605.	366605.	466605.	566605.	156605.	255606.	155506.	355506.	455506.	545506.
565507.	255507.	355507.	455507.	356508.	456508.	556508.	256408.		

(((INSTRUCTION 501)))
0.6555010E 06 0.6555010E 06 0.6955010E 06 0.6555010E 06 0.6595010E 06 0.0 0.1000000E 01

***** ORIGIN ON DUMMY ATCM 6 *****

Table H.1. (Continued)

X VECTOR		Y VECTOR		Z VECTOR							
0.6937587E-01	0.0	0.0	0.0	0.0	0.0	0.1441339E 02	0.0	0.0	0.0	0.0	0.0
0.0	0.1736112E 00	0.0	0.0	0.0	0.0	0.0	0.5759998E 01	0.0	0.0	0.0	0.0
0.0	0.0	0.1967033E 00	0.0	0.0	0.0	0.0	0.0	0.5083797E 01	0.0	0.0	0.0
((((INSTRUCTION 604))))											
0.0	0.0	0.0	0.0	0.3000000E 01	0.0	0.0	0.0	0.0	0.0	0.0	0.0
***** ELLIPSOID SCALE 3.0 *****											
ORIGIN POINT IN PLOTTER COORD. (5.50 , 5.50) IN.											
OVERALL SCALE = 0.555 INCH/ANGSTROM ELLIPSOID SCALE = 3.000											
VIFW DISTANCE 0.0 INCHES											
((((INSTRUCTION 705))))											
0.4000000E 01	0.0	0.1000000E 01	0.0	0.0	0.0	0.0	0.0	0.0	0.0	0.0	0.0
***** TANTALITE STRUCTURE J.D.GRICE *****											
SYMBOL	ATOM CODE	PLOTTER X,Y(IN.)			CARTESIAN X,Y,Z (IN.)			CRYSTAL SYSTEM X,Y,Z			
		(DIRECTION COSINES(I,J),I=1,3),RMSD(J)),J=1,3			FOR PRINCIPAL AXES BASED ON WORKING SYSTEM						
MN	(1,65501)	9.50	4.93	4.000	-0.566	-0.705	1.0000	0.3231	0.2500	0.0	0.0
	0.0 1.0000	0.0	0.13848	0.0989	0.0	0.9951	0.14922	-0.9951	0.0	0.0989	0.17156
MN	(1,55501)	1.50	4.93	-4.000	-0.566	-0.705	0.0	0.3231	0.2500	0.0	0.0
	0.0 1.0000	0.0	0.13848	0.0989	0.0	0.9951	0.14922	-0.9951	0.0	0.0989	0.17156
TA	(2,55501)	2.80	4.47	-2.700	-1.034	0.668	0.1625	0.1766	0.7367	0.0	0.0
	0.0345 0.2994	0.9535	0.06464	-0.0329	-0.9532	0.3005	0.07454	-0.9989	0.0418	0.0230	0.11524
CX1	(3,55501)	2.27	4.20	-3.234	-1.297	-1.240	0.0958	0.0942	0.0605	0.0	0.0
	1.0000 0.0	0.0	0.11587	0.0	1.0000	0.0	0.11587	0.0	1.0000	0.11587	0.0
CX2	(4,55501)	4.85	4.27	-0.654	-1.232	-1.129	0.4183	0.1146	0.0998	0.0	0.0
	1.0000 0.0	0.0	0.15995	0.0	1.0000	0.0	0.15995	0.0	1.0000	0.15995	0.0
CX3	(5,55501)	7.58	4.28	2.078	-1.217	-1.146	0.7597	0.1193	0.0940	0.0	0.0
	-1.0000 0.0	0.0	0.10314	0.0	1.0000	0.0	0.10314	0.0	1.0000	0.10314	0.0
CX3	(5,65502)	7.42	5.12	1.922	-0.381	0.265	0.7403	0.3807	0.5940	0.0	0.0
	-1.0000 0.0	0.0	0.10314	0.0	1.0000	0.0	0.10314	0.0	1.0000	0.10314	0.0
MN	(1,55502)	5.50	4.47	0.0	-1.033	0.705	0.5000	0.1769	0.7500	0.0	0.0
	0.0 1.0000	0.0	0.13948	-0.0989	0.0	0.9951	0.14922	0.9951	0.0	0.0989	0.17156
CX1	(3,55502)	4.73	5.20	-0.766	-0.301	0.171	0.4042	0.4058	0.5605	0.0	0.0
	1.0000 0.0	0.0	0.11587	0.0	1.0000	0.0	0.11587	0.0	1.0000	0.11587	0.0
CX2	(4,55502)	2.15	5.13	-3.346	-0.366	0.282	0.0817	0.3854	0.5998	0.0	0.0
	1.0000 0.0	0.0	0.15995	0.0	1.0000	0.0	0.15995	0.0	1.0000	0.15995	0.0
TA	(2,55402)	4.20	4.94	-1.300	-0.565	-0.743	0.3375	0.3234	0.2367	0.0	0.0
	-0.0345 -0.2994	0.9535	0.06464	-0.0329	-0.9532	0.3005	0.07454	0.9989	-0.0418	0.0230	0.11524
TA	(2,55603)	6.80	4.94	1.300	-0.565	-0.668	0.6625	0.3234	0.2632	0.0	0.0
	-0.0345 0.2994	0.9535	0.06464	0.0329	-0.9532	0.3005	0.07454	0.9989	0.0418	0.0230	0.11524

Table H.1. (Continued)

***** TANTALITE STRUCTURE J.D.GRICE *****

SYMBOL	ATOM CODE	PLCTER X,Y(IN.)			CARTESIAN X,Y,Z (IN.)			CRYSTAL SYSTEM X,Y,Z			
		(DIRECTION COSINES(I,J),I=1,3),RMSD(J),J=1,3			FOR PRINCIPAL AXES BASED ON WORKING SYSTEM						
OX3	(5.5650E)	7.58	6.72	2.078	1.217	0.265	0.7597	0.8807	0.594C		
	-1.0000 0.0	0.0	0.10314	0.0	-1.0000	0.0	0.10314	0.0	0.0	1.0000	0.10314
TA	(2.5640E)	2.80	6.53	-2.700	1.034	-0.743	0.1625	0.8234	0.2367		
	0.0345 -0.2994	0.9535	0.06464	-0.0329	0.9532	0.3005	0.07454	-0.9989	-0.0418	0.0230	0.11524

(((INSTRUCTION E12)))
 0.0 0.0 0.0 0.0 0.0 0.0 0.0 0.0 0.0 0.0
 1 2 3 5 3 0.90000 2.40000 0.06000 0.0 0.0 0.0 0.0 0.0

*** PROJECTED BONDS OUT TO 2.4 A *****

BOND SELECTION CODES

(SEQUENCE(A))	(SEQUENCE(B))	(BOND)	(DISTANCES)	(BOND)	(PERSP.--LABELS)	(NORMAL--LABELS)	(DIGITS)
(MIN MAX)	(MIN MAX)	(TYPE)	(MIN MAX)	(RADIUS)	(HEIGHT OFFSET)	(HEIGHT OFFSET)	(NUMBER)
1 2	3 5	3	0.90 2.40	0.060	0.0	0.0	0.0

(((INSTRUCTION 202)))
 0.200000E 02 0.0 0.0 0.0 0.0 0.0

(((INSTRUCTION -2)))